The Jamuna–Brahmaputra River, Bangladesh

Best, James L. ; Ashworth, Philip J. ; Mosselman, Erik; Sarker, Maminul H.; Roden, Julie E.

DOI
10.1002/9781119412632.ch20

Publication date
2022

Document Version
Final published version

Published in
Large Rivers

Citation (APA)
Best, J. L., Ashworth, P. J., Mosselman, E., Sarker, M. H., & Roden, J. E. (2022). The Jamuna–Brahmaputra River, Bangladesh. In A. Gupta (Ed.), *Large Rivers: Geomorphology and Management* (2nd ed., pp. 579-640). Wiley-Blackwell. https://doi.org/10.1002/9781119412632.ch20

20

The Jamuna–Brahmaputra River, Bangladesh

James L. Best[1], Philip J. Ashworth[2], Erik Mosselman[3,4], Maminul H. Sarker[5], and Julie E. Roden[6]

[1]*Departments of Geology, Geography and Geographic Information Science, and Mechanical Science and Engineering and Ven Te Chow Hydrosystems Laboratory, University of Illinois at Urbana-Champaign, Urbana, IL, USA*
[2]*School of Applied Sciences, University of Brighton, Brighton, UK*
[3]*Deltares, Delft, the Netherlands*
[4]*Department of Hydraulic Engineering, Faculty of Civil Engineering and Geosciences, Delft University of Technology, Delft, the Netherlands*
[5]*Center for Environmental and Geographic Information Services (CEGIS), Dhaka, Bangladesh*
[6]*Henley-on-Thames, UK*

20.1 Background

20.1.1 The River

Bangladesh is dominated by three great rivers – the Jamuna–Brahmaputra, Ganga, and Meghna – that combine to feed sediment into one of the World's largest deltas in the Bay of Bengal (Figure 20.1). Bangladesh has been shaped by, and is dependent upon, its rivers, which provide fertile soils and a diverse flora and aquaculture but also bring significant flood hazard and risk to infrastructure for a large and growing population. Current anthropogenic stresses, in terms of changing climate, water diversions, pollution, and sediment extraction, are posing new pressures to the river and its inhabitants (Best 2019). The people of Bangladesh have adapted their lifestyle for centuries to live with river flooding – frequently moving their temporary bankside homes, planting on newly emergent river bars, and sometimes raising their homesteads above water level in flood periods (Paul 1997). However, a growing population, coupled with the expansion of infrastructure and economic development, has resulted in an increase in the intensity of flood damage (FPCO 1995; Paul 1997; CPD 2004). The lives of many millions of Bangladeshi citizens are reliant on these rivers, with up to 2.3 million people living on the riverine islands alone (Schmuck-Widmann 2001). Bangladesh's rural economy relies upon annual 'normal' floods to bring fish to village ponds and moisture and fresh sediments to the floodplain soils (Paul 1997): for instance, two of the three seasonal rice varieties (*aus* and *aman*) cannot survive without floodwater and the fish caught both on the floodplain during flood season and from the many floodplain ponds ('*beels*') provide the main source of protein for many rural populations (Chowdhury 1994; Paul 1997; de Graaf 2003; Shankar et al. 2004). However, the effect of 'abnormal' floods can be devastating and result in appreciable damage to crops and houses, bank erosion even more severe than during normal floods with consequent loss of homesteads, schools and land, and loss of human lives, livestock, and fisheries (BDER 2021; Shankar et al. 2004). For

Large Rivers: Geomorphology and Management, Second Edition. Edited by Avijit Gupta.

example, in the 1998 flood, over 70% of the land area of Bangladesh was inundated, affecting 31 million people and 1 million homesteads (Chowdhury 2000). The 1998 flood, which had an unusually long duration from July to September, claimed 918 human lives and was responsible for damaging 16 000 and 6000 km of roads and embankment respectively, and affecting 6000 km^2 of standing crops (Chowdhury 2000). In the 2004 floods, over 25% of the population of Bangladesh, or 36 million people, was affected by the floods; 800 lives were lost; 952 000 houses were destroyed and 1.4 million were badly damaged; 24 000 educational institutions were affected, including the destruction of 1200 primary schools; 2 million government and private tubewells were affected, and over 3 million latrines were damaged or washed away, thus increasing the risks of diarrhoea, cholera, and other waterborne diseases. Also, 1.1 million ha of rice crop was submerged and lost before it could be harvested, with 7% of the yearly *aus* (early season) rice crop destroyed; 270 000 ha of grazing land was affected, 5600 livestock perished together with 254 000 poultry, and 63 Mt of lost fish production (BDER 2004; CPD 2004). In the districts that are dominated by the Brahmaputra–Jamuna River, the 2004 flood damage to infrastructure (homes, roads, culverts), tubewells and latrines, with ensuing unemployment of many of the population, had a critical impact. The total cost of the damage caused by the 2004 flood was estimated at $7 billion USD (CPD 2004).

Hence, due to the nature of these devastating floods, and the concentration of especially damaging floods in 1987, 1988, 1998, 2004, and 2007, the possible influences on catastrophic flooding, such as the role of Himalayan deforestation (Kattelman 1990; Mirza et al. 2001), the type of intervention and infrastructural response to flooding (e.g. the Brahmaputra Right Embankment [BRE] from the Teesta to Hurasagar confluences; Figure 20.1) and the nature, scope, and need for the Flood Action Plan (Haggart et al. 1994; Paul 1997) have thus received much attention and debate over recent years (Boyce 1990; Hossain 1993; Haggart et al. 1994; Reavill and Rahman 1995; Paul 1997; Islam 2001). Additionally, political debates concerning water usage and construction of dams have become a major issue for Bangladesh (Patel 1996; Wood 1999; Mirza 2004), since over 90% of the catchments of Bangladesh's three great rivers lies outside the boundaries of the country.

The Brahmaputra–Jamuna and Ganga Rivers combine to form the Padma, which carries the third greatest water discharge of all the World's rivers but is often ranked the highest in terms of sediment discharge (Schumm and Winkley 1994), although a range of values exist for these estimates. The Jamuna is the local name given to the river for its entire length in Bangladesh to the Ganga junction (Figure 20.1; hereafter the river is referred to as the Jamuna). The Jamuna has one principal tributary input, the Teesta River in the north-west, and two major offtakes on the left bank that are the old Brahmaputra (see below) and the Dhaleswari (Figure 20.1). The Jamuna River contributes ~51% of the water discharge and 38% of the sediment yield to the Padma according to Schumm and Winkley (1994), although FAP24 estimates these percentage contributions to the Padma at 66% and 65% for water and sediment discharge respectively (FAP24 1996a), with the sediment yield being estimated at 590 $Mt\,yr^{-1}$ and the sand fraction contributing 34% of this total (Sarker 1996). The Jamuna can have a braidplain width up to 15 km in flood and scour depths of up to 40 m have been recorded (Klaassen and Vermeer 1988). Thus, by any definition, the Jamuna is one of the World's truly great rivers (Best 2019), and has a direct and daily influence on the prosperity of its population and the country's economic growth and political stability.

Since the seminal work of Coleman (1969), much research has been conducted on these rivers, especially in the 1990s as part of the Bangladesh Flood Action Plan (e.g. Haggart et al. 1994; Thorne and Thiagarajah 1994;

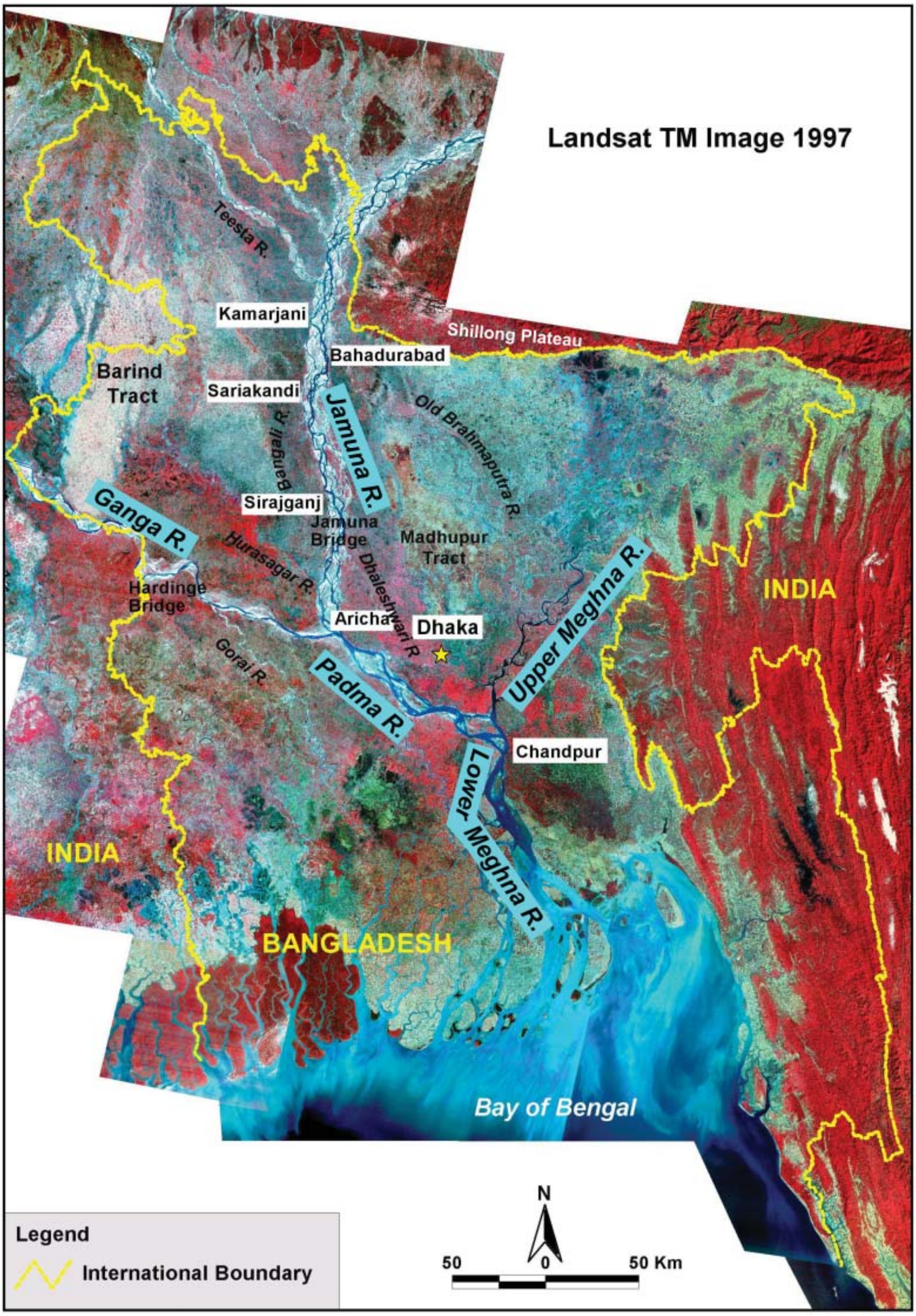

Figure 20.1 Landsat image of Bangladesh, showing the Brahmaputra–Jamuna, Ganga (Ganges), and Meghna Rivers, together with the major features and towns referred to in this chapter.

FAP24 1996a, b, c, d, e, f, g, h; Paul 1997), together with work from organizations such as the Center for Environmental and Geographic Information Services (CEGIS) and Water Resources Planning Organization (WARPO) in Bangladesh, and this has allowed a dramatic increase in our knowledge of the behaviour of the Jamuna River. This work, aided by major advances in monitoring techniques, such as frequent, all-year satellite imagery and whole-flow depth monitoring within the main channels at even the highest discharges, has resulted in the river being characterized in more detail than ever before (Takagi et al. 2007). Hofer and Messerli (2006) provide a detailed account on the history of flooding and hydrology of the Brahmaputra–Jamuna River, as well as highland–lowland linkages and case studies of various flood years. Recent attempts to predict morphological change have also met with some success (EGIS 2002; CEGIS 2003; Mosselman 2006), and together with numerical modelling (Enggrob and Tjerry 1999; Jagers 2003) offer some hope to both understand and predict river channel movement, and establish management plans for such change. Additionally, development of large-scale infrastructure within Bangladesh, such as construction of the Bangabandhu Multipurpose Bridge across the Jamuna, and numerous bank-protection works (Mosselman 2006), has demanded an increased quantification of the alluvial channel processes and prediction of future channel change. This chapter seeks to provide a synthesis on aspects of the geomorphology and sedimentology of the Jamuna River within Bangladesh, between the northern Bangladesh border and its junction with the Ganga some 240 km to the south (Figure 20.1), and examines issues of applied geomorphology in response to the flooding and migration of this huge and largely untamed river. Details of the Brahmaputra River upstream of the Bangladesh border are given by Singh (see Chapter 19), and a synthesis on the water resources of the Brahmaputra Basin in India is provided by Singh et al. (2004), including a chapter on fluvial geomorphology by Bora (2004).

20.1.2 Basinal Setting and Controls on Sedimentation

The Jamuna River has developed in a region of significant tectonic activity associated with Himalayan uplift and development of the Bengal foredeep (Alam et al. 1990; Barua 1994; Goodbred, Jr., et al. 2003; Singh 2007; Brammer 2012; Steckler et al. 2016), and the underlying structural control on the location of the major river systems of Bangladesh has long been debated (Morgan and McIntire 1959; Umitsu 1993; Barua 1994; Reitz et al. 2015; Grimaud et al. 2019). Steckler et al. (2016) show how subduction is still active in the region, with *c.* 13–17 mm yr^{-1} of plate convergence on an active, shallowly dipping and locked megathrust fault. Morgan and McIntire (1959) suggested there is a zone of 'structural weakness' along the present course of the Ganga-Jamuna-Padma rivers due to either a subsiding trough or a fault at depth. The region is known to have suffered major seismic activity in the past 100 years (FAP24 1996a), experiencing 20 earthquakes of Richter magnitude >7 in and around the Bengal Basin in the past 100 years, with the great 1950 Assam earthquake measuring Richter magnitude 8.6 and affecting up to 52 000 km^2 of territory in Assam (Sarker and Thorne 2006; Sarker et al. 2014). Seijmonsbergen (1999) reports on an analysis of Landsat multispectral scanner (MSS) imagery and concludes that many structural lineaments, running broadly NW–SE and WSW–ENE, can be recognized from physical features on the floodplain, and concludes these are small faults that can influence local migration of the channels. Seijmonsbergen (1999) further contends that width changes in the Jamuna may respond to these faults and they may also cause increased sedimentation upstream of the fault. For example, Seijmonsbergen (1999; figures 4 and 7) presents images to argue that a fault downstream of the Bangabandhu Multipurpose Bridge (see Section 20.7) has affected channel migration, although the channel behaviour does not appear to support this contention. The control of uplift and subsidence is, however, clear and Allison (1998), in a review of the geologic and environmental framework of the Ganges–Brahmaputra Delta, highlights the uplifted Pleistocene terraces of the Barind and Madhupur tracts (Figure 20.1) as being first-order controls on the courses of the Jamuna and Ganga Rivers. Barua (1994) also presents a synthesis of the major environmental controls on Bangladesh's river systems and, together with the major controlling factors of regional tectonics, geology, climate, sea-level rise and vegetation, highlights the controls by the 'fluvial loading' that is dictated by water and sediment discharge and sediment calibre. Grimaud et al. (2019) contend that Late Quaternary sediment dynamics indicate subsidence and sediment infilling of *c.* 0.8–2 mm yr^{-1} in the Teesta River megafan area at the foot of the Himalayas, and uplift and erosion in the Barind Tract region at rates of *c.* 0.03–0.11 mm yr^{-1} that allowed the development of mature soils (see Figure 20.1 for location of Teesta River and Barind Tract). This pattern of subsidence in the Teesta River region and uplift of the Barind Tract are argued to indicate the N–S flexural response of the Indian Plate to loading of the Himalayan Mountains (Grimaud et al. 2019). The consequence of this is contended to be abandonment of the Barind Tract by the Pleistocene Brahmaputra River (Grimaud et al. 2019). Reitz et al. (2015) studied the effects of sea-level and tectonic deformation on river path selection, and concluded that tilting due to variable subsidence in Bangladesh, in relation to the channel dynamics, should be sufficient to influence the course of the river. Grall et al. (2018) map subsidence rates over the delta and present a map illustrating the geomorphotectonic domains of the region (Figure 20.2), which can be split into two tectonic and two non-tectonic zones. The regions of tectonic dominance comprise the frontal part of the fold-belt and the Dauki fault system to the north of the region, which contains the northern part of the Jamuna River. The non-tectonic domains consist of the southern tidal region that is dominated by the backwater zone, and to the north a region that is fluvially dominated and encompasses the lower Jamuna River and its transition into the Padma River. These broad domains thus set the context for the behaviour of the river systems of Bangladesh and the relative importance of tectonic, sea-level and autocyclic fluvial controls, and indicate that in the lower Jamuna River autocyclic fluvial processes may be more important. Reitz et al. (2015) present estimates of the avulsion time scale for the Jamuna–Brahmaputra River, and found their modelled avulsion period of 2150 years matched well with that of 1800 years derived from stratigraphically based estimates derived from an array of core data, radiocarbon dating, and seismic profiles.

Deepening of the Bengal Basin has produced huge accumulations of sediment that have been fed from Himalayan erosion, with the thickness of sediment above the Precambrian basement increasing from a few hundred metres in the shelf region to over 18 km in the Bengal foredeep to the south (EGIS 1997). Krien et al. (2019) demonstrate that the influence of the underlying strong Indian craton and the weakened Indo-Burman margin results in significant amplification of the subsidence driven by sediment loading in the eastern part of the Ganges-Brahmaputra-Meghna Delta. Ongoing subsidence in the Bengal Basin, combined with high rates of Himalayan uplift, thus set the tectonic and climatic context for the large water and sediment discharges in the rivers of Bangladesh (Goodbred, Jr. and Kuehl 2000a, b). There is also evidence for a significant Late Quaternary climate signal superimposed on the structural control on sediment supply and channel belt migration (Heroy et al. 2003), and research has also indicated the generation and influence of glacial lake outburst palaeofloods (Montgomery et al.

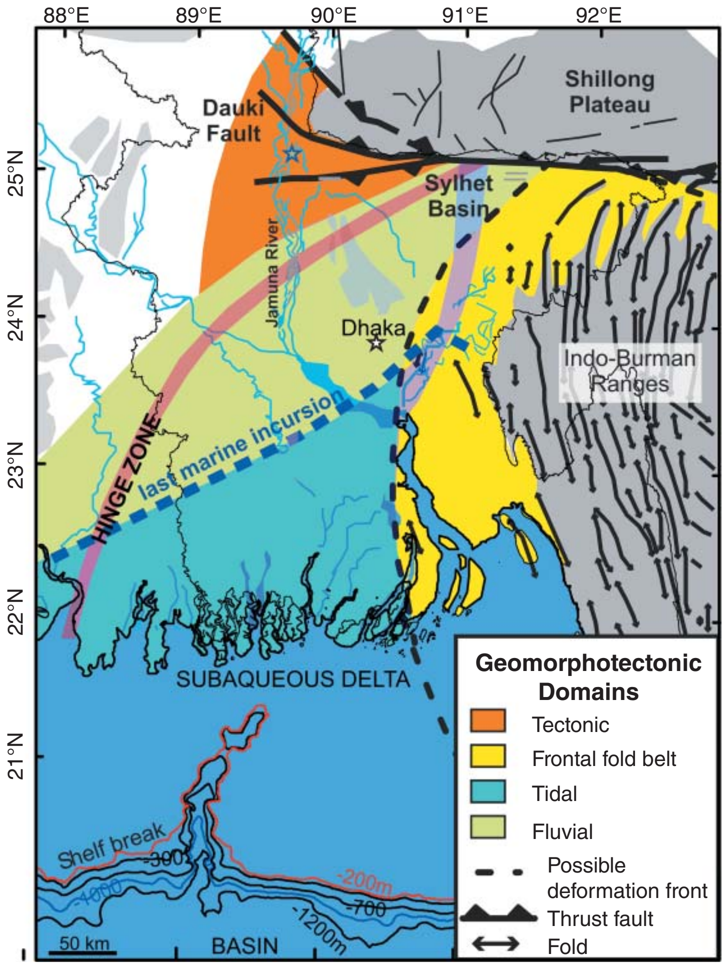

Figure 20.2 Geomorphotectonic domains of the Ganges–Brahmaputra–Meghna delta. The delta is overthrust by the Shillong Plateau and the Indo-Burman foldbelt to the north and east respectively. The edge of the Indian Craton, that is the inherited passive margin, is represented by the Hinge Zone. Two tectonic domains are present: (i) the frontal fold belt and (ii) the Dauki Fault system. The non-tectonic regions of the delta are represented by two domains: (i) the southern tidal domain, which corresponds to the backwater zone, and (ii) the fluvially-dominated domain. The boundary between these two domains is argued by Grall et al. (2018) to follow the maximum extent of the last marine transgression during the Holocene. Source: Modified from Grall et al. (2018).

2004; Pickering et al. 2019) that have been influential in erosion of the Yarlung Tsangpo Gorge (Lang et al. 2013; Huang et al. 2014; Liu et al. 2015). Montgomery et al. (2004) argue that at least two glacially dammed lakes immediately upstream of the Tsangpo River Gorge failed repeatedly throughout the Quaternary, with estimated peak flood discharges of $1\text{–}5 \times 10^6\ m^3\ s^{-1}$. Pickering et al. (2019) found that the base of the Brahmaputra River palaeovalley is >80 km in width and defined by a gravel unit (clasts up to 0.3 m in diameter) that is up to 10 m thick and was detected along a 255 km long seismic transect conducted along the Jamuna River (figure 3 in Pickering et al. 2019). This gravel was deposited between *c.* 9 and 30 ka by glacial-lake outburst floods that were up to *c.* 70 m deep and possessed estimated peak flow velocities of *c.* >3 m s^{-1} (Pickering et al. 2019). Because these outburst floods likely occurred in a period of weakened monsoon and reduced discharge, they were argued to have dominated flows during the late Pleistocene to early Holocene, and allowed exhumation of the flanks of the incising low-stand valley and transport of gravels across the floor of the Brahmaputra palaeovalley (Pickering et al. 2019).

Recent research using strontium as a provenance indicator (Goodbred et al. 2014; Sincavage et al. 2018) has also revealed more details on the Holocene evolution of the rivers of Bangladesh, and their role in constructing the Ganges Delta (Figure 20.3). These data show that the three great rivers of Bangladesh – the Ganga, Jamuna, and Meghna – remained isolated from each other and constrained within their own valleys until around the mid-Holocene (*c.* 7 ka; Figure 20.3a). After this time, and as sea-level continued to rise, the rivers had essentially filled up their palaeovalleys and were then free to avulse and migrate over a wider area: this resulted in numerous channel reorganizations from the mid-Holocene to present (Pickering et al. 2014; Goodbred et al. 2014; Figure 20.3a). These provenance studies also suggest that the basin hydrology may have provided a first-order control upon sedimentation, strongly modifying the potential influence of tectonic subsidence. Evolution of the drainage pathways of these rivers over time has also led to changing patterns of deposition within the Ganges Delta, and lithological and provenance studies have proposed various depocentres that have shifted in time as the rivers have changed course (Figure 20.3b). The nature of sea-level rise and patterns of basin subsidence, together with anthropogenic effects on Bangladesh's rivers such as flood control, water usage, coastal saltwater intrusion following groundwater abstraction and upstream water diversions, and population growth, will clearly take on great importance in the next decades (Grall et al. 2018), especially as the accelerated impact of global climate change starts to bite (Begum and Fleming 1997a, b; Choudhury et al. 1997; Mirza et al. 2001; Mirza 2002; Brammer 2014).

20.1.3 Hydrology, Sediment Yield, and Channel Size

The Ganga and Jamuna rivers are sourced in the Himalayan range, whilst the Meghna River rises in the Sylhet Trough. The Jamuna River has a catchment area of ~560 000 km^2 that receives an average of 1.9 m rainfall yr^{-1} (FAP24 1996a; Sarker and Thorne 2006), with approximately 8.1% of the drainage basin area being within Bangladesh (Ojha and Singh 2004). The rise in the hydrograph of the Jamuna River begins due to Himalayan snowmelt in May, but the hydrograph is dominated by monsoon rainfall, and shows a broad peak between July and September (Figure 20.4; Singh 2007). At Bahadurabad (Figure 20.1), the mean annual discharge is 20 200 $m^3 s^{-1}$, varying from a minimum dry season flow of ~2860 to 100 000 $m^3 s^{-1}$ in the disastrous 1988 flood (EGIS 1997), and a record 102 500 $m^3 s^{-1}$ in the 1998 flood (Chowdhury 2000) that inundated nearly 70% of Bangladesh and affected over 30 million people (Rao et al. 2020). Bankfull discharge is difficult to estimate because the channel bank edge and overbank level are ill-defined, but estimates range from 45 000 to 60 000 $m^3 s^{-1}$ (FAP24 1996e; Thorne et al. 1993). The annual hydrograph shows a yearly change in water stage of ~6 m (FAP24 1996a). The average water slope of the Jamuna is 0.000 076 (76 mm km^{-1}) over the first 130 km and 0.000 065 (65 mm km^{-1}) further downstream (FAP24 1996b). Flow velocities within the main channels are of concern in design considerations and depth-averaged velocities may reach over 3.5 m s^{-1} (FAP24 1996c).

The Jamuna is predominantly a braided river (Ashworth and Lewin 2012), with some anastomosed regions (cf. Sarker and Thorne 2006, their figure 13) and possesses an average braidplain width of 11 km, flow depth of ~5 m

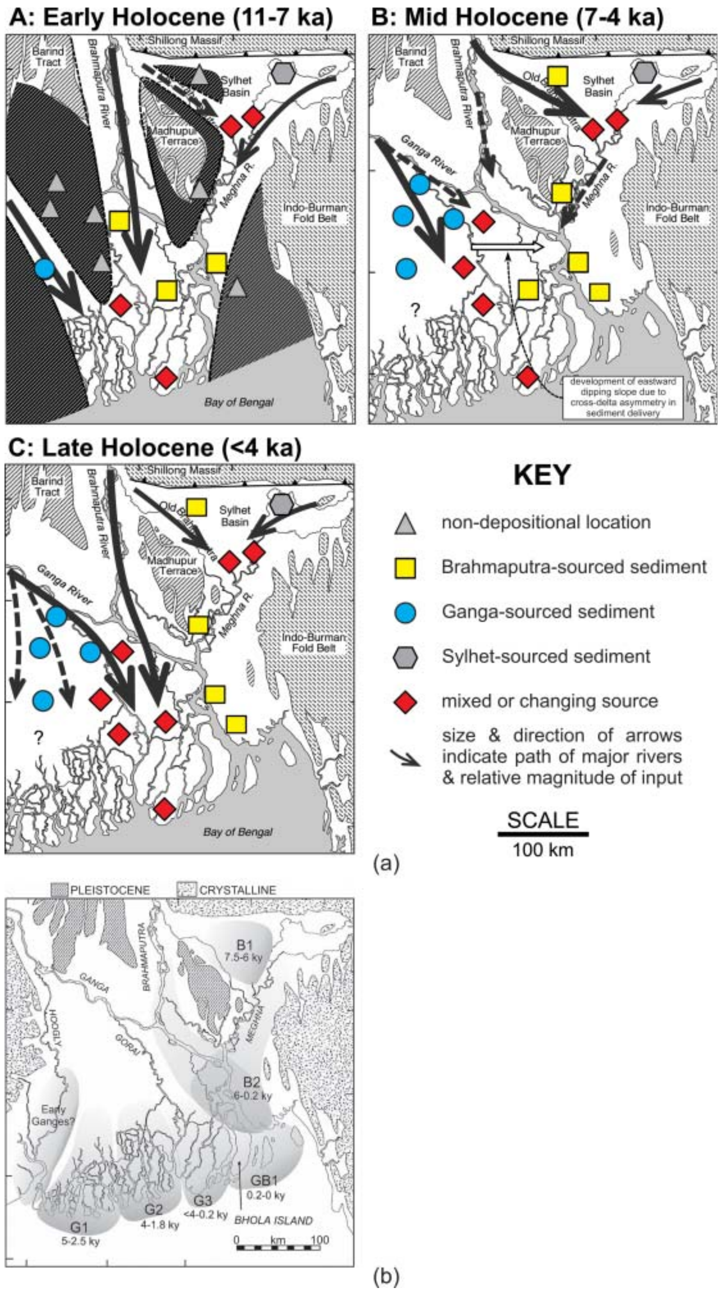

Figure 20.3 (a) Reconstruction of the principal river pathways and patterns of sediment distribution associated with the Ganga, Brahmaputra (Jamuna), and Sylhet sources through the Holocene. A: In the Early Holocene, rivers are constrained within their lowstand valleys, and there is limited influence of the Brahmaputra River in the Sylhet basin. B: In the Mid-Holocene, slower sea-level rise allows rivers to infill their valleys, which subsequently become more mobile across the delta. C: By the Late Holocene, the principal rivers interact on the central delta plain, shifting toward the present-day confluence and the estuary that receives discharge from all the rivers. Source: Modified from Goodbred et al. (2014).
(b) Palaeogeographic reconstruction of the timing and location of river channel change and associated delta lobes during the Middle-Late Holocene. The delta lobes are associated with the Ganga (G1, G2, G3), Brahmaputra (B1, B2) and combined Ganga–Brahmaputra (GB1) river sources. Source: Modified from Akter et al. (2016).

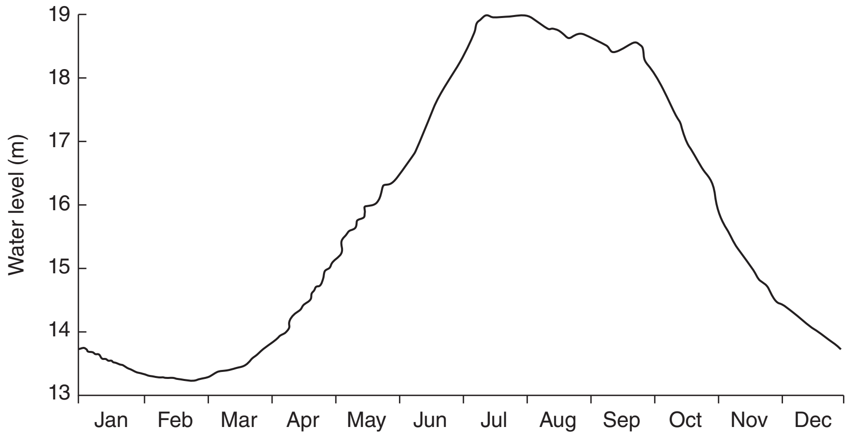

Figure 20.4 The stage-hydrograph of the Jamuna River at Bahadurabad (see Figure 20.1 for location), averaged over a 30-year period. Level is expressed relative to a standard low-water datum derived from long-term records. Source: From Sarker and Thorne (2006). © 2009, John Wiley & Sons.

and a Brice braiding index of 4–6 (FAP24 1996a). Sarker and Thorne (2006) show that when slope is plotted against discharge on the classic empirical channel pattern discrimination diagram proposed for smaller rivers by Leopold and Wolman (1957), the Jamuna, Padma, and Meghna plot in the meandering field, highlighting the controls on channel planform are more complex than solely slope and discharge. The physics-based formula for the transition between meandering and braiding proposed by Crosato and Mosselman (2009) predicts the Jamuna River to be braided. The number of major channels in the braidbelt varies between three in the upper reaches and two in the lower reaches, with the planform being dominated by a range of vegetated and non-vegetated bars that divide the channel into a hierarchy of channel sizes (Bristow 1987). Moreover, the river occupies a large width partly because it is anabranched, which is common for alluvial rivers with mean annual discharges greater than ~17 000 $m^3 s^{-1}$ (Latrubesse 2008). The grain size of the Jamuna River shows a slight fining from north to south, with the median bed material grain size being 260 μm near the Indian border and 165 μm near Aricha (FAP24 1996a), with an average of 220 μm (Barua 1994; Sarker and Thorne 2006). Most of the sediment is fine sand and silt with less than 1% clay (FAP24 1996h). The fine and abundant sediment supply result in sediment transport occurring throughout the year and this, together with high water discharges, gives rise to the massive sediment yields from the Jamuna River, with estimates being of 555 $Mt\,yr^{-1}$ (Coleman 1969), 590 $Mt\,yr^{-1}$ (FAP24 1996a), 792 $Mt\,yr^{-1}$ (Islam et al. 1999), 615 $Mt\,yr^{-1}$ (see summary figure 7 in Rahman et al. 2018) and 1157 $Mt\,yr^{1}$ (see table II in Islam et al. 1999). Various estimates of the percentage of the total load transported as bedload have been proposed, with values between 10% (Islam et al. 1999) and ~30% of the total sediment load as bed material (Sarker et al. 2003). Recent work (Rahman et al. 2018) has also suggested the total load of the Jamuna River may be decreasing by *c.* 6 $Mt\,yr^{-1}$, with the Ganga River decreasing by *c.* 4 $Mt\,yr^{-1}$. This represents a *c.* 10 $Mt\,yr^{-1}$ reduction in sediment supply to the Bay of Bengal, which may have significant implications in future, although it is clear that higher fidelity data are required to test this contention.

20.2 Channel Scale Morphology and Recent Historical Changes in the Course of the Brahmaputra–Jamuna River

The course of the Brahmaputra–Jamuna River has changed dramatically over the past 250 years, with evidence of both large-scale avulsion in the period 1765–1860 (Figure 20.5a) and a predominantly westward migration of the Jamuna channel belt (Figure 20.5b). Avulsion of the Brahmaputra River, and formation of the new Jamuna River, has been described by Bristow (1999) and recently by Bandyopadhyay et al. (2021), who provide new cartographic evidence for the likely date and trigger for the change in channel belt

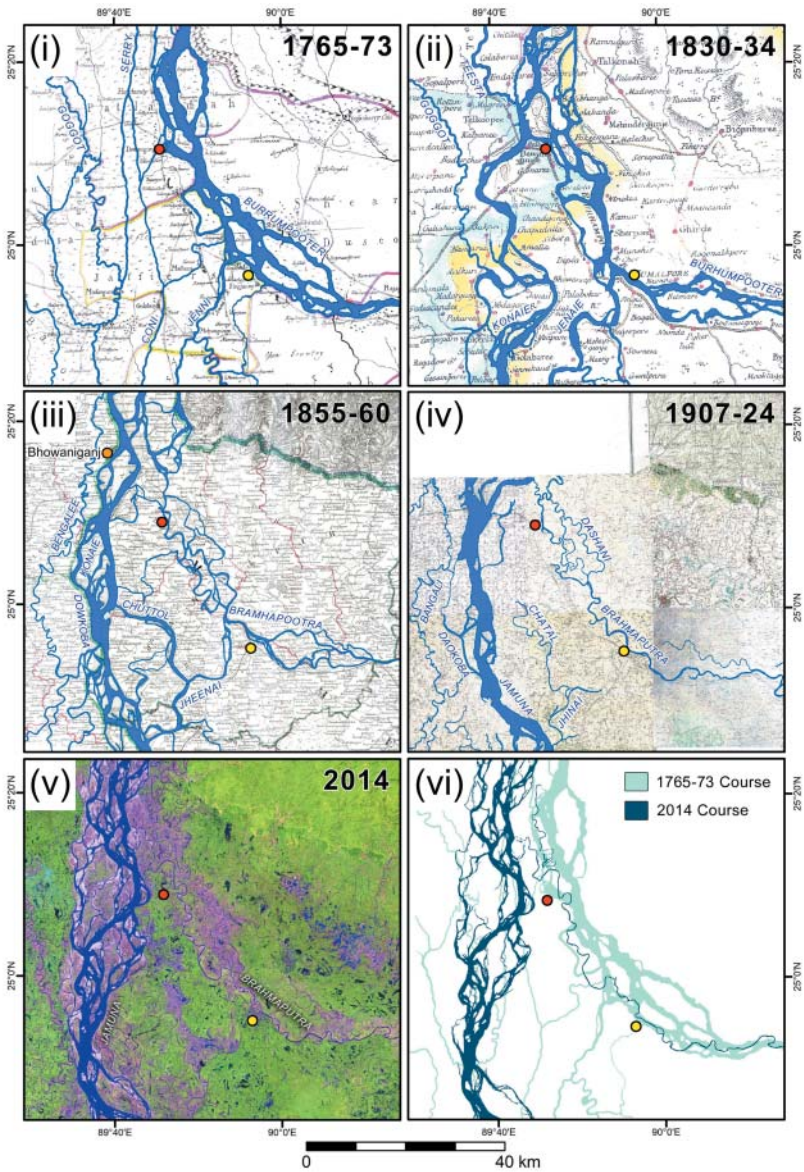

(a)

Figure 20.5 (a) Maps showing the avulsion of the Brahmaputra River into the contemporary course of the Jamuna. These maps illustrate the reduction in flow in the Brahmaputra River (Burrumpooter in (i), now called the Old Brahmaputra) and gradual establishment of an independent Jamuna braidbelt, with flow initially being diverted down the channels of the Konaie and Jenaie rivers (ii, iii). The avulsion was largely complete by 1855–60 (iii). The red and yellow dots show positions of the towns of Dewanganj and Jamalpur, respectively. Source: Modified from Bandyopadhyay et al. (2021). (b) Historical changes in the position of the bankline of the Jamuna River. Source: Based on EGIS (1997).

Figure 20.5 (*Continued*)

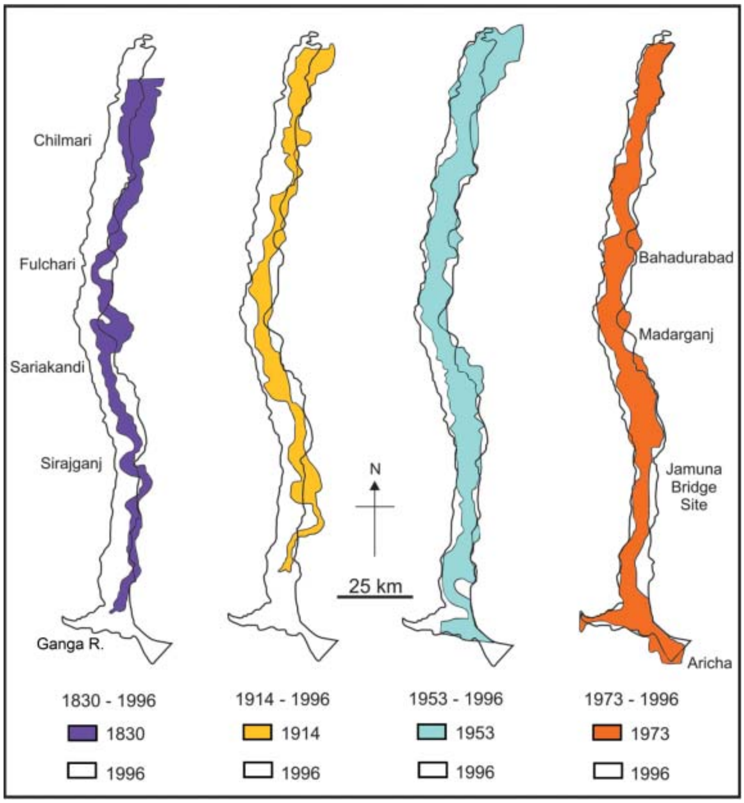

(b)

location. Prior to *c.* 1765, the Brahmaputra flowed within the channel now termed the 'old Brahmaputra' (Figures 20.1 and 20.5a(i)), east of the Madhupur Tract, and joined the Meghna River. The avulsion was initiated sometime between 1765 and 1809 (Bandyopadhyay et al. 2021), with flow occupying the channels of the Konaie and Jenaie rivers (Figure 20.5a(ii)) and eventually leading to a maximum lateral shift in the river course of ~80km, from the east to the west of the Madhupur Tract (Figures 20.1 and 20.6). Studies have suggested a number of reasons for the avulsion, including tectonic activity (Winkley et al. 1994), switches in the upstream course of the Teesta River as it avulsed into the Jamuna River in *c.* 1787 (Morgan and McIntire 1959; Bandyopadhyay et al. 2021), the influence of increased discharge (Coleman 1969), catastrophic floods (La Touche 1910; Bandyopadhyay et al., 2021), and river capture into an old river course (Bristow 1999; Bandyopadhyay et al. 2021). Both Bristow (1999) and Bandyopadhyay et al. (2021) conclude that the avulsion was more likely gradual than catastrophic, and may have been generated by outer (right) bank erosion, perhaps enhanced by flow forced around a large mid-channel bar(s), causing diversion of the channel into existing floodplain channels (Konaie and Jenaie rivers; Figures 20.5a(ii) and 20.6). Bandyopadhyay et al. (2021) argue that westward migration of the Brahmaputra was sufficient to eventually connect to the Konaie channel that led to the avulsion, without the need for avulsion of the upstream Teesta River, but that this erosion may have been hastened by the long duration floods of August 1787. The map of Rennell (1776) clearly shows a sequence of large bars near the offtake of what is now the Jamuna River (Figures 20.5a(i,ii); 20.6a,b,

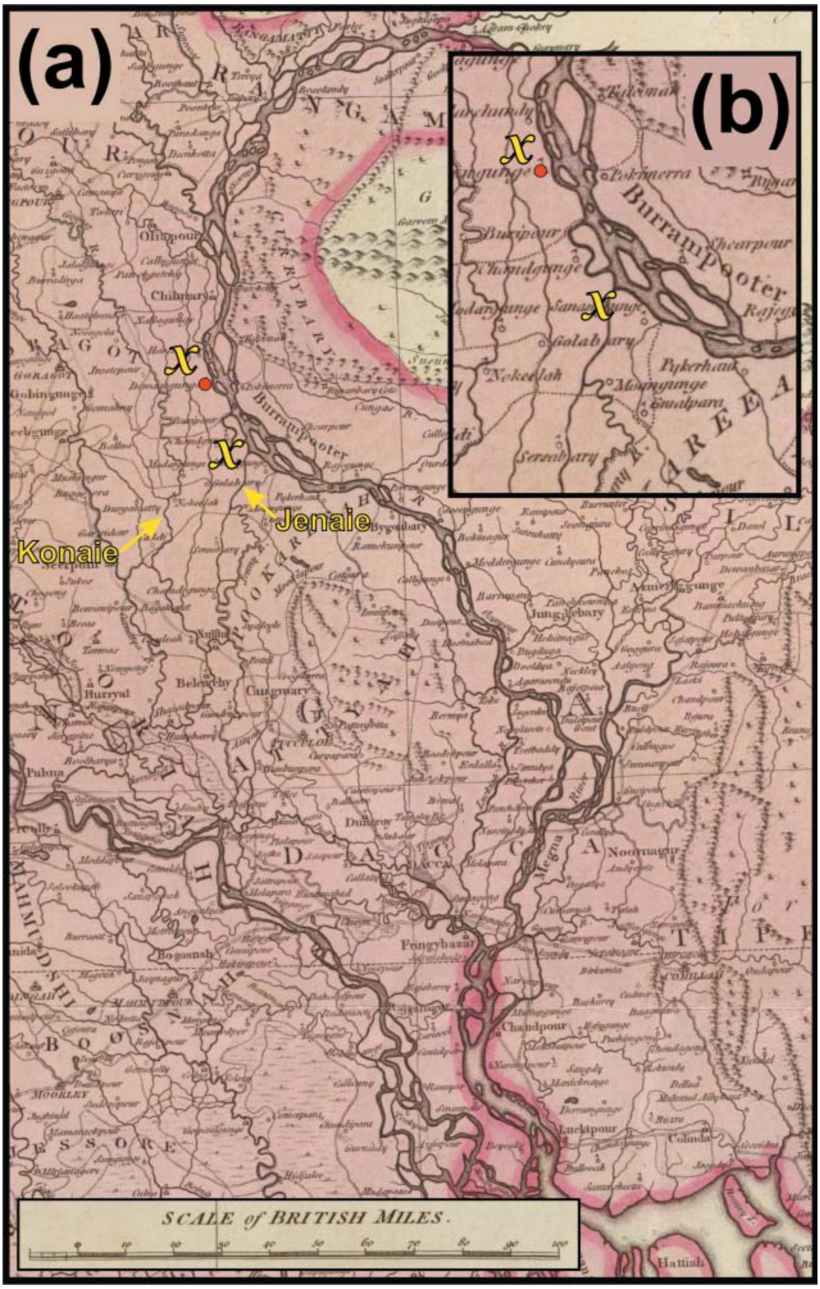

Figure 20.6 (a) Reproduction of part of Rennell's (1776) map illustrating the course of the Old Brahmaputra (Burrampooter) and the course the Jamuna River was to adopt after its avulsion. The red dot shows the position of Dewanganj (see also Figure 20.5a). Source: David Rumsey Map Collection, www.davidrumsey.com. (b) Close up of the region of the avulsion (labelled 'x' in a and b). Note the large bars formed at these locations and the scallops of outer (right) bank erosion that appear in this region. Also compare this map with the image shown in Figure 20.1, and how the course of the Ganga changed after avulsion of the Brahmaputra River. Today the Ganga and Jamuna rivers combine to form the Padma River, which then joins the Meghna River to form one major channel exiting into the Ganges delta (Figure 20.1). In the map of Rennell (1776), the Ganga and Brahmaputra/Meghna rivers form two separate channels flowing through the Ganges delta.

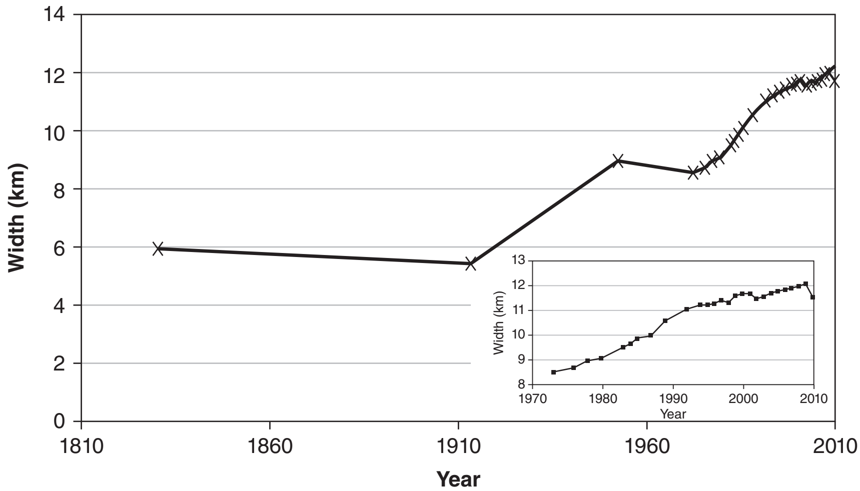

Figure 20.7 Trends in the mean width of the Jamuna River 1830–2010. Inset shows detail from 1970–2010. Source: Modified from Sarker et al. (2014).

label x) and a series of outer bank scallops suggesting local diversion of flow against the banks, which can generate significant lateral bank retreat (Ashworth et al. 2000). Significant flow may have been previously diverted down the future Jamuna offtakes, since the right (west) bank at this point shows two large embayments that would funnel water down the offtakes (Figure 20.6b, label x). The avulsion eventually shortened the course of the river into the Bay of Bengal by *c.* 46km compared to its course through the old Brahmaputra (Bandyopadhyay et al. 2021), and led to a dramatic reorganization of the braid belt (Figure 20.5a(vi)).

Several authors have also described the gradual westward migration of the Jamuna braidbelt (Coleman 1969; Sarker 1996; Khan and Islam 2003) and noted that the braidbelt has widened since the early twentieth century (FAP24 1996c; Sarker 1996; EGIS 1997, their figures 3 and 5). Even given the inherent uncertainties when using old maps to provide quantitative estimates of channel size, the trends in the mean braidplain width for the Jamuna (Figure 20.7) show a significant increase, although the rate of widening decreased from 152 m yr^{-1} between 1973 and 1992, to 20 m yr^{-1} between 1992 and 2010 (EGIS 1997; Sarker and Thorne 2006; Sarker et al. 2014). The rate of widening averaged ~50 m yr^{-1} over the period 1834–1992 (FAP24 1996a), but with significant fluctuations in average rate up to ~170 m yr^{-1} (FAP24 1996a; Khan and Islam 2003), and with *local* erosion rates reaching up to 1 km yr^{-1}. ISPAN (1993) estimated that the length-averaged width of the Jamuna River in 1914 was 5.5 km, which is close to that found in the 1830 map. Later, the width of the river in the 1940s (Coleman 1969) was found to be much higher, with the length-averaged width being ~9 km in 1952 (ISPAN 1993) and, except for the lower reach, braiding was the predominant planform along almost the entire Jamuna River. The development of a braided channel was especially rapid in the period between the maps of 1914 and 1953, with the period between 1830 and 1914 being marked by a reduction in meander amplitude but a westward migration of the river (FAP24 1996c).

River erosion consumes *c.* 2000–5000 ha of mainland floodplain annually, making many tens of thousands of people landless or homeless (Sarker et al. 2014). Sarker et al. (2003) showed that in the period 1984–1992, the Jamuna River eroded 40 000 ha of floodplain but only accreted around 1400 ha. Schmuck-Widmann (2001) reports that some 2.3 million people live on the river islands, or 'chars', with Sarker et al. (2003) placing this number at 600 000, and whose income is reliant on agriculture supplemented by animal husbandry, small businesses, and fishing (Schmuck-Widmann 2001). However, the changing size of these chars due to erosion creates an internally displaced population over periods of years to decades, with estimates of annual population displacement in Bangladesh due to riverbank erosion being *c.* 200 000 people (Sarker et al. 2019). This displaced population faces huge challenges in terms of economic welfare, security, access to food and health services, and issues of mental health, with older people, women, and children being the most vulnerable (Islam and Rashid 2011; Islam et al. 2014; Sarker et al. 2019).

Coleman (1969) related the westward channel migration to uplift of the Madhupur Tract Pleistocene sediment, an argument that has found support from ISPAN (1993), Thorne et al. (1993), and Sarker (1996), although Burger et al. (1988) have rejected this contention. The debate concerning the westward migration of the Jamuna River emerged from the outward movement of both banks of the Jamuna River since the 1970s. During 1973–1992, the rate of eastward migration of the left bank was 79 m yr^{-1} whilst the westward migration of the right bank was 68 m yr^{-1}. This persistent high outward migration rate of both banks caused the apparent eastward migration of the centreline during these two decades, and probably led to the debate concerning the westward migration of the river. However, since the beginning of the 1990s, the eastward migration of the left bank has been greatly reduced to 16 m yr^{-1} and the westward migration of the right bank has been slightly reduced to 44 m yr^{-1}, thus causing the centreline of the Jamuna River to migrate westward (EGIS 1997). These observations indicate that apparently the 'nil or eastward' migration of the centreline of the Jamuna River during 1973–1992 was probably for a short period and related to the very high widening phase of the river. Such westerly migration may be a product of braidplain widening as the channel adapts to its new post-avulsion course, or a response to underlying tectonic control (Morgan and McIntire 1959). Thorne et al. (1993) also linked the location of erosion to the development of bankline curvature in the large-scale planform of the Jamuna and suggested this erosion on the outside of 'large scale meanders' in the braidplain may be used to predict future sites and rates of bank erosion.

The planform analysis of the Jamuna River performed by EGIS (1997, 2000), using time-series satellite images, shows the width (Figure 20.5b) and braiding intensity of the Jamuna River to be changing spatially and temporally, with Klaassen and Vermeer (1988) also documenting changes in the braiding intensity. Brammer (1995, 2012), Goodbred, Jr. et al. (2003), and later Sarker (2009), Sarker and Thorne (2006), and Sarker et al. (2014) have related these changes in morphological and planform parameters, including the braiding intensity in the Jamuna, Padma, and Lower Meghna Rivers, to the propagation of a sediment wave or 'slug' generated from the 15 August 1950 Assam earthquake that had a magnitude, M_w, of 8.6. Sarker and Thorne (2006) divided the Jamuna River into two halves and presented changes in width and braiding intensity for the upstream and downstream reaches (Sarker and Thorne 2006, their figures 6 and 8a). Three points are worthy of note from these studies concerning the braiding intensity of the Jamuna River:

(1) The braiding intensity is less in the downstream reaches of the Jamuna River than in the upstream reaches, possibly in response to a downstream decrease in slope (Klaassen and Vermeer 1988).
(2) The braiding intensity in the upstream reaches of the Jamuna River increased after 1973, but started to decrease from the early 1990s.

(3) In the downstream reaches of the Jamuna River, the braiding intensity decreased in the 1970s, but then increased through the 1980s up to the first half of 1990s. The braiding intensity started to decrease in the downstream reaches of the Jamuna from the mid-1990s.

The rapid increases in channel width and floodplain erosion observed in the Jamuna River during the 1970s and 1980s were argued to have resulted from the arrival of the trailing edge of the sediment wave (Sarker et al. 2014). The fine fraction of the sediment input from the Assam earthquake was suggested to have passed through the fluvial system relatively quickly, but the coarser sand fraction was proposed to have taken approximately 50 years to reach the Bay of Bengal (Sarker and Thorne 2006; Sarker 2009; Sarker et al. 2014). These contentions allowed Sarker et al. (2014) to propose a schematic representation of river response (Figure 20.8) to the forcing variables of avulsion, tectonics, earthquake-induced sediment supply and anthropogenic factors. Avulsion of the river into its new course from the old Brahmaputra was a strong driver of channel change in the Jamuna River in the nineteenth and early twentieth centuries but has now diminished, and recent work suggests that the influence of tectonics may be small compared to other driving factors such as hydrology (Goodbred et al. 2014). Sarker et al. (2014) contend that the influence of the sediment wave generated by the 1950 Assam earthquake had its maximum influence on river morphology in the 1980s, and overwhelmed the westward migration of the braidplain that had prevailed for the previous 150 years. Sarker et al. (2011) and Akter et al. (2016) also suggest that the sediment produced by the 1950 Assam earthquake subsequently led to a period of high net accretion in parts of the Meghna Estuary. Sarker et al. (2011) contend there were two phases of accretion linked to the sediment wave: the first characterized by rapid accretion due to the accumulation of fine silts and clays immediately after the earthquake and that lasted until the early 1970s, and a second phase in the mid-1980s to 1990s due to the arrival of the coarser sediment wave. Lastly, Sarker et al. (2014) indicate that human interventions, such as engineered embankments, hard points, bridges, and guide bunds, will likely have an increasing future effect on morphological change.

However, whilst accepting as indisputable that the sediment wave generated by the 1950 Assam earthquake had significant morphological consequences, RBIP (2015) contend other mechanisms can also explain recent river channel change. In addition to the adjustments in width of the Jamuna River linked to (i) its continuing adjustment to its avulsion from the Old Brahmaputra (Sarker et al. 2014), (ii) the influence of bank protection works (Sarker et al. 2014), and (iii) adjustments due to the arrival of the Teesta River that avulsed from being a Ganga River tributary to becoming confluent with the Brahmaputra River sometime between 1843 and 1868 (Bristow 1999), RBIP (2015) argue that hydrologic variability was likely key in generating river widening. Although recognizing that the annual peak flow has not increased significantly through time, RBIP (2015) argue that the actual peak flows have oscillated in time, with particularly large flood peaks in 1974, 1988, and 1998. Data show that the period between the 1970s and late 1990s (and especially the mid-1980s to late 1990s) had higher peak flows than the periods on either side of this time. RBIP (2015) contend that the period of most rapid morphological change, and critically widening that influenced the entire length of the Jamuna River and the upstream Brahmaputra River in Assam between 1972 and 1989, corresponded with a period of very high flow, and that the beginning of satellite coverage and measurements began in the relatively dry period (1970s) before this period of higher peak flows.

Using satellite images from 1967–2002, Takagi et al. (2007) showed that the temporal

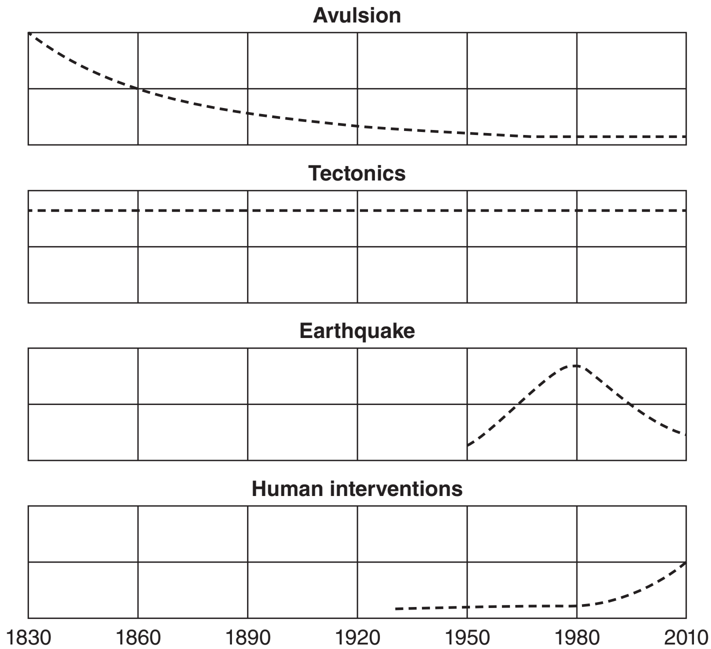

Figure 20.8 A schematic representation of the influence of different forcing variables of morphological change in the Jamuna River (Sarker et al. 2014). Avulsion, after shifting from the course of the Old Brahmaputra, was a strong driver during the nineteenth and early twentieth centuries, but has now diminished. Tectonics will continue to influence channel behavior, but is likely a second order driver of decadal-century scale river channel change. The sediment pulse generated by the 1950 Assam earthquake was an important driver during the second half of the twentieth century, although its influence has now diminished as the sediment pulse has reached the Bay of Bengal. Anthropogenic interventions have grown in their influence since the 1980s. Source: Modified from Sarker et al. (2014).

change in river activity and dynamics may fall into four distinct phases associated with alternating periods of quasi-dynamic equilibrium and more complex conditions. The transition between phases, such as the widening of the channel during the mid-1980s to early 1990s, may have been triggered by significant and frequent flooding events, such as the huge 1987 and 1988 floods. This contention also supports the significance of hydrological variability suggested by RBIP (2015), although this issue still requires further research.

Sarker (1996) and Bristow (1999) noted that the initial planform of the Jamuna after the 1770–1830 avulsion was meandering with a dominantly braided planform in its upstream reaches, and that a fully braided planform has only developed since then. Coleman (1969) surmised that, with the increase in discharge generated by the joining of the Teesta River, the Jamuna started to braid. The date at which, and if, the Teesta River joined the Jamuna is unclear, with Morgan and McIntire (1959) stating this was contemporary with the avulsion of the Brahmaputra River. However, the absence of the Teesta River in the 1828 map of Wilcox makes this uncertain, and only in the map of 1860 is the Teesta River found as a tributary of the Jamuna River. However, maps of 1860 and 1914 show that the planform of the Jamuna River was predominantly meandering, with the presence of a braided planform in some upstream reaches. Coleman (1969) recognized three nodal points along the banks of the Jamuna River, one downstream of Bahadurabad, another near Sirajganj, and the third upstream of Aricha (Figure 20.1). In these areas, which have remained fixed for long periods of time, the river is relatively narrow and deep, and it has been proposed that cohesive clays, together with the slightly more resistant natural levee, do not allow the river to migrate freely here as in other areas (Coleman 1969). Klaassen and Masselink (1992), however, rejected the existence of such nodal points. Thorne et al. (1993) also considered the composition of the bank materials along the Jamuna River to be uniform and that the banks are formed in weakly cohesive silty-sand, which is highly susceptible to erosion. However, they also state that clay deposits exist along the right bank at Sariakandi, 40 km upstream of Sirajganj (Figure 20.1), and in the left bank at Bhuapur opposite Sirajganj, although these locations are not the same as mentioned by Coleman (1969). An analysis of the banklines derived from satellite images over the past three decades suggests the existence of non-erodible bank materials in the left bank around Aricha, which corresponds with the location of the most downstream nodal point identified by Coleman (1969). Except for this location, the characteristics of the bank materials along the Jamuna River appear largely invariant.

A slight deviation from this homogeneity in bank erodibility was observed by EGIS (2002), who report that the erosion rate was higher along bends on the left bank than along right bank bends with similar geometrical characteristics. This feature was attributed to the westward migration of the Jamuna River, which leaves relatively unconsolidated bank materials along its left bank. Analysis of high-resolution satellite images and aerial photographs shows the scars of recent channels on the eastern bank of the Jamuna River, the size of which is comparable with the active channels along this bank. However, such scars are not visible along the western right bank, thus supporting the contention that the river has migrated westwards. At present, the floodplains being eroded by the Jamuna River along its left (eastern) bank are newly formed, unconsolidated sediments, whilst those being eroded along its western, right bank comprise relatively old and consolidated floodplains. These consolidated floodplains are more resistant to erosion, and are also more fertile and productive than the unconsolidated and newly accreted floodplains along the left bank.

Recent studies have also illustrated the great potential of using remote sensing to examine large-scale bankline change within the Jamuna River. Baki and Gan (2012) used Landsat imagery between 1973 and 2003 and showed that the right bank underwent more erosion than the left bank, with the average erosion rate for short- and long-term analysis of the river being 207 and 83 $m\,yr^{-1}$, respectively. They also found that smaller river chars (<50 ha) tended to be very unstable whereas islands larger than *c.* 150 ha tended to be more stable. Bhuiyan et al. (2015) examined images of the lower Jamuna River from 1973–2011 and found two main periods of bankline adjustment: one from 1972–1992, where channel planform changes were irregular, and a second phase between 1992 and 2011 where the channel change was unidirectional and to the east. The second phase was characterized by an average migration rate of 225 $m\,yr^{-1}$ that was three times the rate of the first phase. Bhuiyan et al. (2015) also suggest the influence of river training works on the channel, in that downstream of the Bangabandhu Bridge (see Section 20.7) the river was widening and shifting eastwards, whereas upstream of the bridge a westward migration was occurring.

20.3 Bedform Types and Dynamics

Sediment within the Jamuna River is carried as bed, suspended and wash load, with most of the sediment being carried within the water column (Klaassen et al. 1988). However, the bedload, although only ~10% of the total sediment load, is critical in generating a wide array of bedforms of different scale that drive channel change and migration. Bedload transport occurs at all flow stages in the Jamuna and the role of high-stage flood flow and subsequent reworking, or modification, of the high-stage deposits becomes significant on the falling limb of the flood hydrograph. The synthesis presented herein splits bedforms into two scales: (i) small-scale bedforms that are a small fraction of the flow depth (ripples, upper-stage plane beds) or generally scale with flow depth [dunes, this also including the 'megaripples' of Coleman (1969)] and (ii) bedforms that scale with the channel width and are usually a significant fraction of the flow depth (various types of bars). Figure 20.9 shows some examples of these bedforms and their sedimentary structures.

20.3.1 Small-Scale Bedforms (Ripples, Dunes, and Upper-Stage Plane Beds)

Sand dunes are the predominant smaller-scale bedform within the Jamuna River at all flow stages and in all parts of the channel (FAP24 1996g; Roden 1998); they thus form the nucleus of many larger scale bars (see below) and are a key component of the sedimentary facies (Best et al. 2003). Surveys over a two-year period at Bahadurabad and Sirajganj (Figure 20.10) show that over 40% of the bed is occupied by dunes at any flow stage, and this figure may rise to nearly 100% (Roden 1998). Ripples and smaller dunes are commonly superimposed on larger dunes, but upper-stage plane beds are rare and largely restricted to fast, shallow flows on bar-tops. Dune height and wavelength, plotted from a database of 1400 measurements at three sites (Figure 20.11a,b), range from 0.10 to 6 m (Figure 20.11a–c) and 2 to 331 m respectively. Both distributions are log-normal and the form index of the dunes (height/wavelength) ranges from 0.0005 to 0.27 (Figure 20.11c). The leeside slope angle of these dunes (Figure 20.11d) shows a wide spread from 1° to 58° (steeper than the angle-of-repose probably due to intense eddying in the leeside), with a mean of 8.4°. This demonstrates that many dunes do not possess an angle-of-repose leeside and may be of a form that does not generate permanent flow separation in the leeside, as has been demonstrated in other large rivers (Smith and McLean 1977; Kostaschuk and Villard 1996; Ten Brinke et al. 1999; Best et al. 2001; Best and Kostaschuk 2002; Cisneros et al. 2020). This finding is of considerable importance in considerations of dune form factor and estimates of flow resistance in alluvial channels, since previous work (Ogink 1988) has demonstrated that a considerable reduction in roughness height is present for low-angle dunes due to the lesser effects, or even absence, of permanent flow separation in the dune leeside (Best and Kostaschuk 2002). A plot of the form index of dunes (Figure 20.12) as a function of leeside slope shows the form index is lower at lower leeside slopes: for the average slope of 8.4°, the contribution to the form roughness would decrease to ∼45% of the value for an angle-of-repose dune, whereas for a leeside slope of 4.5° this decrease would be to ∼10% (see figure 4.1 in FAP24 1996c). These figures thus demonstrate that the contribution of dune-related roughness to total roughness may be much smaller than considerations based solely on dune height (FAP24 1996c; Cisneros et al. 2020), a conclusion also reached by Klaassen et al. (1988). Additionally, these data suggest that the shape of the dune must be quantified accurately if bedform tracking is to be used as a method for estimating bedload transport (FAP24 1996g). Ideally this should include quantification of both the dune profile and three-dimensional planform morphology, as available from side-scan sonar (Figure 20.13) and multibeam echo sounding (Parsons et al. 2005; Sambrook Smith et al. 2019; Cisneros et al. 2020).

Plots of dune height and wavelength against flow depth (Figure 20.14) show a wide scatter but illustrate that maximum dune height approximates 0.25–0.33 of the flow depth, and that dune wavelength is generally less than seven times the flow depth (Julien and Klaassen 1995). The scaling of maximum

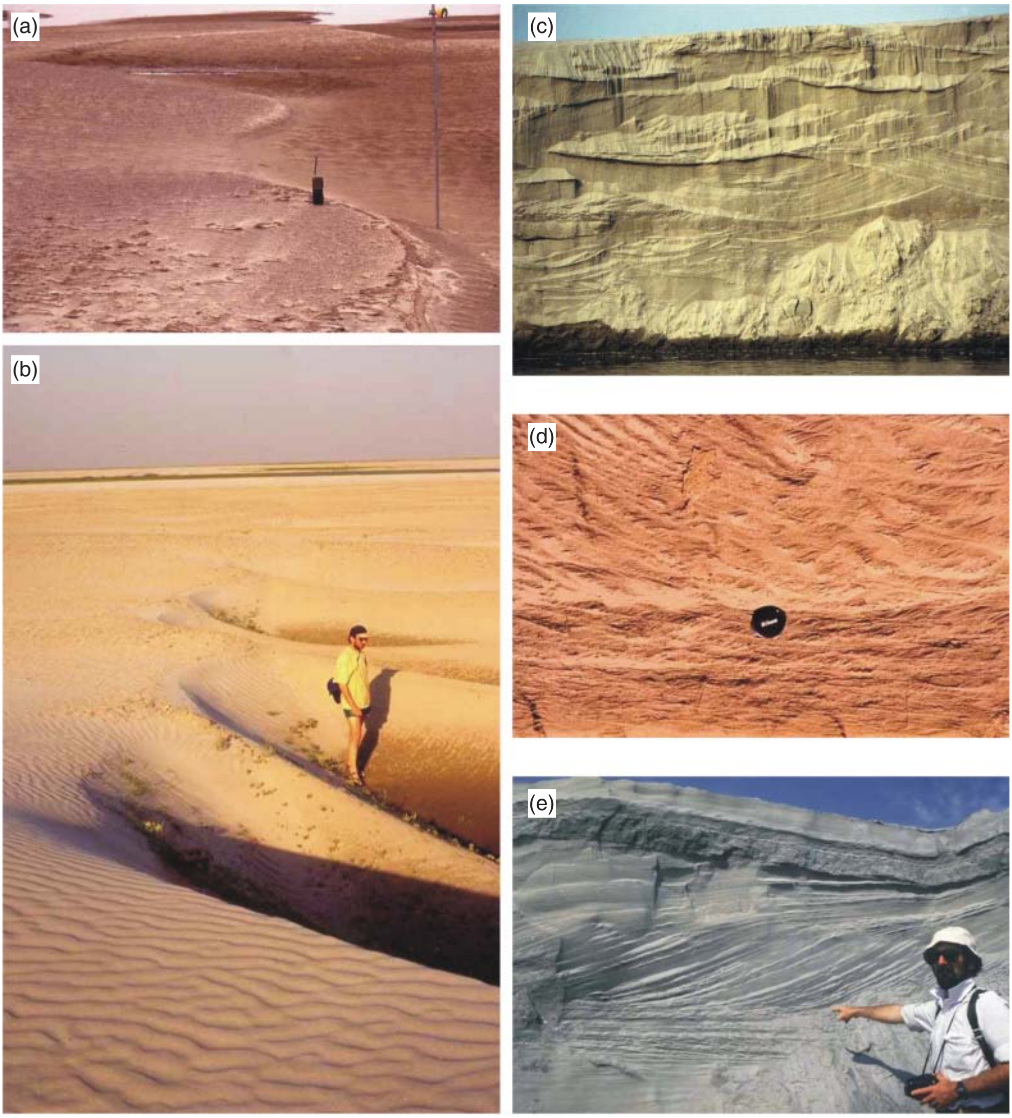

Figure 20.9 Examples of different bedforms and sedimentary structures found within the Jamuna River. (a) Small-scale (up to 0.3 m high) three-dimensional dunes; (b) large-scale (up to 3 m high) dunes; (c) dune trough cross-stratification in a 4 m high cutbank; (d) climbing ripples; and (e) topset, foreset and bottomset preserved in a sand dune in the transitional regime to upper-stage plane beds; the topsets consist of upper stage plane-beds, whilst the toesets contain counter-current ripples, with current ripples overlying upper-stage plane bed laminae. Source: Panel (e) reprinted from Bristow (1993a), with permission from the Geological Society of London.

dune height with flow depth fits well with past work (Jackson 1976; Best 1996), with the smaller dunes either being present under non-equilibrium conditions or growing in response to the boundary layer thickness developed by larger dunes or bars. The planform of the dunes is often both two- and three-dimensional (Figure 20.13). Dune superimposition is ubiquitous, with the height of the secondary dunes generally becoming larger

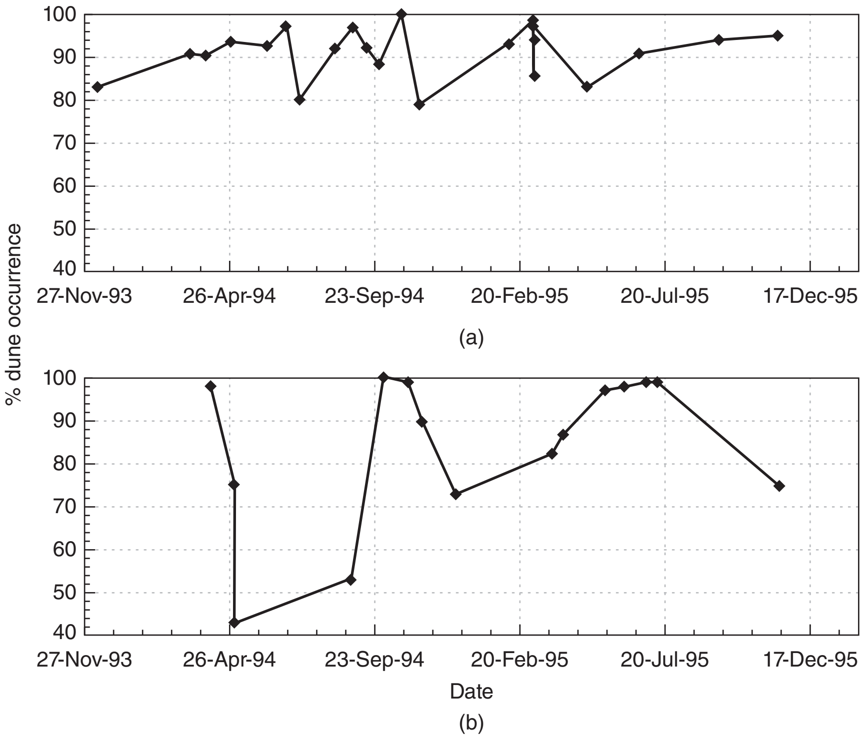

Figure 20.10 Percentage occurrence of dunes in the main channels of the Jamuna River at (a) Bahadurabad and (b) Siraganj, November 1993–December 1995. Source: Based on FAP24 (1996g).

with the size of the primary dune (Figure 20.15) and showing superimposition on the stoss side, shoulder, and leeside of the primary dunes, again confirming the absence of permanent large-scale flow separation in some leesides. This also highlights the likelihood of downstream dipping accretion surfaces, with superimposed smaller cross-stratification, being preserved in the depositional record. Analysis of dune dimensions through the flood hydrograph (Figure 20.16) shows that generally both dune height and wavelength increase with flow velocity, although both positive and negative hysteresis loops are present. However, the form factor of the dunes shows little change and there is little tendency for dunes to flatten as velocity rises: this again demonstrates that the majority of flows within the Jamuna River generate bedforms within the dune stability field and not in the transitional regime to upper-stage plane beds, except in shallow flows on bar-tops (Bristow 1993a; Julien and Klaassen 1995; FAP24 1996a, 1996g; Figure 20.9e). Dune migration rates range from 1.1 to 16.8 $m\,h^{-1}$ for dunes that range in height from 1 to 6 m (FAP24 1996c), although from this limited database there is no indication of any strong link between dune height and migration rate.

The large dunes present in the Jamuna River have also been described in relation to their mean flow field (FAP24 1996g; Roden 1998) and macroturbulence, the latter often seen as eruptions or 'boils' on the water surface (Figure 20.17; Coleman 1969; Roden 1998; Best 2005). Such large-scale turbulence is related to upwellings of fluid over the dune troughs (Figure 20.9b) and has been linked to (i) eddy shedding of Kelvin–Helmholtz instabilities generated along the separation zone shear layer of steep leeside angle dunes, and (ii) temporary shear layer development,

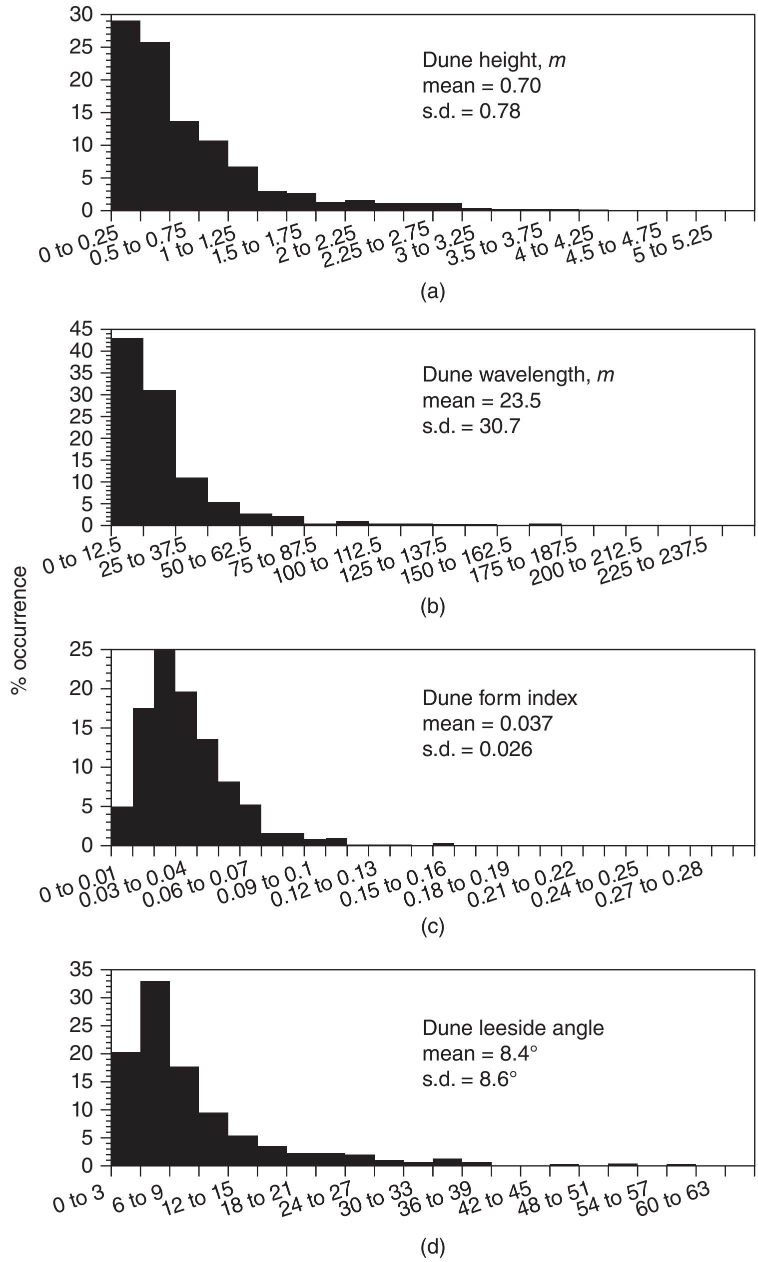

Figure 20.11 Histograms of (a) dune height, (b) dune wavelength, (c) dune form index (height/wavelength), and (d) dune leeside angle, from three study sites in the Jamuna River. Source: FAP24 (1996g) and Roden (1998). Sample size = 1400 dunes.

and possible temporary flow separation (Best and Kostaschuk 2002) in the lee of low-angle dunes, or in response to temporary dune oversteepening, possibly as a result of the migration and amalgamation of superimposed dunes (FAP24 1996g).

Besides dunes, two other small-scale bedforms are present in the Jamuna: ripples (Figure 20.9d) and upper-stage plane beds (Figure 20.9e). Ripples are also ubiquitous and found both superimposed on dunes and also commonly on the bar-tops. The ripples on bar-tops may often be preserved as climbing ripples (Figure 20.9d) with high angles-of-climb, demonstrating the occurrence of high sedimentation rates (Bristow 1993a).

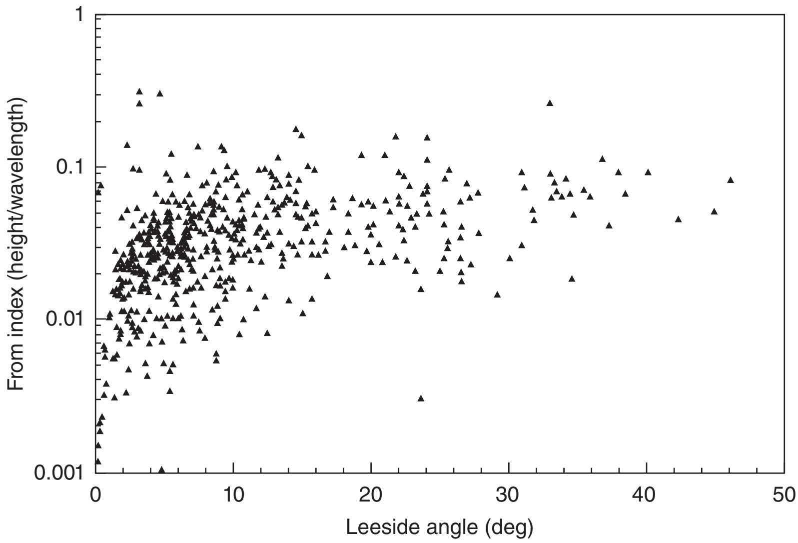

Figure 20.12 Form index of dunes in the Jamuna River as a function of leeside angle. Source: From Roden 1998.

Aeolian erosion and sand transport, as ripples and small barchanoid dunes, may rework the top 0.1–0.5 m of bar surfaces during periods of exposure.

20.3.2 Large-Scale Bedforms (Bars and Bar Complexes)

The Jamuna River contains two different scales of larger bedforms that may be termed 'bars' and 'islands' (Thorne et al. 1993). Bars have lengths of the same order or greater than the channel width and heights that are comparable with the mean depth of the generating flow (ASCE 1966). Islands are vegetated, relatively stable, large bar complexes (known locally as 'chars'), up to 15 km in length and with heights up to the adjacent floodplain level. Bars are frequently found attached to these islands but more commonly within the anabranches that bifurcate around the node-island-node configuration that appears to dominate the downstream configuration of the active Jamuna channel belt (Figure 20.1). The Jamuna River contains all sizes of sand bars ranging from tens of metres to several kilometres in length. The surface geometry of bars in the Jamuna River (expressed as the ratio of long-to-intermediate bar axis) and some aspects of the subsurface facies associated with these bars may be scale independent and share many of the morphological and sedimentological characteristics of other sandy braided rivers (Best et al. 2003; Sambrook Smith et al. 2005).

The most common bar types are the scroll (or point) bar and mid-channel (compound braid) bar (Bristow 1987; Ashworth et al. 2000). Bridge and Lunt (2006) suggest that mid-channel bars in the Jamuna River develop from double-row alternate bars (Fujita 1989; Yalin 1992) which create a 'unit bar' (Bridge 1993, figure 1), although no data are presented to substantiate this hypothesis. Ashworth et al. (2000) tracked the development of a 1.5 km long, 0.5 km wide, 12 m high, symmetrical mid-channel bar over a 28-month period in a major anabranch of the Jamuna River near Bahadurabad (Figures 20.1 and 20.18) and noted that the bar was probably initiated by the stalling and amalgamation of dunes in the main channel thalweg. Supporting evidence for this mode of bar initiation was displayed in Best et al. (2003) using Ground Penetrating Radar (GPR) that imaged the subsurface

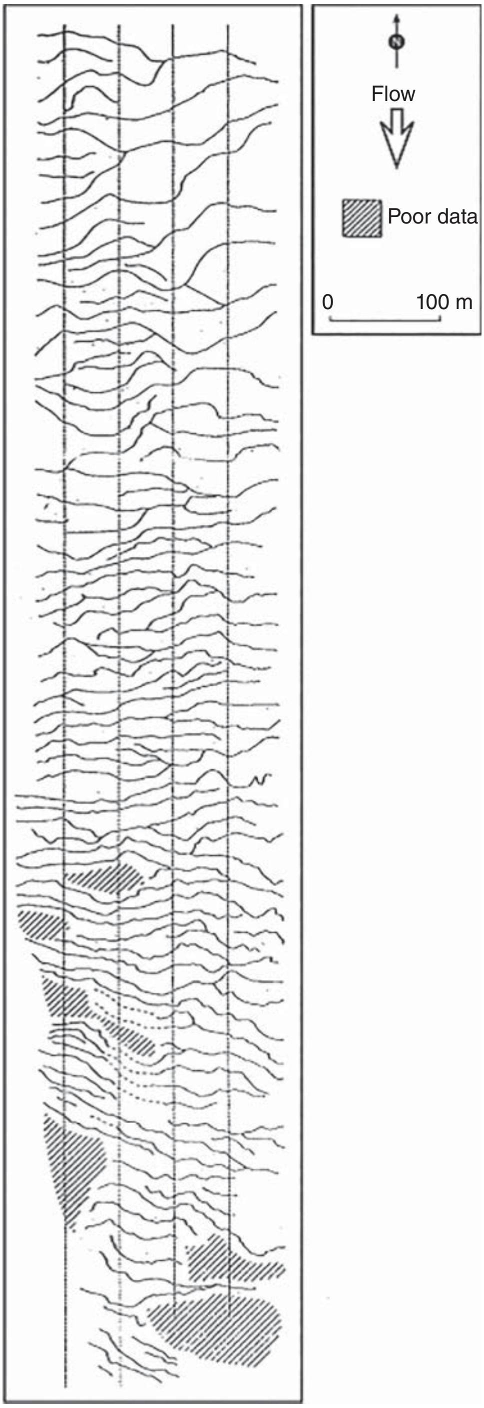

Figure 20.13 Composite tracing of dune crestline planform morphology as derived from sidescan sonar data collected in March 1995 near Bahadurabad. Source: From FAP24 1996g and Roden 1998.

of the same bar down to 12 m and revealed stacked two- and three-dimensional dunes at the base of the bar. Many mid-channel bars in the Jamuna River enlarge (both up-, down-, and across-stream) by the addition of smaller unit bars. Bristow (1987) calculated that up to 57% of the total area of bar deposition in the Jamuna may be through lateral accretion by the successive addition of individual unit or scroll bars to the bar nucleus. Unit bars are dominated by dunes whose crestlines are often oblique to the local anabranch direction (Bridge 1993). Mid-channel bars in the Jamuna River often develop downstream extensions to the bartails that have been termed 'horns' (Cant and Walker 1978), 'limbs' (Ashworth 1996), or 'wings' (EGIS 2002) that may extend for up to 50% of the bar length.

Surprisingly, the Jamuna River does not display many examples of the 'cross-channel bar' that feature strongly in the 'classic' sand braid bar depositional model of Cant and Walker (1978). Many of the kilometre-wide anabranches are devoid of near-emergent lobate unit bars (Figure 20.19a–c), which is very different from observations of many other sand-bed braided rivers (e.g. Platte, South Saskatchewan; cf. Sambrook Smith et al. 2006; Strick et al. 2019). Width-depth ratios of the main anabranch channels are predominantly over 100 (up to 700, cf. Thorne et al. 1993) and can result in a simple flow convergence and divergence around and over bartops, rather than the development of single- and double-cell secondary flow circulation in the anabranches around bars (cf. Richardson and Thorne 1998; McLelland et al. 1999; see Section 20.4).

Figure 20.18 shows a model for sand braid-bar growth in the Jamuna River from Ashworth et al. (2000) based on 12 ship and land surveys, taken in the period 1993–1996, in a 9 × 2.5 km area immediately north of Bahadurabad (location in Figure 20.1). The model shows the creation of a central, symmetrical mid-channel bar from dune stacking in the channel thalweg (stages 2–3, Figure 20.18),

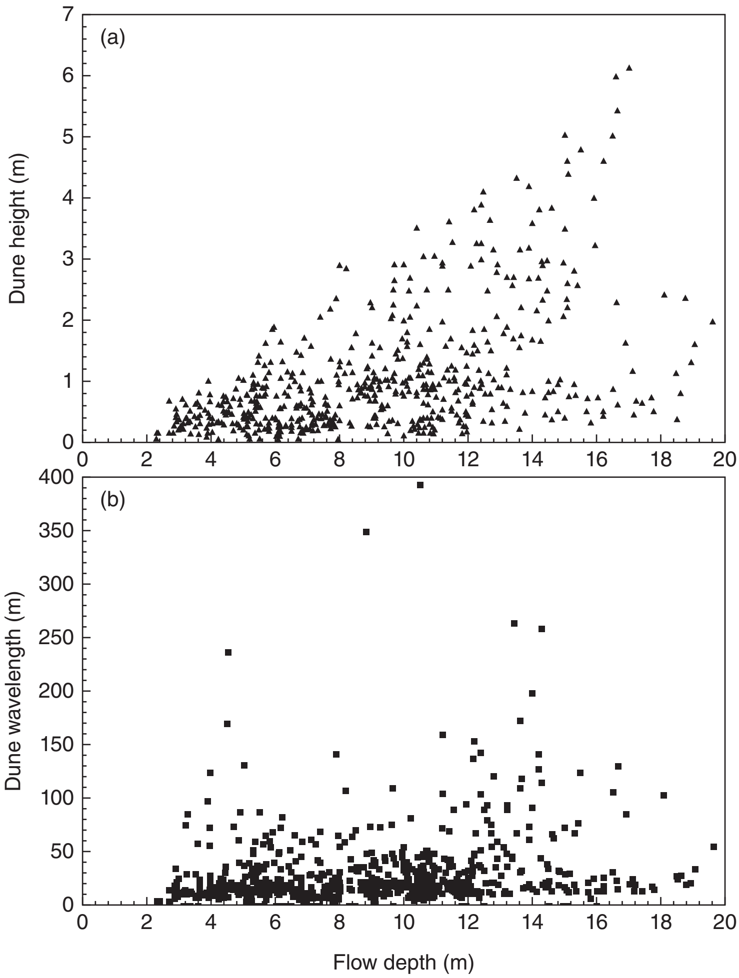

Figure 20.14 Plots of (a) dune height and (b) dune wavelength as a function of flow depth. Source: Based on FAP24 (1996g).

followed by the enhanced development of one anabranch around the bar (stages 4–5, Figure 20.18), which then creates a lobate depositional front (stage 6, Figure 20.18) and an overall planform that resembles an alternate bar rather than a central unit braid bar. The availability of annual low-flow Landsat imagery since 1996 (represented by stage 6 in Figure 20.18) allows evaluation of the longer term stability and development of this particular kilometre-scale bar.

Figure 20.19a shows the morphology for the study reach at the end of the monitoring period described in Ashworth et al. (2000, their figure 5f: p. 540). The emergent mid-channel bar (labelled 1) had a 1 km long bartail and a discontinuous lobate bar front (labelled 2), but there was also deposition of a 3 km long mid-channel bar 2.5 km upstream (labelled 3) and side bars (labelled 4). Figure 20.19b shows that at low flow in 1997 the mid-channel bar under surveillance (labelled 1) appears to have migrated downstream by 3 km but maintained the same overall size and morphology. The lobate bar front (labelled 2) remained in place and became emergent, showing it was not an integral part of the mid-channel bar morphology as suggested in Ashworth et al. (2000). The study reach experienced downstream and lateral accretion of both bars 3 and 4. By 1998 (Figure 20.19c), the mid-channel bar had either been completely reworked or migrated

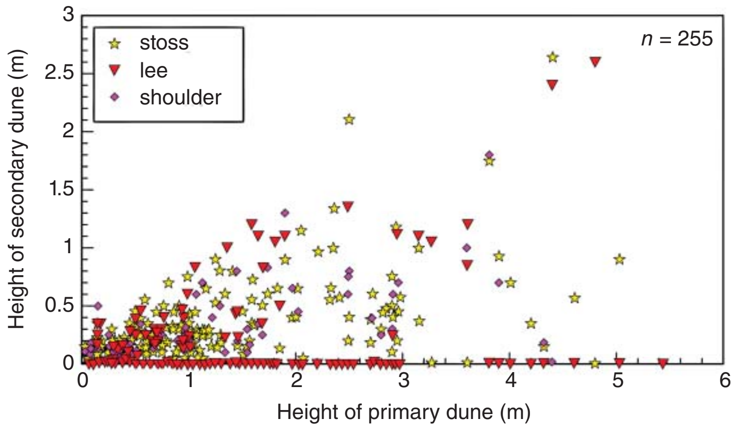

Figure 20.15 Plot of primary dune height against height of secondary dunes that are superimposed on the primary dune. The symbols denote the position on the primary dune where the secondary dunes are superimposed (stoss side, leeside, and on crestal shoulder). Source: Based on FAP24 (1996g).

downstream to accrete onto a bar complex (labelled 5). Bars 3 and 4 continued to grow but the 2 km wide main anabranch was essentially devoid of any partially emergent or newly developing mid-channel bars. Together with the survey data presented in Ashworth et al. (2000), this example of channel evolution near Bahadurabad illustrates that kilometre-scale bars may have a life-cycle of about five years (i.e. more than one flood season but then of limited duration). Mid-channel bars may maintain their basic morphological shape during development even when they migrate kilometres downstream. The annual record of bar evolution shown in Figure 20.19a–c illustrates that in a river the size of the Jamuna, even kilometre-scale bars are extremely mobile and may be transient features in the braidplain depositional record.

20.4 Bifurcations, Offtakes, and Confluences

Within the Jamuna River, the ubiquitous occurrence of bifurcations and confluences is a key aspect of the river channel pattern and dynamics, and these features form important nodes in the braidbelt. The braided nature of the river means that these nodes are present at a range of scales and orders of channel, and are central in dictating local and channel-wide erosion, deposition, and morphological change.

Bifurcations occur as flow divides around the numerous braid bars, and there has been much debate concerning the nature of flow within the distributaries, with Richardson et al. (1996) and Richardson and Thorne (2001) favouring a model that considers the flow similar to two back-to-back meander bends with helical flow developing at the bar-head. However, McLelland et al. (1999) argue that the main features of flow at the barhead bifurcation are convective acceleration as the flow shallows and modification of the primary flow caused by bedforms; they reason that these features, together with the high width:depth ratio of the channels and high relative roughness of dunes, cause a simpler flow pattern to that proposed by Richardson and Thorne (1998, 2001), with simple flow divergence around the barhead bifurcation.

EGIS (2002) report that of the 121 bifurcations considered in their study, 49% were symmetrical in planform whilst 51% were asymmetrical, and that the magnitude and direction of bifurcation migration were independent of angle asymmetry. EGIS (2002) further detail that 17% of the bifurcations migrated upstream, whilst 83% either remained static in position or migrated downstream. The rate of migration of bifurcations in the Jamuna River ranges from −2200 to

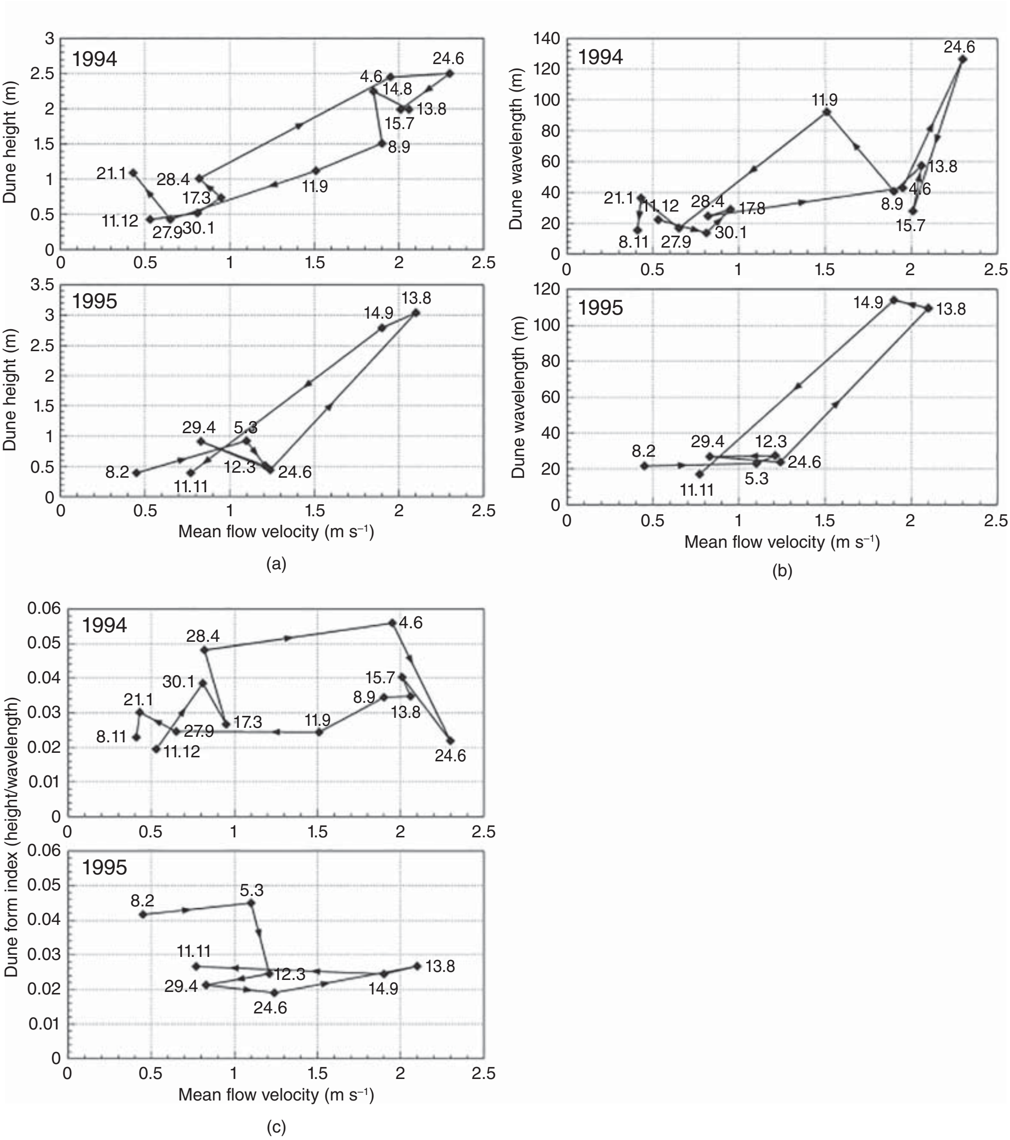

Figure 20.16 Hysteresis plots for 1994 and 1995 hydrographs at Bahadurabad (see Figure 20.1 for location) for (a) dune height, (b) dune wavelength, and (c) dune form index as a function of mean flow velocity (as derived from acoustic Doppler current profiling records). Numbers on graphs refer to day and month of each data point. Source: Based on FAP24 (1996g).

3000 m yr^{-1} (EGIS 2002), whilst the length of the bifurcation, defined as the distance from bifurcation to confluence, varies between 2 and 40 km (EGIS 2002). An important consideration in the evolution of bifurcations is the probability of channel abandonment of one of the distributaries, a process that is common in development of asymmetrical braid bars (Ashworth et al. 2000). Klaassen et al. (1993) and Mosselman et al. (1995) found that higher bifurcation angles are associated with higher rates of channel abandonment (Figure 20.20), with bifurcation angles <20° being very stable. Shampa and Ali (2019) also illustrate the

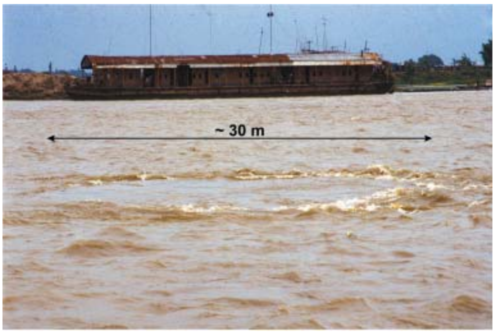

Figure 20.17 Macroturbulence erupting on the water surface of the Jamuna River near Bahadurabad: this locality was above a field of 3–4 m high dunes at the time of survey (Best 2005). Flow left to right, and flow depth ~15 m. For video of such turbulence, see https://www.youtube.com/watch?v=RMfaVJJliK8.

influence of bifurcation angle of flow division at these nodes, with higher bifurcation angles (>30°) sharing a smaller fraction of the total flow being routed into one of branches, thus favouring abandonment.

Besides bifurcations around braid bars, channel offtakes, which are more permanent divisions of flow, are key elements of the river morphology in Bangladesh. The dynamics of such offtakes have undoubtedly been of great significance during channel avulsions, such as (i) the occupation of the current Jamuna channel and abandonment of the Old Brahmaputra (Figures 20.5a and 20.6), (ii) the division of flow from the Jamuna into the Dhaleswari, and (iii) the current concern regarding the flow reduction and infilling of the Gorai channel, which is an offtake from the Ganga just upstream of the Jamuna–Ganga confluence (Figure 20.1). The reduction in flow discharge down the Gorai River over the past decades has meant that during low flow the south-western region of Bangladesh receives much less fresh water, and therefore there is greater intrusion of the saline wedge from the Bay of Bengal into the distributary channels – a factor that has changed the livelihood of largely rural subsistence farmers (Alam 1984). Study of the Gorai offtake (FAP24 1996f) using historical data, satellite images, and two-dimensional morphological modelling, highlights the influence of curvature in the upstream Ganga channel in affecting flow at the offtake and also the significant influence of flow stage in determining the division of flow. Rising flow stages appear to favour shallowing and widening of the channel at the offtake and during falling stage the channel becomes narrower and deeper. However, the influence of large, severe floods is significant, and sediment accumulation in a bar at the mouth of the offtake generated during a very high flow can remain during subsequent years of normal floods (FAP24 1996f).

Channel confluences are also key sites within the Jamuna River, and have been documented as important sites of bed scour (Klaassen and Vermeer 1988; FAP24 1996a; Best and Ashworth 1997; EGIS 2002; Dixon et al. 2018; Sambrook Smith et al. 2019). The depth of the central confluence scour shows some dependence on the junction angle (Figure 20.21), with higher confluence angles possessing scour depths up to six times that of the confluent channels. Local factors, such as hydrograph shape, upstream channel curvature, and low-stage modification may make this junction angle–scour depth relationship more complex, but the predictive equation of Klaassen and Vermeer (1988) is a reasonable estimate of scour depth (Sarker 1996), and is given by:

$$h_{cs}/h = 1.292 + 0.037\theta$$

where h_{cs} is the confluence scour depth, h is the mean flow depth of the upstream channels, and θ is the junction angle in degrees. Additionally, research comparing Jamuna scour data with other rivers in the World (Sambrook Smith et al. 2005) has suggested that scour depth relative to mean channel depth may be scale invariant over a threefold order of channel depths. Detailed bathymetric maps of the Jamuna–Ganga junction have shown the scale and rapidity of bed morphological change (Best and Ashworth 1997), with the 30 m deep

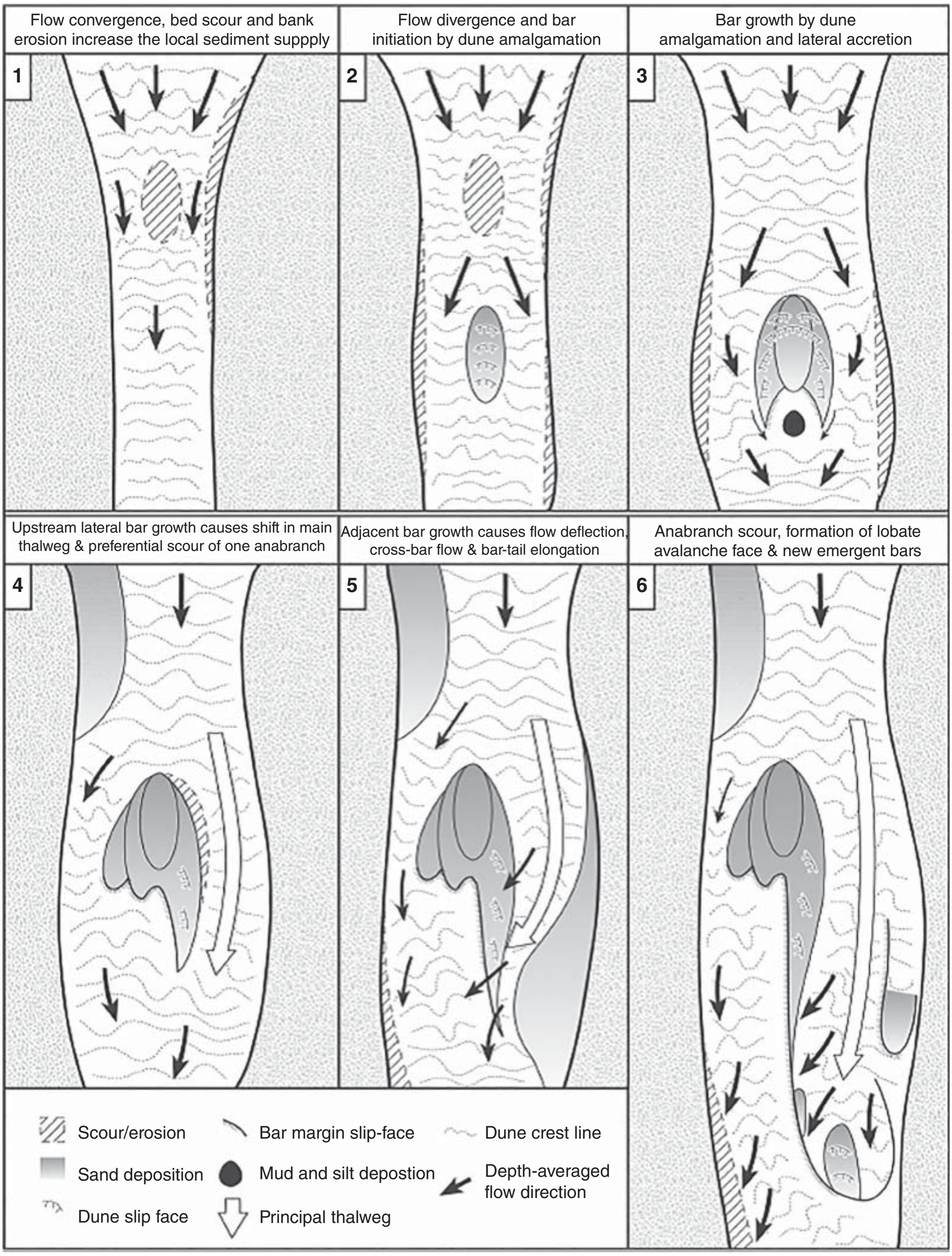

Figure 20.18 Summary model of the key stages in the evolution of a kilometre-scale mid-channel sand bar. Dune orientations and flow directions at the bed are inferred from the data presented in Roden (1998) and McLelland et al. (1999). Source: From Ashworth et al. (2000). © 2000, John Wiley & Sons.

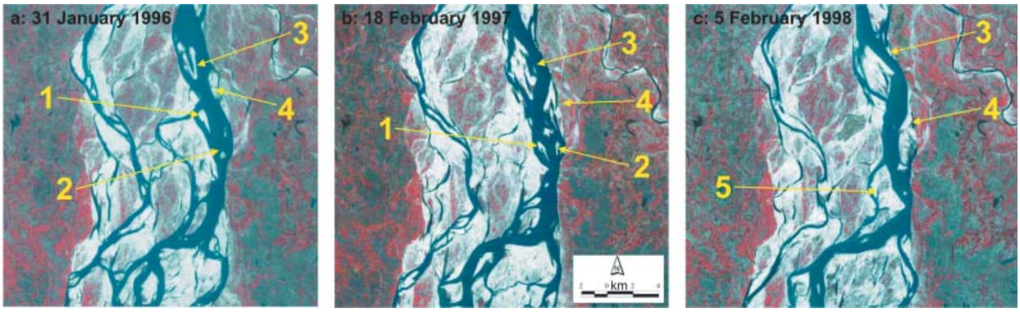

Figure 20.19 Morphological evolution of the reach studied by Ashworth et al. (2000) at Bahadurabad: (a) January 1996 (which represents stage 6 in Figure 20.18); (b) February 1997; and (c) February 1998. Source: Ashworth et al. (2000).

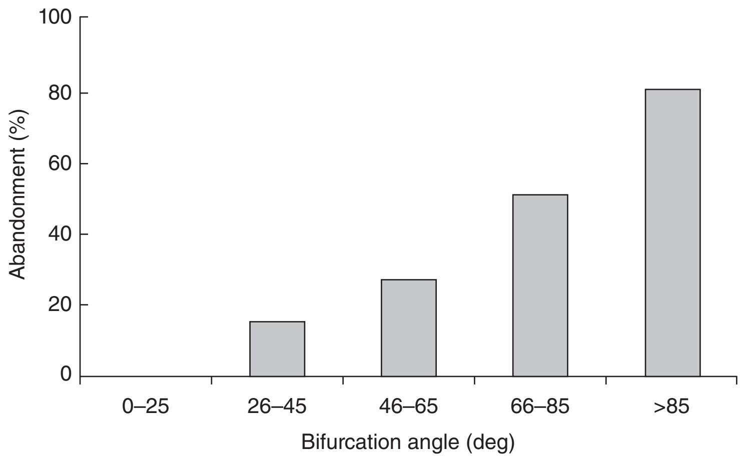

Figure 20.20 Distribution of channel abandonment as a function of bifurcation angle for bifurcations without appreciable barforms. Sources: EGIS (2002), Klaassen et al. (1993) and Mosselman et al. (1995).

confluence scour migrating 2 km in two flood seasons (Figure 20.22). Dixon et al. (2018) analysed satellite images from 1973–2014 and found that the junction between the Jamuna and Ganga rivers responded to changes in the north-south migration of the Ganga River at the junction, as well as to periodic changes in the orientation and position of the dominant thalwegs in the Jamuna River. Consequently, over this 40-year time period, the confluence encompassed a region 14 km long and 4.2 km wide.

20.5 Floodplain Sedimentation

ISPAN (1995) provide a summary of sedimentation on the Jamuna River floodplain, where most land is seasonally flooded, and which is characterized by an irregular relief. The nature of floodplain sedimentation and inundation is vital in planning annual crop growth and may adopt great significance in the ongoing debate on the sources, causes, and accumulation of arsenic in the groundwaters of Bangladesh (see Ahmed et al. (2004) for a review). ISPAN (1995) define several principal types of relief within the Jamuna River floodplain (Figure 20.23):

(1) Bars, scroll bars, and sand dunes: Generated by flood waters at the edge of the floodplain, often on the margins of the main or cross-floodplain channels. The difference in elevation between the top and bottom of this channel topography is rarely more than 1–2 m.

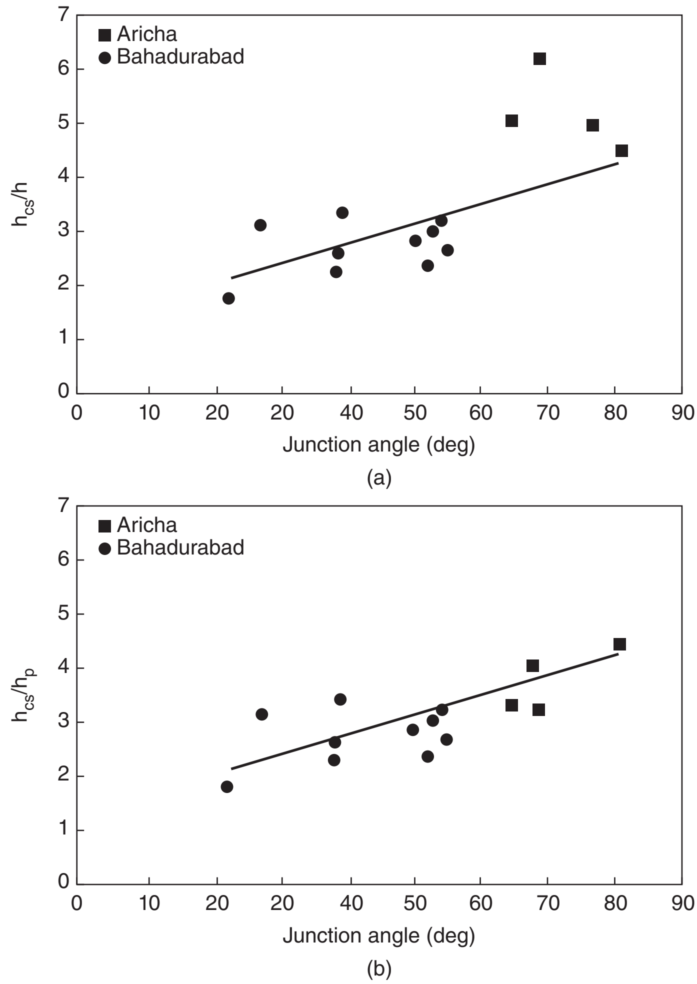

Figure 20.21 Confluence scour depth as a function of junction angle for data collected on the Jamuna River at Bahadurabad and Aricha: (a) with scour depth, h_{cs}, expressed in relation to flow depth at the time of measurement, h; (b) with scour depth, h_{cs}, expressed in relation to average flow depth in the upstream channels during the flood season, h_p. (b) shows a better relationship between junction angle and flow depth. Source: Based on FAP (1996d).

(2) River levees: Found along the edges of the active channels and formed by deposition from overbank flow, with grain size and deposition rate decreasing exponentially with distance from the channel. The height difference between the levee top and surrounding floodplain can be ~1 m over a distance of 100 m along small channels, but 2–3 m over 500 m or more alongside the major channels.

(3) Crevasse splays: Initiated due to a breach in the levee that forms a lobe of sediment which progrades onto the adjacent floodplain. The grain size of crevasse splays decreases with distance from the initial breach.

(4) Flood basin: Nearly enclosed depressions between the levees of adjacent rivers that usually drain out through small channels on their downstream side. Subsidiary levees can form along these smaller channels and the flood basins may contain silts and clays that settle out in quiet water, whilst more permanently flooded areas in older floodbasins contain peat accumulations.

The older parts of the floodplain thus become more complex in topography (ISPAN 1995), with the initial topography being smoothed out but with clay deposits up to 1 m thick. Elevation differences are generally 2–3 m over a lateral distance of 0.5–1 km. Soils within the Jamuna

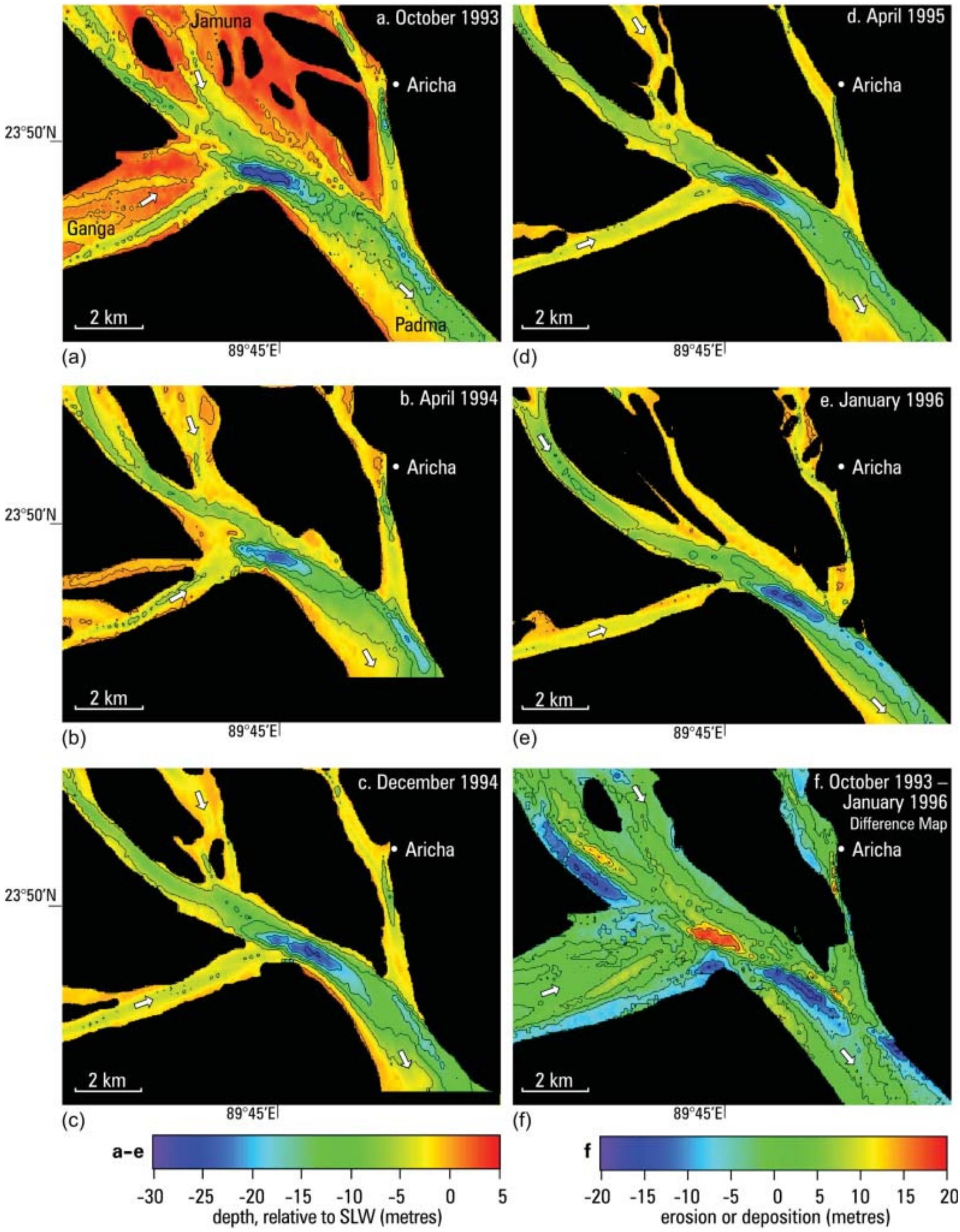

Figure 20.22 Plots of bed morphology and channel change at the junction of the Jamuna and Ganga rivers. SLW refers to Standard Low Water level. Source: Modified from Best and Ashworth (1997).

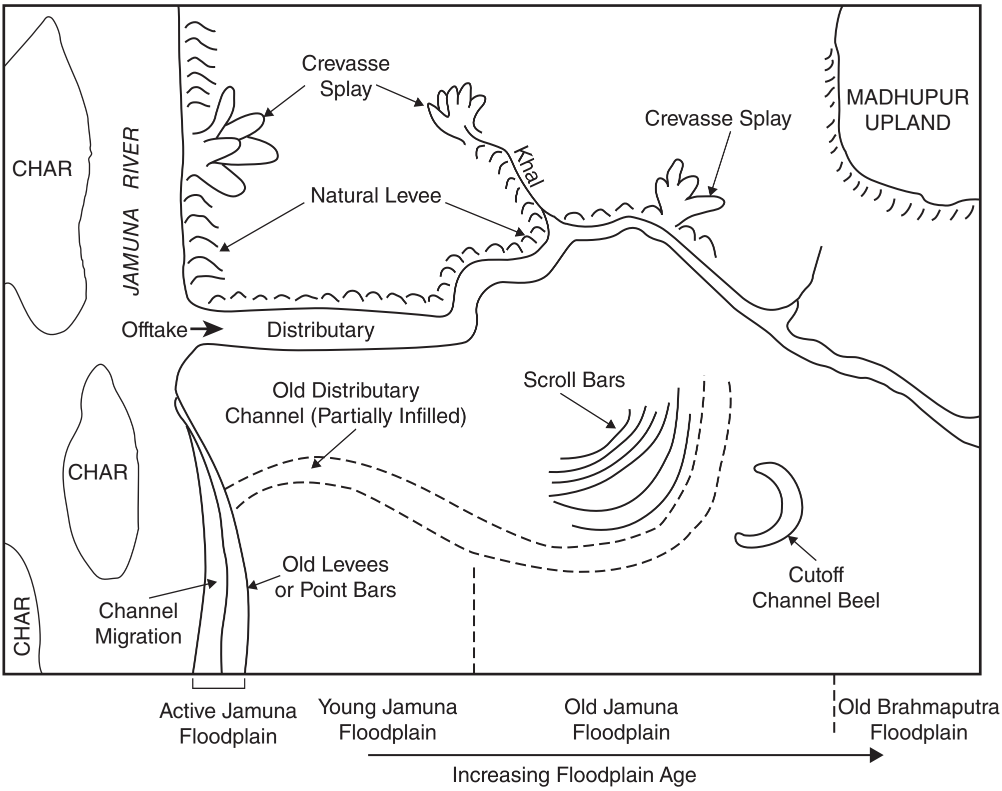

Figure 20.23 Representative landforms of the Jamuna River floodplain. Source: Modified from ISPAN (1995).

River floodplain change from east to west, from stratified alluvium on the active Jamuna floodplain to soils with well-developed profiles on the older floodplain and Old Brahmaputra. The main changes in soil-forming processes across this transect from east to west (Figure 20.24) involve increasing acidification, destruction of clays, and accumulation of organic matter, with the soils increasingly displaying greater biotic mixing, mottling, coatings around peds, and developing soil structure.

The depth of floodplain inundation is critical to farmers as this determines the annual cropping pattern and which type of rice will be grown. A classification of inundation on the floodplain (Table 20.1) shows the normal water depths in various categories of floodplain, although the effects of local ground subsidence (for instance earthquakes) and flood protection schemes, such as localized embankments that may increase flood inundation levels outside the embankments, may change the local floodplain water depths. ISPAN (1995) report average annual sedimentation rates of 7.6 mm yr^{-1} obtained from a GIS study, with a range from 0 to 76 mm yr^{-1}. Allison et al. (1998) also report accumulation rates of ~40 mm yr^{-1} on the levees to <10 mm yr^{-1} within a few tens of kilometres into the floodplain flood basin. Allison et al. (1998) state that the important controls on local sedimentation rate are proximity to distributary channels, local topography, and interannual variability of the flood pulse. Model results suggest that between 31% and 71% of the total alluvial sediment budget may be trapped landward of the Ganga–Brahmaputra mouth, and highlight the key role of floodplain storage in controlling the sediment yield to the oceans (Allison et al. 1998). Islam et al. (1999) estimate that

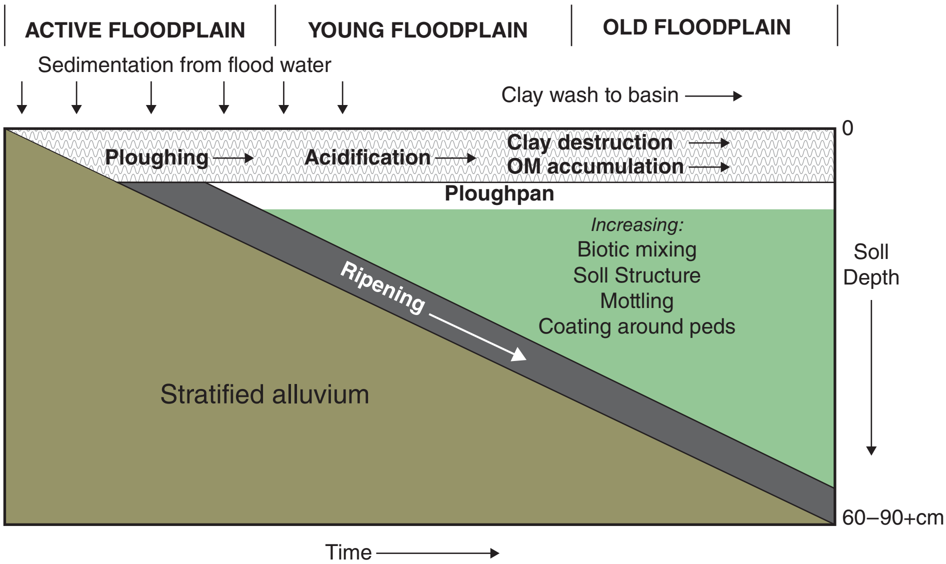

Figure 20.24 Stages of floodplain soil development in Bangladesh (after ISPAN 1995). See text for discussion of lateral changes in soil characteristics. Source: Modified from ISPAN (1995).

Table 20.1 Classification of floodplain water depths.

Agro-ecological zone	Normal maximum water depth during flood (cm)
Highland	0
Medium highland-1	0–30
Medium highland-2	30–90
Medium lowland	90–180
Lowland	180–300
Very low lowland	>300
Bottomland	Mainly >300, but includes perennial wetland in other depth classes

Source: Modified from ISPAN (1995).

~49% of the total load is deposited before the coastal region, with 28% being deposited on the floodplain and 21% within the active channels. Islam et al. (1999) contend this deposition thus leads to significant aggradation within the channels as well as on the floodplain.

The nature of the annual flood hydrograph exerts a strong control on the grain size of floodplain sedimentation, and hence the contribution to soil fertility and subsequent crop success. For example, the large floods of 1998 and 2004 were very different, with overbank flows experienced for 65 and 45 days, respectively (CPD 2004). The nutrient-rich silt deposited during the longer duration 1998 flood led to a record *boro* rice crop the next year (BDER 2004). However, the relatively fast-rising and receding monsoon flood in 2004 resulted in more overbank sand than silt deposition, and there was concern as to the impact this would have on the 2005 rice yields (BDER 2004).

20.6 Sedimentology of the Jamuna River

The surface geomorphology of the braided Jamuna River, together with descriptions of the numerous cutbanks and use of ground-penetrating radar, allows an insight into the depositional facies of the Jamuna. The principal papers concerning the sedimentology of the Jamuna River are those of Coleman (1969),

Radar Facies No.	Radar Characteristics	Vertical & Lateral Extent	Sedimentary Characteristics & Interpretation
1	**1a.** Steeply dipping (angle-of-repose) planar or subplanar reflections and low-angle (10 – 15°) planar or subplanar reflections dipping into anabranch channel on western edge of bar.	up to 8 m high and extend laterally for >100 m	1a. Large-scale cross-stratification either at angle-of-repose, with large sets (a) dipping from bar margin into thalweg, or lower angle sets (b) that occur in deeper part of radar profile and on western side of bar, sloping into anabranch channels. May contain internal reactivation surfaces.
	1b. Planar and asymptotic dipping reflections in lens-shaped packages. Sometimes bounded by erosion surface at base or top.	up to 4 m high and extend laterally and downstream up to 100 m	1b. Large-scale cross-stratification (c) caused by deposition at the margins of the barhead by diverging flow.
2	**2a.** Strong, trough-shaped reflections that are laterally discontinuous, often with steeply dipping or low-angle internal reflections.	1 – 3 m high; 5 – 300 m lateral continuity	2a. Medium-scale trough (d) cross-stratification associated with preservation of large dunes.
	2b. Weak undulating reflections at depth often lacking internal dipping reflections (because foresets are beneath radar resolution).		2b. Medium-scale cross-stratification produced by large dunes in the deeper parts of radar profiles are identified from basal erosion surfaces (e) and the lack of discernible foresets.
	2c. Discontinuous sigmoidal packages of concave/convex dipping reflections.	2 – 4 m high; 20 – 200 m lateral continuity	2c. Complex sets of medium-scale cross-stratification (f) due to oblique migration of large dunes and superimposed dunes descending the bar margin. Sets may contain internal reactivation surfaces (g) and variable dip angles.
3	Small discontinuous reflections with weak concavity from trough shaped structures at the limits of radar resolution.	0.5 – 2 m high; 5 – 30 m wide	Small-scale trough cross-stratification (h) produced by dune deposition on the bar flanks. Set size increases with depth, larger sets are found on the bar western side and smaller sets on the eastern side.
4	High-amplitude, continuous, undulating reflections	~ 0.5 m high; ~ 40 m wide	Mud drape (i)

(a)

Figure 20.25 (a) The four principal ground-penetrating-radar facies documented from the GPR survey lines presented in Best et al. (2003), with (b) representative GPR examples and sedimentary interpretation. Vertical exaggeration = 1.58. Source: Best et al. (2003). © 2003, Society for Sedimentary Geology.

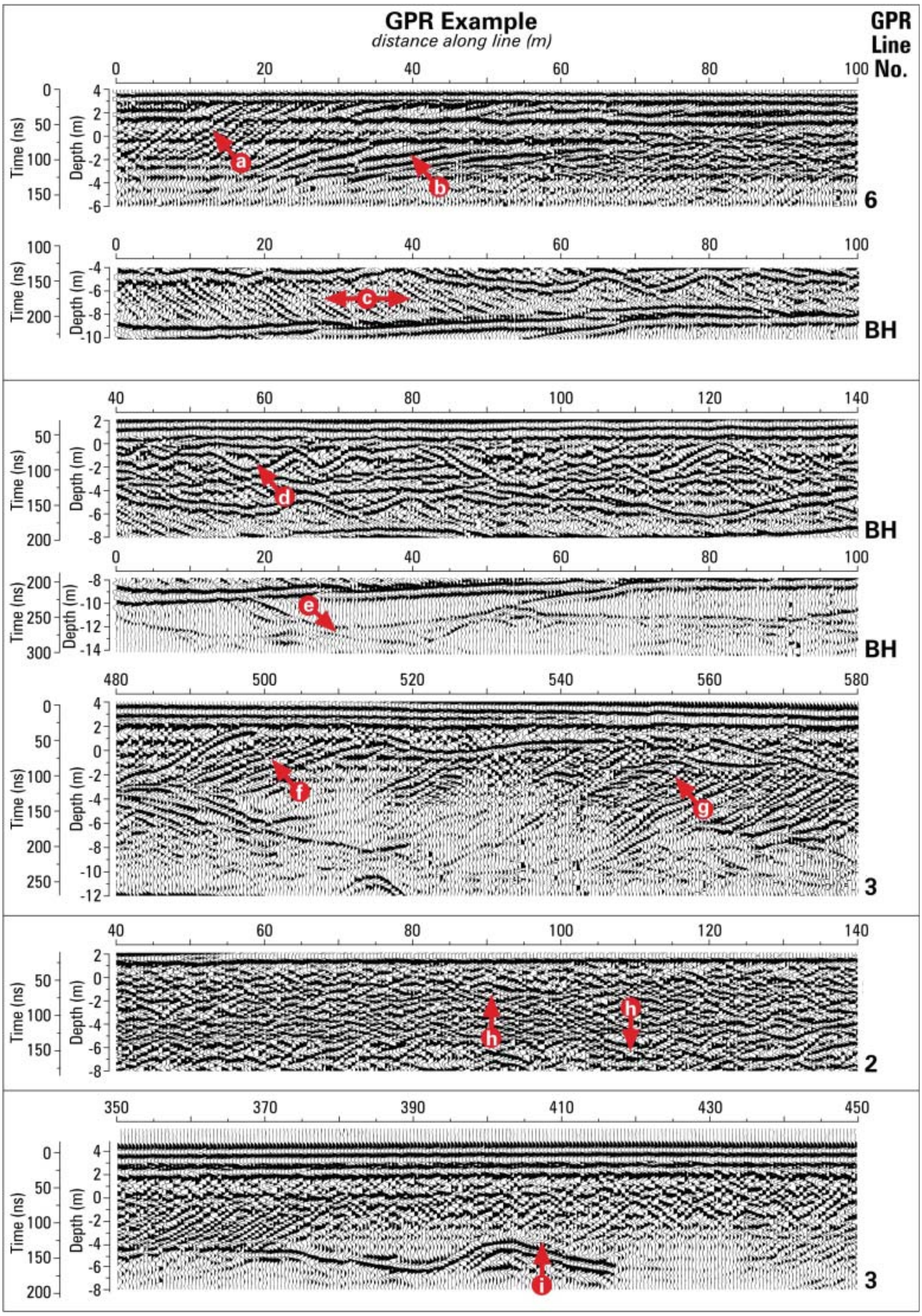

(b)

Figure 20.25 (*Continued*)

Bristow (1993a), and Best et al. (2003) and these are used below to highlight the depositional form of a braid bar within the Jamuna River. The Jamuna River has also been used as an analogue for deposition in other large ancient braided channels (e.g. see Bristow 1993b; Miall and Jones 2003) and thus description of a facies model is important for reconstructions of ancient alluvial architecture. Sambrook Smith et al. (2019) also examined the sedimentology of river channel confluences and used geophysical data from the Jamuna River to illustrate the internal structure of these bars. Best et al. (2003), using a combination of detailed GPR (Figure 20.25) and trench/core logging tied into surveys over an evolving, newly formed mid-channel braid bar (Ashworth et al. 2000), document four principal depositional facies: (i) large bar-margin slipfaces, up to 8 m high, that are generated as steep avalanche faces at the downstream end of actively migrating braid bars and are often associated with oblique flow over the braid bar; (ii) medium-scale dune cross-stratification, 1–4 m high, generated by large-scale dunes within the active channels, or possibly as unit bars; (iii) small-scale dune cross-stratification, 0.5–1 m high, generated by sinuous-crested sand dunes; and (iv) mud-drapes formed in quiet water regions, such as in the lee of mid-channel bars. These four facies were found to generate seven styles of deposition (Figure 20.26):

(1) *Bar-margin slipface*: A dominant style of deposition within mid-channel bars that is created by oblique downstream growth and cross-channel bar-margin accretion. This deposition often occurs through amalgamation of complex sets of dune-scale cross-stratification and bar-margin slipface accretion with both large, low-angle and angle-of-repose foresets. Large bar-margin slipfaces may become progressively steeper until reaching the angle-of-repose.
(2) *Vertical accretion in channel*: Sets of trough cross-stratification, produced by sand dunes within the channels and decreasing in size towards the bar-top, are found in all areas of the bar and formed a significant proportion of the sedimentary facies.
(3) *Vertical accretion on bar-top*: Sets of trough cross-stratification are found on the bar-head, bar-tail, and along the bar-margin, and are formed from deposition by small (<1.5 m high) three-dimensional dunes.
(4) *Upstream accretion*: Restricted to the upper 2–3 m of sediments in the mid-bar region and probably formed in response to dune stacking over the bar-top in shallow flows. The upstream accretion surfaces were separated by small-scale sets of trough cross-stratification, and mirror the observations of bar-top deposition by Bristow (1993a) (Figures 20.26 and 20.27).
(5) *Lateral accretion*: This was documented on one side at the upstream end of the bar studied by Best et al. (2003) and attributed to deposition during the falling stage of the hydrograph as flow was diverted around the bar-head. Lateral accretion surfaces were separated by trough cross-stratification generated by small, three-dimensional dunes.
(6) *Downstream/oblique accretion*: Occurred on the central and downstream regions of the bar, representing downstream and oblique accretion of dunes across the bar, forming complex downstream-dipping surfaces.
(7) *Mud drapes*: Present as low-stage, fine-grained drapes that develop in the bar lee where fine-grained silt and clay are deposited from suspension.

Apart from this model of deposition within the entire braid bar, Bristow (1993a) presents a model of bar-top sedimentation in the Jamuna River (Figure 20.27) that matches well with the later GPR surveys of Best et al. (2003) and is characterized by: (i) upstream accretion on the upstream part of the bar-top, which is formed from trough cross-stratification and rare upper-stage plane beds. The upstream

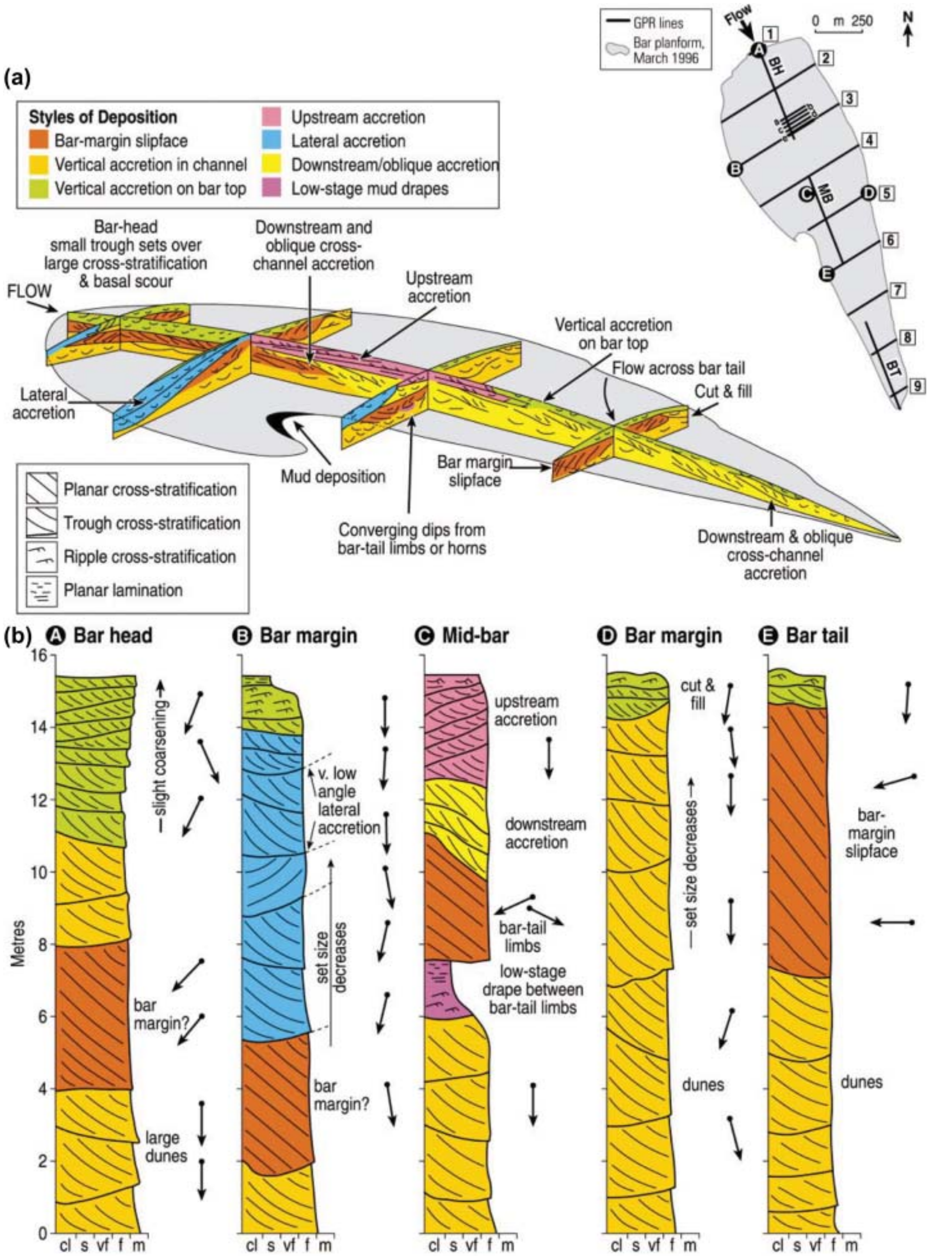

Figure 20.26 Styles of deposition and vertical facies profiles for a mid-channel bar in the Jamuna River. (a) Three-dimensional diagram of the principal styles of deposition quantified within a Jamuna braid-bar (see text for details). The scale of the bar is 3 km long, 1 km wide and 12–15 m high. The different styles of deposition are coloured and the main sedimentary structures are labelled. (b) Schematic sedimentary logs at five localities within the large braid bar (see inset for location), illustrating the characteristic sedimentary structures, large-scale bedding surfaces, and styles of deposition (see a). Arrows depict the approximate flow directions for sedimentary structures at various heights in each profile, with flow down the page (e.g. profile A, bar head at 2 m) indicating flow parallel to the mean flow direction (see arrow on inset location map). Deviations in flow from this direction are shown, such as the oblique, cross-channel movement of the bar-margin slipface (e.g. profile E, bar-tail at 8.5 m). Source: From Best et al. (2003). © 2003, Society for Sedimentary Geology.

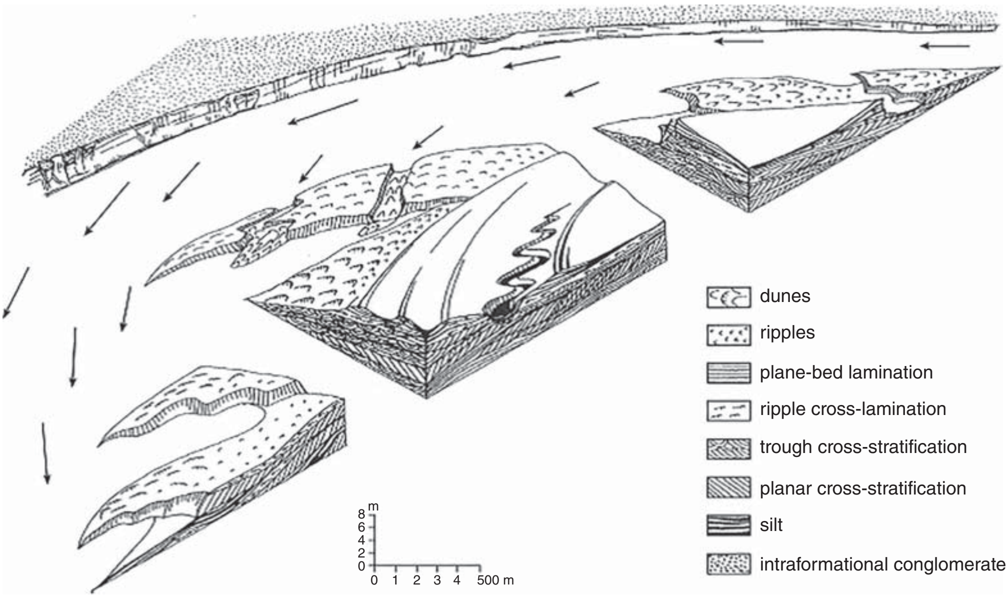

Figure 20.27 Facies model for bar-top deposition in the Jamuna River. Source: From Bristow (1993a). © 1993, Geological Society of London.

part of the bar-top was found to sometimes be erosional with cantilever bank failures; and (ii) the central section of the bar-top was characterized by both vertical and lateral accretion, containing dune-scale trough cross-stratification, upper-stage plane beds, and ripple cross-lamination. Bristow (1993a) proposed a characteristic vertical sequence of upper-stage plane beds to trough cross-stratification and then ripple lamination, which reflects declining flow velocities and increasing aggradation rates within these bar-top sediments. The downstream ends of the bar-top were found to be more variable in composition, with dunes and scroll-bars (unit bars) migrating around the downstream bar margin (see also model of braid bar growth, Figure 20.18). Bristow (1993a) found that the downstream bar margins may become steepened to form avalanche faces and that flow separation/reduced velocities in the bar-lee can lead to deposition of current ripples and fine-grained drapes. Bristow (1993a) also highlights the role of falling-stage modification in forming bar-top channels, with low-stage flow being unable to rework the bar-surface.

In a study examining the sedimentology of river channel confluences, Sambrook Smith et al. (2019) used a Boomer system to collect seismic reflection profiles at the junction of the Jamuna and Ganga rivers (Figure 20.28). These seismic data were georeferenced to the 1973–2014 Landsat imagery of Dixon et al. (2018), as well as the earlier bathymetric analysis of Best and Ashworth (1997). Rather than showing the dominance of depositional surfaces produced by the uninterrupted migration of bars into the confluence scour, as suggested in other models of junction sedimentation (Bristow 1993a, b), these seismic sections show the dominance of low-angle (*c.* 2°–4°) erosion surfaces (labelled R1–R3 in Figure 20.28a) down to a depth of *c.* 14 m, which represent reworking of the bar surfaces over a distance of up to 1–2 km. In a section towards the base of the scour (Figure 20.28b), although the same reflections R1–R3 are present, more of the reflections show clear truncations, and are only *c.* 400 m in length. Sambrook Smith et al. (2019) interpret these shorter and more complex reflections to likely be the product of the channel thalweg moving back across a location, as revealed in the satellite imagery of Dixon et al. (2018), and reworking its deposits.

Sambrook Smith et al. (2005) considered the morphology and depositional facies of a range of braided rivers, including the Jamuna River, and found that the surface planform morphology of braid bars, and the maximum relative depth of confluence scour, displayed a scale invariance over many different types and sizes of braided river. They also concluded that the subsurface sedimentary facies of three sandy braided rivers, which covered a twofold order of magnitude in channel width, exhibited a degree of scale invariance with the ubiquitous occurrence of trough cross-stratification associated with migrating dunes. However, the occurrence of bar-margin, high-angle planar cross-stratification and low-angle stratification was variable both between rivers and between bars within the same river. Sambrook Smith et al. (2005) concluded that the relative presence of these two facies within the stratigraphy is related to a wide range of factors, including the discharge regime, local bar/channel topography, the channel width:depth ratio, and the presence and abundance of vegetation. Hence, although the models described above for the Jamuna River may share common characteristics with many other braided rivers, much work remains to be conducted to document and quantify the full range of depositional facies within large sandy braided rivers, especially in bars that are a complex product of successive periods of erosion and deposition.

20.7 Applied Geomorphology and Engineering in the Jamuna River

The Jamuna River is one of the most dynamic rivers in the World with little to stop sustained channel migration, bank erosion, bar creation, and destruction. The banks of the Jamuna River consist of weakly cohesive sand and silts, commonly with less than 1% clay and hardly any deep-rooted vegetation to bind the soil (FAP24 1996h). However, even deep roots would be insufficient to stop bank erosion along the 20–30 m deep channels of the river. Banks erode usually through large-scale slab failure due to toe scouring (Figure 20.29), and the slump blocks disintegrate rapidly after failure, so there is no potential for temporary stabilization of the bank through the accumulation of bank failure debris at the toe (Thorne et al. 1993). This bank erosion is a major source of poverty (Elahi et al. 1991). Banks along the Brahmaputra–Jamuna River can retreat hundreds of metres in a single flood season (Klaassen et al. 1993; Ashworth et al. 2000), devouring property and infrastructure on their way. The stabilization of riverbanks is thus of vital importance for alleviating poverty. In cost-benefit analyses, the major benefit of stabilization is derived from avoiding erosion and the collapse of embankments that protect land and infrastructure from flooding, such as the Brahmaputra Right Embankment [BRE] built in the 1960s. Other benefits arise from the stabilization of the distributary river offtakes of the Old Brahmaputra and Dhaleshwari that supply water to the capital city Dhaka. Riverbank stabilization projects along the Jamuna River also encounter pressures from sand mining and efforts to narrow the river to reclaim land and improve navigability. These additional interventions, however, are not justified by cost-benefit analyses. Rather, they give rise to concerns about adverse effects, which can be expected within Bangladesh as well as upstream in India.

River training works have been implemented in Bangladesh for over 100 years (Oberhagemann et al. 2020) and bank protection systems have been developed along the Jamuna–Brahmaputra River since the 1990s. Although several systems built between 1998 and 2004 failed (BDER 2021), earlier and later projects have been successful. Flood Action Plan projects FAP1 and FAP21/22, as well as river training works for the Bangabandhu Bridge, were realized in the 1990s. FAP1 stabilized banks to protect the BRE, thus

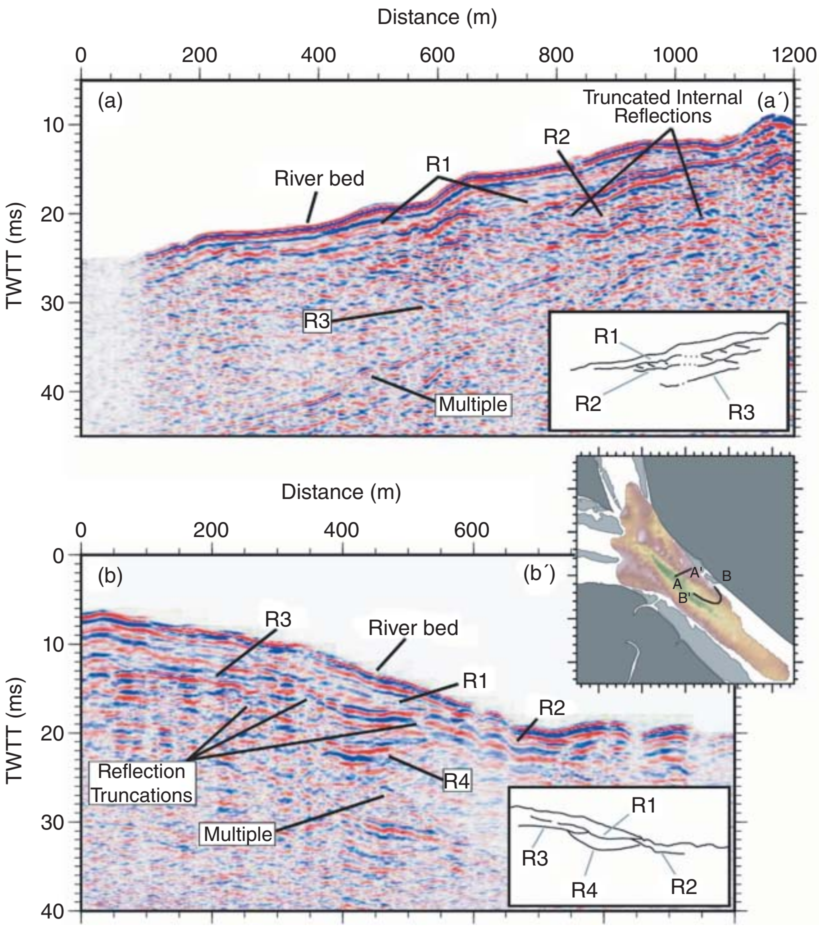

Figure 20.28 Plots of seismic data and their interpretations from the confluence of the Jamuna and Ganga rivers (see inset for bathymetry and location of seismic lines). (a) Seismic section a-a′. Three broadly parallel reflections, labelled R1–R3, were interpreted by Sambrook Smith et al. (2019) as erosion surfaces that could be traced across the east side of the confluence. (b) Seismic section b-b′, showing a series of relatively short cross-cutting reflections (R1–R4) that show migration and reworking of sediment by the scour zone. Reflections R1–R3 refer to the same features in both (a) and (b). Source: From Sambrook Smith et al. (2019). © 2019, John Wiley & Sons.

preventing avulsion into the Bengali River, securing the city of Sirajganj and the Fulchari railway ferry terminal, and preventing future outflanking of the Bangabandhu Bridge. FAP21/22 piloted new designs and new materials for more affordable structures: permeable groynes on the right bank at Kamarjani and revetments on the left bank at Bahadurabad and Guthail (Mosselman 2006). Figure 20.30 shows that the revetments are still in place after 25 years, despite strong fluvial attack. The project concluded that revetments are to be preferred for works that merely aim to stabilize the banks. Groynes and spurs require more material and create deep scour holes that threaten the stability of the structures. Although levees, such as the BRE, have contributed to economic development, their cost can be very high and may lead to dependency on foreign investors and loans (Ferdous et al. 2019b). In addition, levees can increase the potential damage from levee breaching, since

Figure 20.29 Large-scale slab failure by bank undercutting near Shailabari (~4 km upstream of Sirajganj). Photograph taken at low flow. During seasonal floods, the water level would be up to bankfull.

property owners may feel more secure due to their presence and therefore invest more in their own infrastructure (Ferdous et al. 2019b).

In addition, the Bangabandhu Bridge, 5 km south of Sirajganj (Figures 20.31 and 20.32), is the first and at present only bridge to span the Jamuna River. Built at a cost of *c.* US$ 550 million and opened on 23 June 1998 (Mottaleb and Rahut 2019), the bridge is 4.8 km long with 49 spans and used 80 m long piles driven 60 m into the river bed. The bridge deck is 18.5 m wide with four road lanes and a dual-gauge railway, as well as a 750 mm diameter gas pipeline attached underneath. Concrete pylons above carry high-voltage power and telecommunication lines. The Bangabandhu Bridge is located at a position where the Jamuna River braid belt narrows. This was one of the narrower, and deeper, reaches that Coleman (1969) identified as a nodal point, although these points were later found to be transient, and not permanent, nodes (Klaassen and Masselink 1992). The Bangabandhu Bridge allowed linking of the poorer northwest parts of Bangladesh with the more economically advanced eastern parts of the country (Mottaleb and Rahut 2019) and has been shown to have improved the daily wages in the northwestern Rangpur region, and encouraged migration of labour out of the northwestern parts of Bangladesh, which has improved the economic status of the

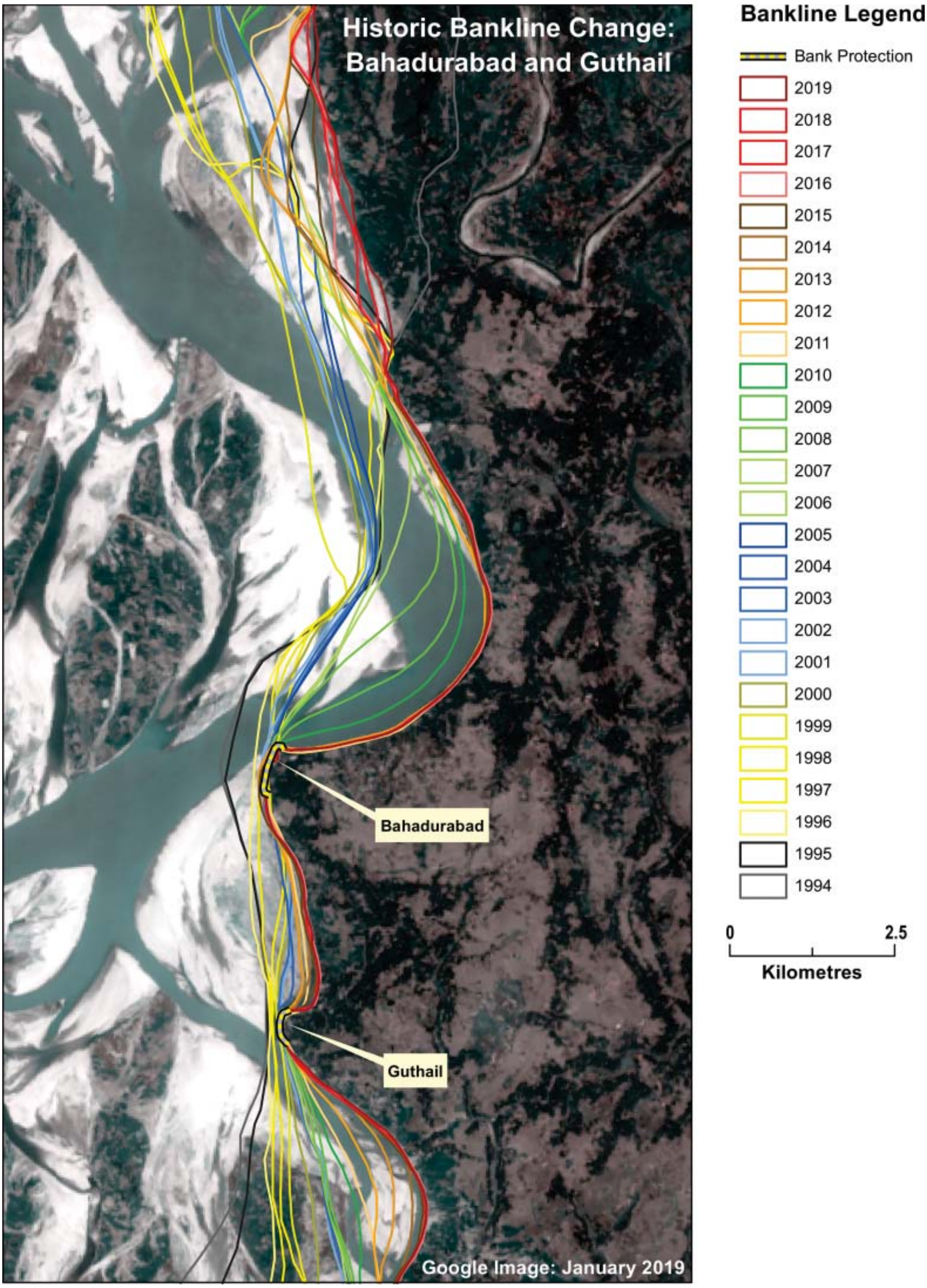

Figure 20.30 Bankline positions on the east (left) bank of the Jamuna River over 25 years near Bahadurabad, showing the success of revetments at Bahadurabad and Gutail in preventing bank erosion at these key sites. Source: Figure courtesy of Knut Oberhagemann and Saleh Adib Turash (FRERMIP) and the Center for Environmental and Geographic Information Services (CEGIS).

most vulnerable day-labourers (Mottaleb and Rahut 2019). In addition, the bridge improved cropping intensity by permitting better access to markets (Mottaleb and Rahut 2019) and also facilitated a shift from farm to non-farm employment, while decreasing household unemployment (Mahmud and Sawada 2018). Although construction of such large infrastructure appears to promote overall gains for Bangladesh, it still remains debatable as to whether the additional employments represent a net gain or merely a displacement of jobs from one region to the other (Mahmud and Sawada 2018).

The major challenge in constructing bridges across dynamic braid belts is to prevent the migrating channels eroding the approach embankment, and thus outflanking the bridge. In the nineteenth century, Horace Bell and Francis Spring developed a system based on guide bunds, originally termed ‘guide banks’ or ‘Bell’s bunds’, to protect the bridge abutments, and the roads or railways on the approach embankments, against erosion (Spring 1903). These arcuate embankments extend far enough upstream to prevent sinuous bends from breaching the approach embankment, whilst the upstream head of a guide bund is curved so that it can cope with channel and flow approach from different directions. The downstream tail is also curved, in order to locate the vulnerable termination of the structure outside any zone of deep scouring. The guide bunds of the Bangabandhu Bridge (Figures 20.31 and 20.32) are 2.1 km (West) and 2.2 km (East) long in upstream direction, and their slopes are relatively flat (1V : 5H and 1V : 6H) in order to reduce potential scour.

Whilst the Bangabandhu Bridge has withstood several years of high flows, including the largest flood of the twentieth century in 1998, the bridge site requires continual and sustained river engineering management, as revealed in satellite imagery over the period 1999–2019 (Figures 20.31 and 20.32). Klaassen et al. (2012) reviewed the performance of the river training works at the bridge in the period 1997–2009. They found the local bed scour depth at the western guide bund was almost 45 m below the average flood level, deeper than anticipated in the original design and tentatively ascribed to flow separation near the head of the guide bund. Such flow separation can create increased local flow velocities and turbulence, thereby aiding bed scour. Islam et al. (2017) examined the changing bar morphology 35 km upstream and downstream of the Bangabandhu Bridge, finding that the bridge construction induced an increase in both the area of bars and bar migration rates, which subsequently also generated problems with local bank erosion (see below).

The narrower river channel between the guide bunds hinders downstream migration of meander bends. Such migrating bends jam against the narrowed section and increase in amplitude: they become wider. Therefore, hard points were created upstream of the Bangabandhu Bridge in a funnel-shaped planform alignment, in order to guide migrating bends under the bridge without widening. Without such hard points, a danger would remain that bends would outflank the guide bunds, despite the upstream lengths of the bunds. The hard point at Sirajganj is one of the largest fixed, hard engineering structures on the Jamuna River, and its 2 km long embankment, termed the ‘B2 hardpoint’ (Figures 20.31 and 20.32), was constructed at an approximate cost of US$ 65 million to protect the large ferry terminal and market town. The B2 hardpoint was constructed of a ridge of locally dredged river sand and silt covered by a plastic and geotextile membrane, then superimposed by broken bricks and topped with 0.45 or 0.65 m^3 concrete blocks (Figure 20.33). Although largely successful, the B2 hardpoint suffered major failures between 15 August and 18 September during the 1998 flood season (Figure 20.34; Bashar 1999) when construction was 94% complete. A 32-m deep scour hole developed immediately downstream of the hardpoint ‘nose’, reaching a maximum during the height of the monsoon flood that was especially

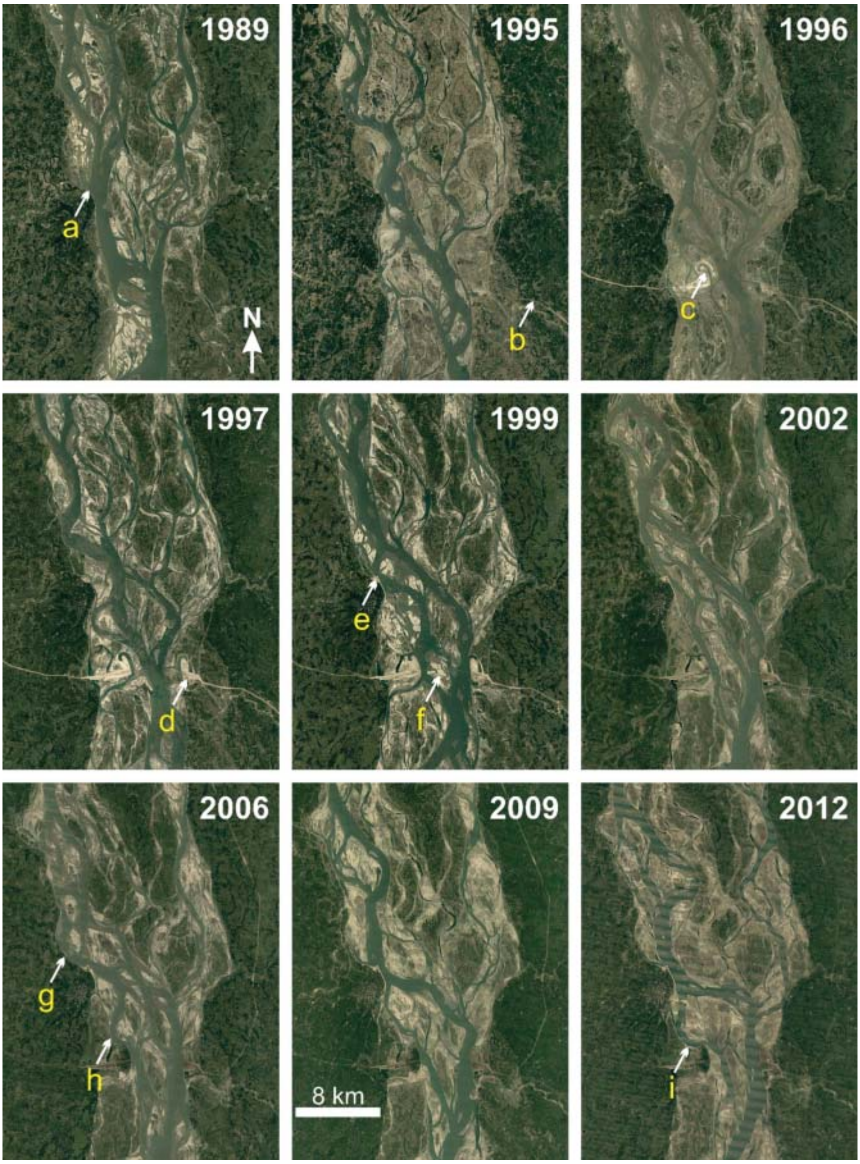

Figure 20.31 Landsat images of the Jamuna River in the vicinity of the B2 hardpoint at Sirajganj and the Bangabandhu Bridge, 1989–2012. Arrow label 'a' in 1989 denotes the location of the future B2 hardpoint, whilst label 'b' higlights the access road built for the Bangabandhu Bridge in 1995. Construction of the western and eastern guide bunds for the Bangabandhu Bridge is evident in 1996 (label 'c') and 1997 (label 'd'), respectively. The upstream nose of the Sirajganj B2 hardpoint is clearly evident in 1999 (label 'e') following severe west bank erosion in 1997 and 1998. This led to failures of the B2 hardpoint in 1998. A large sand bar has formed under the Bangabandhu Bridge by 1999 (label 'f'): this bar caused flow deflection, and erosion, on either side that resulted in the channel abutting both guide bunds (compare the areas of sediment around the guide bunds between 1997 and 1999). Note continued development of this bar in 2002, and changes to the complex of bars upstream and under the Bangabandhu Bridge in 2006–2012. Severe west bank erosion is evident upstream of the B2 hardpoint in 2006 (label 'g') and the Bangabandhu Bridge western guide bund (label 'h'), with the latter still experiencing intense erosion in 2012 that threatened outflanking of the Bangabandhu Bridge and its western guide bund. Source: Images courtesy of Google Earth.

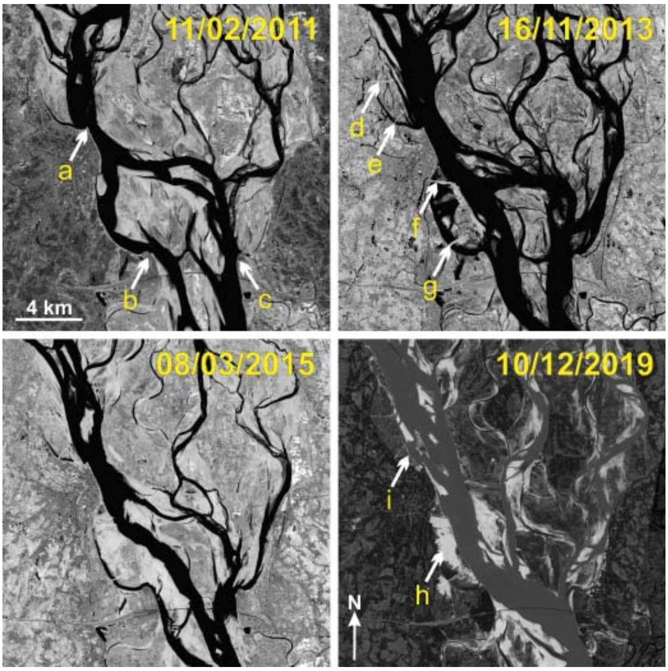

Figure 20.32 CubeSat images of the Jamuna River in the vicinity of the B2 hardpoint at Sirajganj and the Bangabandhu Bridge, 2011–2019. In 2011, the nose of the B2 hardpoint (label 'a') is clearly evident protruding into the main channel. The upstream nose of the western guide bund for the Bangabandhu Bridge (label 'b') is also evident as is the severe bank erosion occurring upstream of this site. The eastern guide bund (label 'c') also has the river channel adjacent to its structure. Severe bank erosion upsteam of the B2 hardpoint and western guide bund prompted the beginning of construction of four cross-bar groynes by 2013 (labels 'd, e, f, g') with infilling of these regions by sand dredging and pumping by 2015. Such bank protection is an ongoing task, with renewed erosion just upstream of the B2 hardpoint being evident in 2019 (label 'i') and the manifestation of ongoing sediment infill being shown by label 'h'. Source: Images courtesy of Planet Labs Inc.

prolonged in 1998, and caused collapse of at least four sections of the embankment. Repair costs were estimated in excess of US$ 10 million. Although now repaired and functioning well, the scale and cost of the damage that was inflicted on the B2 hardpoint illustrates the erosional threat of the Jamuna River and the magnitude of the problem faced by river engineers and geomorphologists working in such a dynamic alluvial environment. Similar to the diagnosis outlined by Klaassen et al. (2012) for unexpectedly deep scour at the head of the western guide bund, flow separation was an important factor in generating the deep scour near the 'nose' of the B2 hardpoint as confirmed by subsequent flow velocity measurements in 2008/2009 (Nakagawa et al. 2013). In addition, the changing planform configuration of the channels upstream of the nose of the hard point over the construction period in 1995–1999 (Figure 20.31) resulted in very different flows across the hard point nose that exacerbated the size, and erosive potential, of flow separation. This illustrates the key role of assessing the changing channel planform when assessing likely scour around such structures. However, contrary to the exacerbation of morphological conditions upstream of the river training works at Siraganj, the guide bunds at the Bangabandhu Bridge appear to have stabilized the channel pattern downstream of the bridge.

The complexity of morphological change, and the continuous need to assess channel

(a)

(b)

Figure 20.33 Construction of the B2 hardpoint at Sirajganj showing: (a) dredged river silt covered with geotextile membrane filter, then covered by broken brick and concrete cubes.
Source: Photograph courtesy of Mr Bob Courtier, W.S. Atkins Ltd. (b) 0.45 m^3 concrete blocks in place, view looking downstream from the hardpoint 'nose'.

change when managing large-scale infrastructure in the Jamuna River, is clearly shown over the last 30 years at the site of the B2 hardpoint and Bangabandhu Bridge (Figures 20.31 and 20.32). Once construction of the Bangabandhu Bridge had begun in 1995–1996, sedimentation underneath the main bridge span generated a mid-channel bar (Islam et al. 2017) that deflected flow to each side and caused erosion towards the west and east guide bunds (see 1999 image in Figure 20.31). Continuing sedimentation in the vicinity of the bridge also formed a large bar complex immediately upstream and adjacent to the bridge (see label f, Figure 20.31), which resulted in bank erosion on the west bank that threatened to outflank the bridge. As detailed above, erosion adjacent to the B2 hardpoint was caused by the changing alignment of the upstream channel, which was still causing flow to run across the hardpoint in the period 2006–2009 (see label 'g' in Figure 20.31). These two sites have been the location of major engineering works since 2013 (Figure 20.32) that have sought to reclaim land, and protect the west bank upstream of the B2 hardpoint and Bangabandhu Bridge, in order to lessen erosion problems in this region. In 2011, the B2 hardpoint and western guide bund (see labels 'a' and 'b' respectively in Figure 20.32) were exposed and vulnerable, and led to beginning of construction of four groynes (labels d–g, Figure 20.32) in 2013. The presence of these groynes, and sedimentation by sand that was pumped from adjacent channels and bars, allowed infill of these two regions, such that by 2015 these two areas were far better protected and the reclaimed land was already being farmed. An image from December 2019 shows that infilling by dredged sand is still ongoing in the southern area just north of the Bangabandhu Bridge (see label 'h', Figure 20.32) but that the B2 hardpoint and western guide bund are more stable. However, it is clear that monitoring and maintenance of these sites will be a continual practice, for even areas of recently reclaimed land are subject to continued erosion (label 'i', Figure 20.32). The images shown in Figure 20.32 over a period of eight years also illustrate the rapidly changing nature of sedimentation underneath the bridge (see Islam et al. 2017), and thus the changing velocities experienced at the guide bunds as flows are deflected by these bars.

Bank revetments and guide bunds are made of rocks or concrete cement blocks ('CC blocks'). However, rocks are expensive as they need to be imported, and producing concrete blocks consumes precious river sand and emits CO_2. Geobags are thus a cost-effective alternative (Oberhagemann and Hossain 2010; Asian Development Bank 2019). The Flood

Figure 20.34 Image of the B2 hardpoint in 1998 showing the multiple failures (white arrows) formed at the height of the 1998 flood. Flow towards viewer and the upstream nose of the B2 hardpoint is labelled. Source: Photograph courtesy of Mr. Bob Courtier, W.S. Atkins Ltd.

and Riverbank Erosion Risk Management Investment Program (FRERMIP) has applied geobags successfully for riverbank stabilization along the Jamuna River at Chauhali (Figure 20.35). Irrespective of the material used, all bank stabilization and river training structures require monitoring and, wherever necessary, repairs by dumping additional rocks, blocks, or geobags.

Engineers in South Asia have longstanding experience with using relatively light structures in the dry season to create, and deepen, navigation channels that connect ports and ferry landings to the main channels of the river. This annually repeated improvement of navigation channels is called 'bandalling'. Bandals refer to screens placed on poles at an angle to the flow, and oriented towards the channel axis downstream (see images and description in Nakagawa et al. 2013). These bandals aim to concentrate the upper, fast flows in the centre of the channel while generating sediment transport underneath towards the channel margins. They were originally called 'jhámp', whereas the present term 'bandal' originally referred to brushwood fascines

Figure 20.35 Sand-filled geotextile bags, or geobags, used for bank protection at Chauhali, Jamuna River. View looking upstream.

that were placed in channels to favour erosion of another, parallel channel. Spring (1903) therefore conjectured the word 'bandal' to be a vernacular corruption of the English word 'bundle' for 'fascine', used by crew members of steamers plying the rivers of British India. FAP21/22 piloted a similar type of screen on poles for flood conditions (see Mosselman 2006), but this high-water bandal became so massive that it lost the advantage of a light and flexible recurrent structure. Moreover, the functioning of bandals depends sensitively on their orientation with respect to the flow, which may vary considerably due to morphological changes occurring in the flood season. Bandals thus remain excellent for correcting the river bed at low flows but are not well suited for flood conditions.

Prioritization, planning, design, and implementation of river training and bank stabilization works require predictions of morphological development two to three years ahead, when the river may still be hundreds of metres away from the future structure (see example of B2 hardpoint above; Figure 20.31). For forward planning, land thus needs to be acquired, the population must be relocated, a construction camp set up, and equipment and materials imported to the area. Meanwhile, the river should not erode the site during these preparations. Moreover, a requirement within the FAP21/22 project was that the structure would be subjected to fluvial attack immediately after completion and within the monitoring period of the project so that its effectiveness could be assessed. These planning needs thus pose a great challenge to forecasting morphological developments. FAP21/22 developed an empirical prediction method, based on studying the year-to-year changes of the dry-season braided-anabranched channel pattern visible on satellite images. The method produced predictors for channel width changes, bend migration, and bifurcation development, including channel creation and abandonment (Klaassen and Masselink 1992; Klaassen et al. 1993; Mosselman 1995; Mosselman et al. 1995). The method was formulated in a probabilistic way, assigning probabilities of exceedance to rates of bank retreat and elaborating different cascades of downstream effects depending on the probabilities of channel creation and channel abandonment.

Jagers (2001, 2003) subsequently coded the empirical prediction method into a computer program that he called the 'branches model'. He also trained an artificial neural network on a set of dry-season satellite images of consecutive years, and compared the predictions from this network and the branches model with the erosion that occurred in reality (Figure 20.36). Although the agreement may seem poor at first sight, the models are successful in identifying the locations where the predictability of erosion was relatively good. This approach was successful in aiding the selection of suitable sites for pilot projects under FAP21/22.

The FAP19 project of the Flood Action Plan developed another empirical prediction method for riverbank erosion, also based on satellite images, but valid for shorter time spans. This method relies on the identification of a series of key sedimentary features, or bar forms, which are indicators for the ongoing morphological development of the Jamuna River planform. EGIS (2002) terms these features 'contraction bars', 'sharpened bars', 'sand wings', 'sand tongues', and 'bankside bars'. The lengths of downstream wings on either side of a bar, for instance, indicated on which side the river was the most active. EGIS (2002) merged the FAP19 and FAP21/22 methods into a single prediction method that is still operational at CEGIS in Dhaka. Figure 20.37 shows an example flow chart using this type of methodology that may be used to predict the rate of bank erosion on the outer banks of the Jamuna River. The empirical prediction depends strongly on the presence or absence of a bar ('sedimentary feature') downstream of the channel and the radius of curvature of the channel (ratio of the radius of the outer bank of the curved channel to the low flow width of the channel). Data on channel radius of curvature, channel width, and rate of annual bank erosion were derived from Landsat images for the period 1992–2000 to build upon earlier data reported by Klaassen and Masselink (1992) and Klaassen et al. (1993).

In parallel to the development of empirical prediction methods, Enggrob and Tjerry (1999) and Jagers (2003) pioneered the application of physics-based numerical models of fluvial morphodynamics to the Jamuna-Brahmaputra River. The Institute of Water Modelling (IWM) in Dhaka and several consultancy firms now use such models routinely to assess the effectiveness and impacts of interventions in the rivers of Bangladesh. For example, Schuurman et al. (2013, 2015) systematically studied numerical simulations of the morphological evolution of the Jamuna River, finding that their models reproduced the cascades of effects of the FAP21/22 method and the relation between sand wings and morphological activity of the FAP19 method. However, shortcomings remain. Because the numerical models are depth-averaged, and their computational cells are larger than the water depth, they do not represent the relevant details of subgrid processes such as bank erosion and structure-induced local scour. These shortcomings form key areas for further research and development.

Riverbank stabilization in the past 25 years, and the development of a variety of prediction methods, have shown that predicting and influencing channel change is possible in even the largest and most mobile of sand-bed braided rivers. Further development of our understanding and modelling of the controlling morphodynamic processes holds great potential for helping to maintain and implement bank protection structures along the Jamuna River. The most recent comprehensive reviews are provided by Oberhagemann et al. (2020), Van der Wal et al. (2020) and the reports of the Flood and Riverbank Erosion Risk Management Investment Program (FRERMIP: McLean et al. 2020). The latter program is being implemented by the Bangladesh Water Development Board (BWDB) from mid-2014

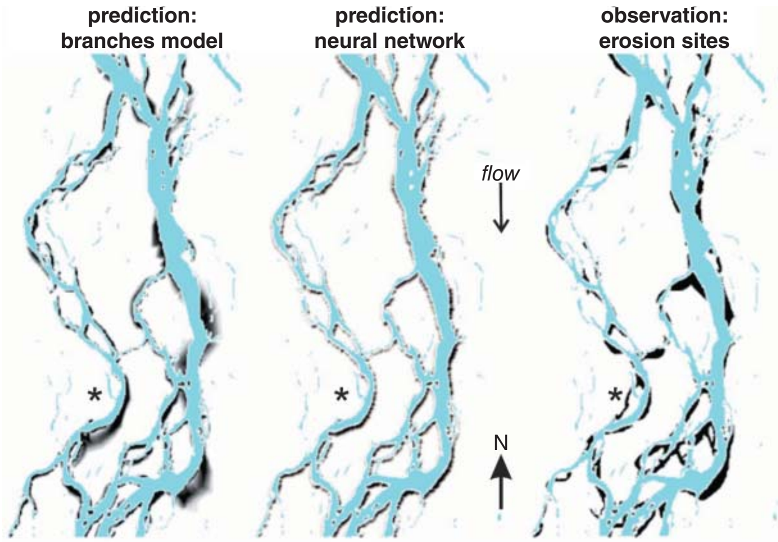

Figure 20.36 Comparison of bank erosion predictions by the branches model (left), the neural network (centre) and observations (right). Erosion of high mainland and island banks appears to be more predictable than the erosion of the margins of low chars. Source: Modified from Jagers (2001).

to mid-2023 and aims to address the stability of the Jamuna River.

20.8 Summary: What Does the Future Hold?

The Jamuna–Brahmaputra River is one of the World's truly great rivers and forms a dynamic and highly variable alluvial environment that has a huge impact on the daily lives of the growing population of Bangladesh. The past three decades have seen a massive increase in our knowledge of the behaviour of this dynamic river, and a growing realization that a holistic management approach is required to plan for, cope with, and benefit from floods (Yang et al. 2016; Barua 2018; Ferdous et al. 2018, 2019a). The early plans for large-scale engineering works along the Jamuna River (see reviews in Hossain 1994; Yakub 1994) have been shown to be inappropriate from a community and environmental perspective, let alone considerations of costs, but have set the agenda for some key schemes and approaches that have borne great benefits. Although the Flood Action Plan has had many critics and the nature of FAP changed greatly over the years (see papers in Haggart et al. 1994), hindsight now shows many highly valuable outputs from the FAP projects, including both a far-improved understanding of the processes and dynamics of the rivers of Bangladesh (Jagers 2003), and establishment of long-lived remote sensing, field survey and modelling capabilities that have led to better predictive tools for assessing channel change (EGIS 2002; Jagers 2003; Schuurman et al. 2015). This will be increasingly important in key infrastructural protection works, such as shown herein for the Bangabandhu Bridge, as well as bridges such as the Muktarpur Bridge across the Dhaleswari River and the multipurpose bridge across the Padma River, which is due for completion in 2022 at a total cost of $3.69 billion USD. Such remote sensing, field surveys, and numerical models will also provide better assessment of the impact of future river planform change, such as the potential movement of the Jamuna River into the channel of the Bangali River, near Sariakandi and Mathurapara (Figure 20.1).

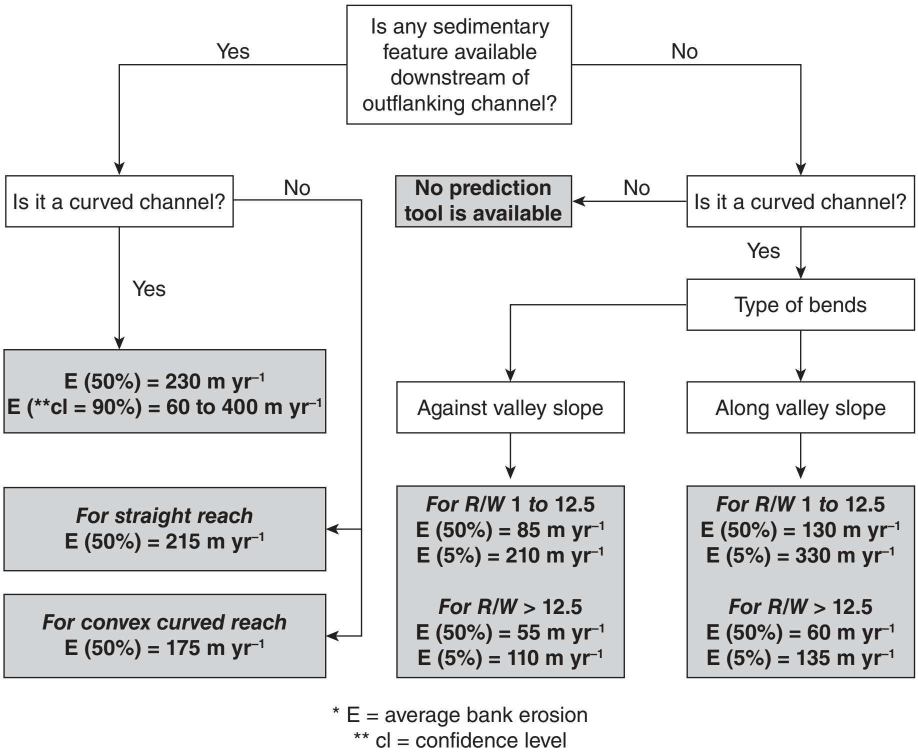

Figure 20.37 Flow diagram for predicting bank erosion along the outflanking channels of the Jamuna River. Data were obtained from 213 bends from sequential dry-season satellite images from 1992 to 2000. R and W are the radius of curvature to the outer bank line and the channel wetted width at low flow, respectively. Source: Modified from EGIS (2002).

It is also evident that the hydrology of the Ganga–Brahmaputra–Meghna basin will change in the future, with most models indicating an increased frequency and intensity of flood events (Arnell and Gosling 2016; Ali et al. 2019; Best 2019), with reductions in the return period of the current 100-year magnitude flood event (Hirabayashi et al. 2013). This change in river hydrology, and thus sediment transport and morphological change, will also have to be set in the context of human interventions as regards hydropower construction, water abstraction, and diversions (Yang et al. 2016; Best 2019), which could change markedly the amount of water routed along the Jamuna, with potential detrimental downstream effects as have been realized by construction of the Farraka Barrage across the Ganga River (Mirza 1998). The Jamuna River will also face increasing pressures from pollution, both from agricultural and urban sources, sand mining, as well as threats to its natural ecology, and fish yield.

Thus on a large spatial and temporal scale, Bangladesh faces many challenges in coping with changing water resources dictated by decisions taken outside its borders, and the potential effects of climatic change on the intensity of the monsoon and sea-level rise. The sustainable development of this transboundary river thus calls for an integrated approach across the climate-water-energy and food nexus, with major implications for security and international relations (Yang et al. 2016) and one in which transnational water diplomacy will be vital (Barua 2018). Barua (2018) views multitrack diplomacy as being essential to develop inclusive governance within the

Brahmaputra River Basin, and further progress in the 'Brahmaputra Dialogue' as being vital in the sustainable development of water resources that will play a vital role in poverty alleviation and raising living standards. It is also clear that management and governance must be rooted within socio-hydrological space (Ferdous et al. 2018) and that the co-evolution of social behavior, natural processes, and technological interventions give rise to different landscapes, styles of living, and ways to organize livelihoods in specific locations (Ferdous et al. 2018). Such a framework provides a more holistic way to assess adjustments to flooding, such as by adaptation and settling away from the river, or fighting the river by rising levees or dikes (Ferdous et al. 2018). The past twenty years have witnessed the immense benefits of adopting a multidisciplinary and multinational approach to studying these large rivers in Bangladesh. With the successful and continued development of infrastructure and expertise in Bangladesh (e.g. CEGIS, IWM, Bangladesh Water Development Board (BWDB)), working in close collaboration with Government policy (i.e. WARPO), and developing technologies for monitoring river and sediment flows from space, the future for assessing, predicting, and managing river channel change should become more attainable and therefore sustainably and environmentally acceptable.

Acknowledgements

We are very grateful to a wide range of organizations and individuals who have fostered, aided, and enthused our interests and research in Bangladesh over the past four decades. We are pleased to acknowledge the logistical and financial support of Delft Hydraulics and the Danish Hydraulics Institute as main contractors of the Flood Action Plan 24, the Flood Plan Coordinating Organization (FPCO) as client and the European Union as funding agency for FAP24. We are indebted to Gerrit Klaassen, Johan Grijsen, Maarten van der Wal, Hans Høyer, Dilip J. Barua, Zahirul Khan, and Kim Kyle for their considerable advice and support in the FAP24 River Survey Project, together with Captain Monjoor and the crew of DH survey vessel-A, whose skill and dedication in the field were central to the success of our projects. Part of the work conducted by JLB, PJA, and JR was funded by the UK Natural Environment Research Council through grant GR9/02034 and a NERC studentship to Roden, for which we are grateful. We would also like to acknowledge and sincerely thank the CEGIS for their assistance and provision of several of the Landsat images used in this paper. We are also very grateful to Sunando Bandyopadhyay, Steve Goodbred, Celine Grall, and Mike Steckler for providing copies of the artwork from their papers. Sadiul Chyon is thanked for information relating to the B2 hardpoint and Bangabandhu Bridge. The David Rumsey map collection is thanked for permission to reproduce Rennell's beautiful 1776 map (access to a wide range of historical maps can be found at www.davidrumsey.com). JLB gratefully acknowledges the Jack and Richard Threet chair in Sedimentary Geology, University of Illinois at Urbana-Champaign, for support in updating this chapter. We are grateful to David Appleyard and Alison Manson for their preparation of some of the original figures and to Chris Fielding for his thorough review of the original manuscript. Finally, we are very grateful to Avijit Gupta for his invitation to write this chapter and its revised version, his review comments, and his continuing enthusiasm and encouragement to complete it, which have again allowed us the opportunity to synthesize and incorporate some of the more recent work on this most beautiful and inspirational river.

References

Ahmed, K.M., Bhattacharya, P., Hasan, M.A. et al. (2004). Arsenic enrichment in groundwater of the alluvial aquifers in Bangladesh: an overview. *Applied Geochemistry* 19: 181–200.

Akter, J., Sarker, M.H., Popescu, I., and Roelvink, D. (2016). Evolution of the Bengal Delta and its prevailing processes. *Journal of Coastal Research* 32: 1212–1226.

Alam, M. (1984). Other natural hazards. In: *Rivers of Life* (eds. K. Haggart, S. Huq, A.A. Rahman, et al.), 151–170. Dhaka: Bangladesh Centre for Advanced Studies\Panos.

Alam, M.K., Hasan, A.K.M.S., Khan, M.R., and Whitney, J.W. (1990). *Geological Map of Bangladesh*. Geological Survey of Bangladesh.

Ali, M.H., Bhattacharya, B., Islam, A.K.M.S. et al. (2019). Challenges for flood risk management in flood-prone Sirajganj region of Bangladesh. *Journal of Flood Risk Management* 12 https://doi.org/10.1111/jfr3.12450.

Allison, M.A. (1998). Geologic framework and environmental status of the Ganges-Brahmaputra River. *Journal of Coastal Research* 14: 826–836.

Allison, M.A., Kuehl, S.A., Martin, T.C., and Hassan, A. (1998). The importance of floodplain sedimentation for river sediment budgets and terrigenous input to the oceans: insights from the Brahmaputra-Jamuna Rivers. *Geology* 26: 175–178.

Arnell, N.W. and Gosling, S.N. (2016). The impacts of climate change on river flood risk at the global scale. *Climate Change* 134: 387–401.

Asian Development Bank (2019). Project Performance Evaluation Report for Jamuna-Meghna River Erosion Mitigation Project in Bangladesh (Loan 1941). Asian Development Bank, Philippines, 17. https://www.adb.org/documents/bangladesh-jamuna-meghna-river-erosion-mitigation-project-0.

ASCE (1966). Nomenclature for bed forms in alluvial channels. Task force on bedforms in alluvial channels. *Journal of the Hydraulics Division* 92: 51–64.

Ashworth, P.J. (1996). Mid-channel bar growth and its relationship to local flow strength and direction. *Earth Surface Processes and Landforms* 21: 103–123.

Ashworth, P.J. and Lewin, J. (2012). How do big rivers come to be different? *Earth-Science Reviews* 114: 84–107. https://doi.org/10.1016/j.earscirev.2012.05.003.

Ashworth, P.J., Best, J.L., Roden, J.E. et al. (2000). Morphological evolution and dynamics of a large, sand braid-bar, Jamuna River, Bangladesh. *Sedimentology* 47: 533–555.

Baki, A.B.M. and Gan, T.Y. (2012). Riverbank migration and island dynamics of the braided Jamuna River of the Ganges-Brahmaputra basin using multi-temporal Landsat images. *Quaternary International* 263: 148–161.

Bandyopadhyay, S., Das, S. and Kar, N.S. (2021). Avulsion of the Brahmaputra in Bangladesh during the 18th–19th century: A review based on cartographic and literary evidence, Geomorphology, 384, 107696. https://doi.org/10.1016/j.geomorph.2021.107696.

Bangladesh Disaster and Emergency Sub-Group (BDER) (2004). Monsoon Floods 2004: Post Flood Needs Assessment Summary Report, 36, Dhaka, Bangladesh (https://reliefweb.int/sites/reliefweb.int/files/resources/0601496727BB568AC1256F230033FBC5-lcg-bang-6oct.pdf).

Barua, A. (2018). Water diplomacy as an approach to regional cooperation in South Asia: a case from the Brahmaputra basin. *Journal of Hydrology* 567: 60–70.

Barua, D.K. (1994). On the environmental controls of Bangladesh river systems. *Asia Pacific Journal on Environment and Development* 1: 81–98.

Bashar, M.A. (1999). A review of the bank protection works at Sirajganj, Unpublished Mechanical Engineering Thesis, Department of Water Resources Engineering, Bangladesh University of Engineering and Technology, 91 pp.

Begum, S. and Fleming, G. (1997a). Climate change and sea level rise in Bangladesh, Part I: numerical simulation. *Marine Geodesy* 20: 33–53.

Begum, S. and Fleming, G. (1997b). Climate change and sea level rise in Bangladesh, Part II: effects. *Marine Geodesy* 20: 55–68.

Best, J.L. (1996). The fluid dynamics of small-scale alluvial bedforms. In: *Advances in Fluvial Dynamics and Stratigraphy* (eds. P.A. Carling and M.R. Dawson), 67–125. Chichester: Wiley.

Best, J.L. (2005). The kinematics, topology and significance of dune-related macroturbulence: some observations from the laboratory and field. In: *Fluvial Sedimentology VII* (eds. M.D. Blum, S.B. Marriott and S. Leclair), Special Publication of the International Association of Sedimentologists, no. 35, 41–60. Oxford: Blackwell.

Best, J. (2019). Anthropogenic stresses on the world's big rivers. *Nature Geoscience* 12: 7–21. https://doi.org/10.1038/s41561-018-0262-x.

Best, J.L. and Ashworth, P.J. (1997). Scour in large braided rivers and the recognition of sequence stratigraphic boundaries. *Nature* 387: 275–277.

Best, J.L. and Kostaschuk, R.A. (2002). An experimental study of turbulent flow over a low-angle dune. *Journal of Geophysical Research* 107: 3135–3153.

Best, J.L., Kostaschuk, R.A., and Villard, P.V. (2001). Quantitative visualization of flow fields associated with alluvial sand dunes: results from the laboratory and field using ultrasonic and acoustic Doppler anemometry. *Journal of Vizualization* 4: 373–381.

Best, J.L., Ashworth, P.J., Bristow, C.S., and Roden, J.E. (2003). Three-dimensional sedimentary architecture of a large, mid-channel sand braid bar, Jamuna River, Bangladesh. *Journal of Sedimentary Research* 73: 516–530.

Bhuiyan, M.A.H., Kumamoto, T., and Suzuki, S. (2015). Application of remote sensing and GIS for evaluation of the recent morphological characteristics of the lower Brahmaputra-Jamuna River, Bangladesh. *Earth Science Informatics* 8: 551–568.

Bora, A.K. (2004). Fluvial geomorphology. In: *The Brahmaputra Basin Water Resources* (eds. V.P. Singh, N. Sharma and C.S.P. Ojha), 88–112. Dordrecht: Kluwer Academic Publishers.

Boyce, J.K. (1990). Birth of a megaproject: political economy of flood control in Bangladesh. *Environmental Management* 14: 419–428.

Brammer, H. (1995). *Geography of Soils of Bangladesh*. Dhaka, Bangladesh: The University Press.

Brammer, H. (2012). *The Physical Geography of Bangladesh*, 547. Dhaka, Bangladesh: The University Press Ltd.

Brammer, H. (2014). Bangladesh's dynamic coastal regions and sea-level rise. *Climate Risk Management* 1: 51–62.

Bridge, J.S. (1993). The interaction between channel geometry, water flow, sediment transport and deposition in braided rivers. In: *Braided Rivers* (eds. J.L. Best and C.S. Bristow), 13–71. London, UK: Geological Society of London, Special Publication, no. 75.

Bridge, J.S. and Lunt, I. (2006). Depositional models of braided rivers. In: *Braided Rivers: Process, Deposits, Ecology and Management* (eds. G.H. Sambrook Smith, J.L. Best, C.S. Bristow and G. Petts), Special Publication of the International Association of

Sedimentologists, no. 36, 11–50. Oxford: Blackwell.

Bristow, C.S. (1987). Brahmaputra River: channel migration and deposition. In: *Recent Developments in Fluvial Sedimentology* (eds. F.G. Ethridge, R.M. Flores and M.D. Harvey), 63–74. Tulsa, OK: Society of Economic Palaeontologists and Mineralogists, Special Publication, no. 39.

Bristow, C.S. (1993a). Sedimentary structures in bar tops in the Brahmaputra River, Bangladesh. In: *Braided Rivers* (eds. J.L. Best and C.S. Bristow), 277–289. London, UK: Geological Society of London, Special Publication, no. 75.

Bristow, C.S. (1993b). Sedimentology of the rough rock: a Carboniferous braided river sheet sandstone in northern England. In: *Braided Rivers* (eds. J.L. Best and C.S. Bristow), 291–304. Geological Society, Special Publication, no. 75.

Bristow, C.S. (1999). Avulsion, river metamorphosis and reworking by underfit streams: a modern example from the Brahmaputra River in Bangladesh and a possible ancient example in the Spanish Pyrenees. In: *Fluvial Sedimentology VI* (eds. N.D. Smith and J. Rogers), 221–230. International Association of Sedimentologists, Special Publication, no. 28.

Burger, J.W., Klaassen, G.J., and Prins, A. (1988). Bank erosion and channel processes in the Jamuna River, Bangladesh. In: *Proceedings of the International Symposium on the Impact of River Bank Erosion, Flood Hazard and the Problem of Population Displacement*, 1–17. Dhaka, Bangladesh.

Cant, D.J. and Walker, R.G. (1978). Fluvial processes and facies sequences in the sandy braided South Saskatchewan River, Canada. *Sedimentology* 25: 625–648.

Center for Environmental and GIS Support Project for Water Sector Planning (CEGIS) (2003). *Morphological Analyses and Prediction for the Jamuna River around the PIRDP Site*, Prepared for Jamuna-Meghna River erosion Mitigation Project, BWDB, Dhaka, Bangladesh.

Centre for Policy Dialogue (CPD) (2004) *Rapid Assessment of Flood 2004: Interim Report*, August 12 2004, Dhaka, 47 pp. (see http://www.cpd-bangladesh.org/flood.pdf and http://www.cpd-bangladesh.org).

Choudhury, A.M., Haque, M.A., and Quadir, D.A. (1997). Consequences of global warming and sea level rise in Bangladesh. *Marine Geodesy* 20: 13–31.

Chowdhury, M. (1994). Fisheries. In: *Rivers of Life* (eds. K. Haggart, S. Huq, A.A. Rahman, et al.), 95–120. Dhaka: Bangladesh Centre for Advanced Studies\Panos.

Chowdhury, M.R. (2000). An assessment of flood forecasting in Bangladesh: the experience of the 1998 flood. *Natural Hazards* 22: 139–169.

Cisneros, J., Best, J., van Dijk, T. et al. (2020). Dunes in the world's big rivers are characterized by low-angle lee-side slopes and a complex shape. *Nature Geoscience* 13: 156–162.

Coleman, J.M. (1969). Brahmaputra River: channel processes and sedimentation. *Sedimentary Geology* 3: 129–239.

Crosato, A. and Mosselman, E. (2009). Simple physics-based predictor for the number of river bars and the transition between meandering and braiding. *Water Resources Research.* 45: W03424.

de Graaf, G. (2003). The flood pulse and growth of floodplain fish in Bangladesh. *Fisheries Management and Ecology* 10: 241–247.

Dixon, S.J., Sambrook Smith, G.H., Best, J.L. et al. (2018). The morphodynamics of river confluences: insights from analysis of remotely sensed imagery. *Earth-Science Reviews* 176: 1–18.

Elahi, K.M., K.S. Ahmed & M. Mafizuddin (1991) *Riverbank erosion, flood and population displacement in Bangladesh*. Riverbank erosion impact study, Publ. Jahangirnagar Univ., Dhaka, Bangladesh.

Enggrob, H.G. and Tjerry, S. (1999). Simulation of morphological characteristics of a braided river. In: *Proceedings of the IAHR Symposium* *on River, Coastal and Estuarine Morphodynamics*, Genova, 6–10 September 1999, vol. I, 585–594.

Environmental and GIS Support Project for Water Sector Planning (EGIS) (1997) *Morphological Dynamics of the Brahmaputra-Jamuna River*. Prepared for Water Resources Planning Organization, Dhaka, Bangladesh, 76 pp.

Environmental and GIS Support Project for Water Sector Planning (EGIS) (2000) *Remote Sensing, GIS and Morphological Analyses of the Jamuna River, 2000, Part II*, Dhaka, Bangladesh.

Environmental and GIS Support Project for Water Sector Planning (EGIS) (2002) *Developing and Updating the Empirical Methods for Predicting the Morphological Changes in the Jamuna River*, EGIS Technical Note Series 29, Dhaka, Bangladesh.

Ferdous, M.R., Wesselink, A., Brandimarte, L. et al. (2018). Socio-hydrological spaces in the Jamuna River floodplain in Bangladesh. *Hydrology and Earth System Science* 22: 5159–5173.

Ferdous, M.R., Wesselink, A., Brandimarte, L. et al. (2019a). The costs of living with floods in the Jamuna floodplain in Bangladesh. *Water* 11 https://doi.org/10.3390/w11061238.

Ferdous, M.R., Wesselink, A., Brandimarte, L. et al. (2019b). The levee effect along the Jamuna River in Bangladesh. *Water International* 44: 496–519.

Flood Action Plan 24; Delft Hydraulics and DHI (1996a) *FAP24 River Survey Project, Final Report, Main Volume* (prepared for FPCO), Dhaka, Bangladesh, 280 pp.

Flood Action Plan 24; Delft Hydraulics and DHI (1996b) *FAP24 River Survey Project, Final Report – Annex 3: Hydrology* (prepared for FPCO), Dhaka, Bangladesh.

Flood Action Plan 24; Delft Hydraulics and DHI (1996c) *FAP24 River Survey Project, Final Report – Annex 4: Sedimentology*, (prepared for FPCO), Dhaka, Bangladesh.

Flood Action Plan 24; Delft Hydraulics and DHI (1996d) *FAP24 River Survey Project, Final Report – Annex 5: Morphological Characteristics* (prepared for FPCO), Dhaka, Bangladesh.

Flood Action Plan 24; Delft Hydraulics and DHI (1996e) *FAP24 River Survey Project, Special Report 6, Floodplain levels and bankfull discharge* (prepared for FPCO), Dhaka, Bangladesh.

Flood Action Plan 24; Delft Hydraulics and DHI (1996f) *FAP24 River Survey Project, Special Report 10, Morphology of the Gorai Offtake* (prepared for FPCO), Dhaka, Bangladesh, 158 pp and Appendices.

Flood Action Plan 24; Delft Hydraulics, DHI and Leeds University (1996g) *FAP24 River Survey Project, Special Report 9, Bedform and bar dynamics in the main rivers of Bangladesh* (prepared for FPCO), Dhaka, Bangladesh, 107 pp.

Flood Action Plan 24; Delft Hydraulics and DHI (1996h) *FAP24 River Survey Project, Special Report 14, Physical properties of river sediments* (prepared for FPCO), Dhaka, Bangladesh, 36 pp.

Flood Plan Coordinating Organisation (FPCO) (1995) *Bangladesh Water and Flood Management Strategy*, FPCO, Dhaka, Bangladesh, 22 pp.

Fujita, Y. (1989). Bar and channel formation in braided streams. In: *River Meandering*, Water Research Monograph, vol. 12 (eds. S. Ikeda and G. Parker), 417–462. Washington, DC: American Geophysical Union.

Goodbred, S.L. Jr., and Kuehl, S.A. (2000a). The significance of large sediment supply, active tectonism, and eustasy on sequence development: Late Quaternary stratigraphy and evolution of the Ganges-Brahmaputra delta. *Sedimentary Geology* 133: 227–248.

Goodbred, S.L. Jr., and Kuehl, S.A. (2000b). Enormous Ganges-Brahmaputra sediment load during strengthened early Holocene monsoon. *Geology* 27: 559–562.

Goodbred, S.L. Jr.,, Kuehl, S.A., Steckler, M.S., and Sarker, M.H. (2003). Controls on facies distribution and stratigraphic preservation in the Ganges-Brahmaputra delta sequence. *Sedimentary Geology* 155: 301–316.

Goodbred, S.L., Paolo, P.M., Ullah, M.S. et al. (2014). Piecing together the Ganges-Brahmaputra-Meghna River delta: use of sediment provenance to reconstruct the history and interaction of multiple fluvial systems during Holocene delta evolution. *Geological Society of America Bulletin* 126: 1495–1510.

Grall, C., Steckler, M.S., Pickering, J.L. et al. (2018). A base-level stratigraphic approach to determining Holocene subsidence of the Ganges–Meghna–Brahmaputra Delta plain. *Earth and Planetary Science Letters* 499: 23–36.

Grimaud, J.-L., Grall, C., Goodbred, S. et al. (2019). Flexural deformation controls on Late Quaternary sediment dispersal in the Garo-Rajmahal Gap, NW Bengal Basin. *Basin Research* https://doi.org/10.1111/bre.12425.

Haggart, K., Huq, S., Rahman, A.A. et al. (eds.) (1994). *Rivers of Life*. Dhaka: Bangladesh Centre for Advanced Studies\Panos, 244 pp.

Heroy, D.C., Kuehl, S.A., and Goodbred, S.L. Jr., (2003). Mineralogy of the Ganges and Brahmaputra rivers: implications for river switching and Late Quaternary climate change. *Sedimentary Geology* 155: 343–359.

Hirabayashi, Y., Mahendran, R., Koirala, S. et al. (2013). Global flood risk under climate change. *Nature Climate Change* 3: 816–821.

Hofer, T. and Messerli, B. (2006). *Floods in Bangladesh: History, Dynamics and Rethinking the Role of the Himalayas*. Tokyo: United Nations University Press, 468 pp.

Hossain, M.M. (1993). Economic effects of riverbank erosion: some evidence from Bangladesh. *Disasters* 17: 25–32.

Hossain, M. (1994). Existing embankments. In: *Rivers of Life* (eds. K. Haggart, S. Huq, A.A. Rahman, et al.), 51–76. Dhaka: Bangladesh Centre for Advanced Studies\Panos.

Huang, S.Y., Chen, Y.G., Burr, G.S. et al. (2014). Late Pleistocene sedimentary history of multiple glacially dammed lake episodes along the Yarlung-Tsangpo River, southeast Tibet. *Quaternary Research* 82: 430–440.

Islam, M.F. and Rashid, A.N.M.B. (2011). Riverbank erosion displacees in Bangladesh: need for institutional response and policy intervention. *Bangladesh Journal of Bioethics* 2: 4–19.

Islam, M.R., Begum, S.F., Yamaguchi, Y., and Ogawa, K. (1999). The Ganges and Brahmaputra rivers in Bangladesh: basin denundation and sedimentation. *Hydrological Processes* 13: 2907–2923.

Islam, M.S., Sultana, S., Saifunnahar, and Miah, M.A. (2014). Adaptation of char livelihood in flood and river erosion areas through indigenous practice: a study on Bhuapur riverine area in Tangail. *Journal of Environmental Science and Natural Resources* 7: 13–19.

Islam, N. (2001). The open approach to flood control: the way to the future in Bangladesh. *Futures* 33: 783–802.

Islam, R., Islam, M.N., and Islam, M.N. (2017). Impacts of Bangabandhu Jamuna Multi-purpose Bridge on the dynamics of bar morphology at the Jamuna River in Bangladesh. *Modeling Earth Systems and Environment* 3: 903–925.

ISPAN (FAP 16 and FAP 19), (1993) *The Dynamic Physical and Human Environment of Riverine Charlands: Jamuna*, Dhaka, Bangladesh.

ISPAN (FAP 16 and FAP 19) (1995) *A Study of Sedimentation in the Brahmaputra-Jamuna Floodplain*, Dhaka, Bangladesh.

Jackson, R.G. (1976). Sedimentological and fluid-dynamic implications of the turbulence bursting phenomenon in geophysical flows. *Journal of Fluid Mechanics* 77: 531–560.

Jagers, B. (2001). A comparison of prediction methods for medium-term planform changes in braided rivers. In: *Proc. 2nd IAHR Symp. River, Coastal and Estuarine Morphodynamics* (ed. S. Ikeda), 10-14 Sept. 2001, 713–722. Obihiro, Japan.

Jagers, H.R.A. (2003) *Modelling planform changes of braided rivers*, PhD thesis, University of Twente, The Netherlands, 313 pp.

Julien, P.Y. and Klaassen, G.J. (1995). Sand-dune geometry of large rivers during flood. *Journal of Hydraulic Engineering* 121: 657–663.

Kattelman, R. (1990). Conflicts and cooperation over floods in the Himalaya-Ganges region. *Water International* 15: 189–194.

Khan, N.I. and Islam, A. (2003). Quantification of erosion patterns in the Brahmaputra-Jamuna River using geographical information system and remote sensing techniques. *Hydrological Processes* 17: 959–966.

Klaassen, G.J. and Vermeer, K. (1988). Confluence scour in a large braided river with fine bed material. In: *Proceedings of the International Conference on Fluvial Hydraulics*, Budapest, Hungary, 395–408. Budapest: International Association of Hydraulic Research.

Klaassen, G.J. and Masselink, G. (1992). Planform changes of a braided river with fine sand as bed and bank material. In: *Proceedings of the 5th International Symposium on River Sedimentation* (eds. P. Larson and N.E. Eisenhauer), 459–471. Karlsruhe, Germany.

Klaassen, G.J., Vermeer, K., and Uddin, N. (1988). Sedimentological processes in the Jamuna (Lower Brahmaputra) river, Bangladesh. In: *Proceedings of the International Conference on Fluvial Hydraulics*, 381–394. Budapest, Hungary.

Klaassen, G.J., Mosselman, E., and Brühl, H. (1993). On the prediction of planform changes of braided sand-bed rivers. In: *Advances in Hydroscience and Engineering* (ed. S.S.Y. Wang), 134–146. Washington, DC: University of Mississippi.

Klaassen, G.J., Van Duivendijk, H., and Sarker, M.H. (2012). Performance review of Jamuna Bridge River Training Works 1997-2009. In: *River Flow 2012* (ed. R.E.M. Muñoz). ISBN: 978-0-415-62129-8, Proc. Int. Conf. on Fluvial Hydraulics, San José, Costa Rica, 5-7 September 2012.

Kostaschuk, R. and Villard, P. (1996). Flow and sediment transport over large subaqueous dunes: Fraser River, Canada. *Sedimentology* 43: 849–863.

Krien, Y., Karpytchev, M., Ballu, V. et al. (2019). Present-day subsidence in the Ganges-Brahmaputra-Meghna Delta: Eastern amplification of the Holocene sediment loading contribution. *Geophysical Research Letters* 46: 10764–10772.

Lang, K.A., Huntington, K.W., and Montgomery, D.R. (2013). Erosion of the Tsangpo Gorge by megafloods, Eastern Himalaya. *Geology* 41: 1003–1006.

Latrubesse, E.M. (2008). Patterns of anabranching channels: The ultimate end-member adjustment of mega rivers. *Geomorphology* 101: 130–145.

La Touche, T.H.D. (1910). Relics of the great Ice Age in the plains of northern India, reprinted (1919). In: *Report on the Hooghly River and its Head waters*, vol. I, 21–22. Calcutta: The Bengal Secretariat Book Depot.

Leopold, L.B. and Wolman, M.G. (1957) River channel patterns: braided, meandering and straight, *Professional Paper United States Geological Survey*, 262-B, 51 pp.

Liu, W., Lai, Z., Hu, K. et al. (2015). Age and extent of a giant glacial-dammed lake at Yarlung Tsangpo gorge in the Tibetan Plateau. *Geomorphology* 246: 370–376.

Mahmud, M. and Sawada, Y. (2018). Infrastructure and well-being: employment effects of the Jamuna bridge in Bangladesh. *Journal of Development Effectiveness* 10: 327–340.

McLean, D., Oberhagemann, K., Wiebe, H. and Bennett, S. (2020). River Stabilization and Development: Jamuna-Padma and Dependent Areas, Main Report, Northwest Hydraulic Consultants and Euroconsult Mott MacDonald, Edmonton, Canada, 160pp.

McLelland, S.J., Ashworth, P.J., Best, J.L. et al. (1999). Flow structure and transport of sand-grade suspended sediment around an evolving braid-bar, Jamuna River, Bangladesh. In: *Fluvial Sedimentology 6* (eds. N.D. Smith and J. Rogers), 43–57. International

Association of Sedimentologists, Special Publication, no. 28.

Miall, A.D. and Jones, B.G. (2003). Fluvial architecture of the Hawkesbury Sandstone (Triassic), near Sydney, Australia. *Journal of Sedimentary Research* 73: 531–545.

Mirza, M.M.Q. (1998). Diversion of the Ganges water at Farakka and its effects on salinity in Bangladesh. *Environmental Management* 22: 711–722.

Mirza, M.M.Q. (2002). Global warming and changes in the probability of occurrence of floods in Bangladesh and implications. *Global Environmental Change* 12: 127–138.

Mirza, M.M.Q. (ed.) (2004). *The Ganges Water Diversion: Environmental Effects and Implications*, 367. Dordrecht: Kluwer Academic Publishers.

Mirza, M.M.Q., Warrick, R.A., Ericksen, N.J., and Kenny, G.J. (2001). Are floods getting worse in the Ganges, Brahmaputra and Meghna basins? *Environmental Hazards* 3: 37–48.

Montgomery, D.R., Hallet, B., Yuping, L. et al. (2004). Evidence for Holocene megafloods down the Tsangpo River gorge, southeastern Tibet. *Quaternary Research* 62: 201–207. https://doi.org/10.1016/j.yqres.2004.06.008.

Morgan, J.P. and McIntire, W.G. (1959). Quaternary geology of the Bengal Basin, East Pakistan and India. *Bulletin of the Geological Society of America* 70: 319–342.

Mosselman, E. (1995). A review of mathematical models of river planform changes. *Earth Surface Processes and Landforms* 20 (7): 661–670.

Mosselman, E., Huisink, M., Koomen, E., and Seymonsbergen, A.C. (1995). Morphological changes in a large braided sand-bed river. In: *River Geomorphology* (ed. E.J. Hickin), 235–247. Wiley.

Mosselman, E. (2006). Bank protection and river training along the braided Brahmaputra-Jamuna River, Bangladesh. In: *Braided Rivers: Process, Deposits, Ecology and Management* (eds. G.H. Sambrook Smith, J.L. Best, C.S. Bristow and G. Petts), Special Publication of the International Association of Sedimentologists, No. 36, 277–288. Oxford: Blackwell.

Mottaleb, K.A. and Rahut, D.B. (2019). Impacts of improved infrastructure on labor allocation and livelihoods: the case of the Jamuna Multipurpose Bridge, Bangladesh. *European Journal of Development Research* 31: 750–778.

Nakagawa, H., Zhang, H., Baba, K., and Teraguchi, H. (2013). Hydraulic characteristics of typical bank-protection works along the Brahmaputra/Jamuna River, Bangladesh. *Journal of Flood Risk Management* 6: 345–359. https://doi.org/10.1111/jfr3.12021.

Oberhagemann, K., Aminul Haque, A.M., and Thompson, A. (2020). A century of riverbank protection and river training in Bangladesh. *Water* 12: 3018. https://doi.org/10.3390/w12113018.

Oberhagemann, K. and Hossain, M.M. (2010). Geotextile bag revetments for large rivers in Bangladesh. *Geotextiles and Geomembranes* https://doi.org/10.1016/j.geotexmem.2010.12.003.

Ogink, H.J.M. (1988) *Hydraulic roughness of bedforms*, Delft Hydraulics Report M2017.

Ojha, C.S.P. and Singh, V.P. (2004). Introduction. In: *The Brahmaputra Basin Water Resources* (eds. V.P. Singh, N. Sharma and C.S.P. Ojha), 1–16. Dordrecht: Kluwer Academic Publishers.

Parsons, D.R., Best, J.L., Lane, S.N. et al. (2005). The morphology and flow fields of 3D dunes, Rio Paraná, Argentina: results from simultaneous multibeam echo sounding and acoustic Doppler profiling. *Journal of Geophysical Research, Earth Surface* 110: F04503. https://doi.org/10.1029/2004JF00231.

Patel, T. (1996) Bridge over troubled water, *New Scientist*, November, 12–13.

Paul, B.K. (1997). Flood research in Bangladesh in retrospect and prospect: a review. *Geoforum* (2): 121–131.

Pickering, J.L., Diamond, M.S., Goodbred, S.L. et al. (2019). Impact of glacial-lake paleofloods on valley development since glacial termination II: a conundrum of hydrology and scale for the lowstand Brahmaputra-Jamuna paleovalley system. *GSA Bulletin* 131: 58–70.

Pickering, J.L., Goodbred, S.L., Reitz, M.D. et al. (2014). Late Quaternary sedimentary record and Holocene channel avulsions of the Jamuna and Old Brahmaputra River valleys in the upper Bengal delta plain. *Geomorphology* 227: 123–136.

Rahman, M.M., Dustegir, M., Karim, R. et al. (2018). Recent sediment flux to the Ganges-Brahmaputra-Meghna delta system. *Science of the Total Environment* 643: 1054–1064.

Rao, M.P., Cook, E.R., Cook, B.I., et al. (2020). Seven centuries of reconstructed Brahmaputra River discharge demonstrate underestimated high discharge and flood hazard frequency. Nature Commun., 11: 6017, https://doi.org/10.1038/s41467-020-19795-6.

Reavill, L.R.P. and Rahman, T.G. (1995). A systems-science-based analysis of the factors that influence and aggravate the effects of flooding in Bangladesh. *Technological Forecasting and Social Change* 49: 89–101.

Reitz, M.D., Pickering, J.L., Goodbred, S.L. et al. (2015). Effects of tectonic deformation and sea level on river path selection: theory and application to the Ganges-Brahmaputra-Meghna River delta. *Journal of Geophysical Research: Earth Surface* 120: 671–689.

Rennell, J.J. (1776). *An actual survey of the provinces of Bengal, Bahar etc. by Major General James Rennell, Surveyor to the Honourable East India Company* (as referenced in Bristow, 1999).

Richardson, W.R.R. and Thorne, C.R. (1998). Secondary currents around braid bar in Brahmaputra River, Bangladesh. *Journal Hydraulic Engineering* 124: 325–328.

Richardson, W.R.R. and Thorne, C.R. (2001). Multiple thread flow and channel bifurcation in a braided river: Brahmaputra-Jamuna River, Bangladesh. *Geomorphology* 38: 185–196.

Richardson, W.R.R., Thorne, C.R., and Mahmood, S. (1996). Secondary flow and channel changes around a bar in the Brahmaputra River, Bangladesh. In: *Coherent Flow Structures in Open Channels* (eds. P.J. Ashworth, S.J. Bennett, J.L. Best and S.J. McLelland), 520–543. Chichester: Wiley.

River Bank Improvement Program (RBIP) (2015). Morphology. Feasibility Report and detailed design priority reach, Annex A Volume 1 Final Report, May 2015, Volume 2. Part 2: Sediment Wave Assessment, 63 pp.

Roden, J.E. (1998) *Sedimentology and dynamics of mega-sand dunes, Jamuna River, Bangladesh, PhD thesis*, University of Leeds, 310 pp.

Sambrook Smith, G.H., Ashworth, P.J., Best, J.L. et al. (2005). The morphology and facies of sandy braided rivers: some considerations of scale invariance. In: *Fluvial Sedimentology VII* (eds. M.D. Blum, S.B. Marriott and S. Leclair), International Association of Sedimentologists, 145–158. Oxford: Blackwell.

Sambrook Smith, G.H., Ashworth, P.J., Best, J.L. et al. (2006). Alluvial architecture and sedimentology of the sandy braided South Saskatchewan River, Canada. *Sedimentology*: 53. https://doi.org/10.1111/j.1365–3091.2005.00769.x.

Sambrook Smith, G.H., Nicholas, A.P., Best, J.L. et al. (2019). The sedimentology of river confluences. *Sedimentology* 66: 391–407.

Sarker, M.H. (1996) Morphological processes in the Jamuna River, MSc thesis, International Institute for Hydraulic and Environmental Engineering, Delft, the Netherlands, 175 pp.

Sarker, M.H. (2009) Morphological response of the Brahmaputra–Jamuna–Padma–Lower Meghna River to the Assam earthquake of 1950. PhD thesis, University of Nottingham, UK, 297 pp.

Sarker, M.H. and Thorne, C.R. (2006). Morphological response of the Brahmaputra-Padma-Lower Meghna River system to the Assam earthquake of 1950. In: *Braided Rivers: Process, Deposits, Ecology and Management* (eds. G.H. Sambrook Smith, J.L. Best, C.S. Bristow and G. Petts), Special Publication of the International Association of

Sedimentologists, no. 36, 289–310. Oxford: Blackwell.

Sarker, M.H., Huque, I., Alam, M., and Koudstaal, R. (2003). Rivers, chars, and char dwellers of Bangladesh. *International Journal of River Basin Management* 1: 61–80.

Sarker, M.H., Akter, J., Ferdous, M.R., and Noor, F. (2011). Sediment dispersal processes and management in coping with climate change in the Meghna Estuary, Bangladesh. In: *Proceedings of the Workshop on Sediment Problems and Sediment Management in Asian River Basins*, vol. 349, 203–218. (Hyderabad, India, IAHS), Publication.

Sarker, M.H., Thorne, C.R., Aktar, M.N., and Ferdous, M.R. (2014). Morpho-dynamics of the Brahmaputra-Jamuna River, Bangladesh. *Geomorphology* 215: 45–59.

Sarker, M.N.I., Wu, M., Alam, G.M.M., and Shouse, R.C. (2019). Livelihood vulnerability of riverine-island dwellers in the face of natural disasters in Bangladesh. *Sustainability* 11 https://doi.org/10.3390/su11061623.

Schmuck-Widmann, H. (2001) *Facing the Jamuna: indigenous and engineering knowledge in Bangladesh*, Bangladesh Resource Centre for Indigenous Knowledge, Dhaka, Bangladesh, 242 pp.

Schumm, S.A. and Winkley, B.R. (1994). The character of large alluvial rivers. In: *The Variability of Large Alluvial Rivers* (eds. S.A. Schumm and B.R. Winkley), 1–13. New York: American Society of Civil Engineers.

Schuurman, F., Kleinhans, M.G., and Marra, W.A. (2013). Physics-based modeling of large braided sand-bed rivers: bar pattern formation, dynamics, and sensitivity. *Journal of Geophysical Research* 118: 2509–2527.

Schuurman, F., Kleinhans, M.G., and Middelkoop, H. (2015, 2015). Network response to internal and external perturbations in large sand-bed braided rivers. *Earth Surface Dynamics Discussions* 3 (1): 197–250.

Seijmonsbergen, A.C. (1999). The influence of neo-tectonics on river patterns in Bangladesh; a preliminary study based on Landsat MSS imagery. *Geologie en Mijnbouw* 77: 129–135.

Shampa and Ali, M.M. (2019). Interaction between the braided bar and adjacent channel during flood: a case study of a sand-bed braided river, Brahmaputra–Jamuna. *Sustainable Water Resources Management* 5: 947–960.

Shankar, B., Halls, A., and Barr, J. (2004). Rice versus fish revisited: on the integrated management of floodplain resources in Bangladesh. *Natural Resources Forum* 28: 91–101.

Sincavage, R., Goodbred, S., and Pickering, J. (2018). Holocene Brahmaputra River path selection and variable sediment bypass as indicators of fluctuating hydrologic and climate conditions in Sylhet Basin, Bangladesh. *Basin Research* 30: 302–320.

Singh, S.K. (2007). Erosion and weathering in the Brahmaputra River system. In: *Large Rivers: Geomorphology and Management* (ed. A. Gupta), 373–393. Chichester: Wiley.

Singh, V.P., Sharma, N., and Ojha, C.S.P. (eds.) (2004). *The Brahmaputra Basin Water Resources*, 632. Dordrecht: Kluwer Academic Publishers.

Smith, J.D. and McLean, S.R. (1977). Spatially-averaged flow over a wavy surface. *Journal of Geophysical Research* 82: 1735–1746.

Spring, F.J.E. (1903). The training of certain great rivers in Northern India, so that they may not outflank the works which span them. Tech. paper No. 153, Railway Board, Government of India.

Steckler, M., Mondal, D., Akhter, S. et al. (2016). Locked and loading megathrust linked to active subduction beneath the Indo-Burman Ranges. *Nature Geoscience* 9: 615–618.

Strick, R.J.P., Ashworth, P.J., Sambrook Smith, G.H. et al. (2019). Quantification of bedform dynamics and bedload sediment flux in sandy braided rivers from airborne and satellite imagery. *Earth Surface Processes and Landforms* 44: 953–972.

Takagi, T., Oguchi, T., Matsumoto, J. et al. (2007). Channel braiding and stability of the Brahmaputra River, Bangladesh, since 1967: GIS and remote sensing analyses. *Geomorphology* 85: 294–305.

Ten Brinke, W.B.M., Wilbers, A.W.E., and Wesseling, C. (1999). Dune growth, decay and migration rates during a large-magnitude flood at a sand and mixed sand-gravel bed in the Dutch Rhine river system. In: *Fluvial Sedimentology VI* (eds. N.D. Smith and J. Rogers), 15–32. International Association of Sedimentologists, Special Publication, no. 28.

Thorne, C.R. and Thiagarajah, R.I. (1994). Discussion of 'Twelfth Hunter Rouse Hydraulic Engineering Lecture: Future Trends and Needs in Hydraulics'. *Journal of Hydraulic Engineering* 120: 672–676.

Thorne, C.R., Russell, A.P.G., and Alam, M.K. (1993). Planform pattern and channel evolution of the Brahmaputra River, Bangladesh. In: *Braided Rivers* (eds. J.L. Best and C.S. Bristow), 257–276. Geological Society of London, Special Publication, no. 75.

Umitsu, M. (1993). Late Quaternary sedimentary environments and landforms in the Ganges delta. *Sedimentary Geology* 83: 177–186.

Van der Wal, M. (2020). Bank protection structures along the Brahmaputra-Jamuna River; A study of flow slides. *Water* 12: 2588. https://doi.org/10.3390/w12092588.

Winkley, B.R., Lesleighter, E.J., and Cooney, J.R. (1994). Instability problems of the Arial Khan River Bangladesh. In: *The Variability of Large Alluvial Rivers* (eds. S.A. Schumm and B.R. Winkley), 269–284. New York: ASCE Press.

Wood, G. (1999). Contesting water in Bangladesh: knowledge, rights and governance. *Journal of International Development* 11: 731–754.

Yakub, N.N. (1994). Overview. In: *Rivers of Life* (eds. K. Haggart, S. Huq, A.A. Rahman, et al.), 1–30. Dhaka: Bangladesh Centre for Advanced Studies\Panos.

Yalin, M.S. (1992). *River Mechanics*. Oxford: Pergamon Press, 219 pp.

Yang, Y.C.E., Wi, S., Ray, P.A. et al. (2016). The future nexus of the Brahmaputra River Basin: climate, water, energy and food trajectories. *Global Environmental Change* 37: 16–30.